

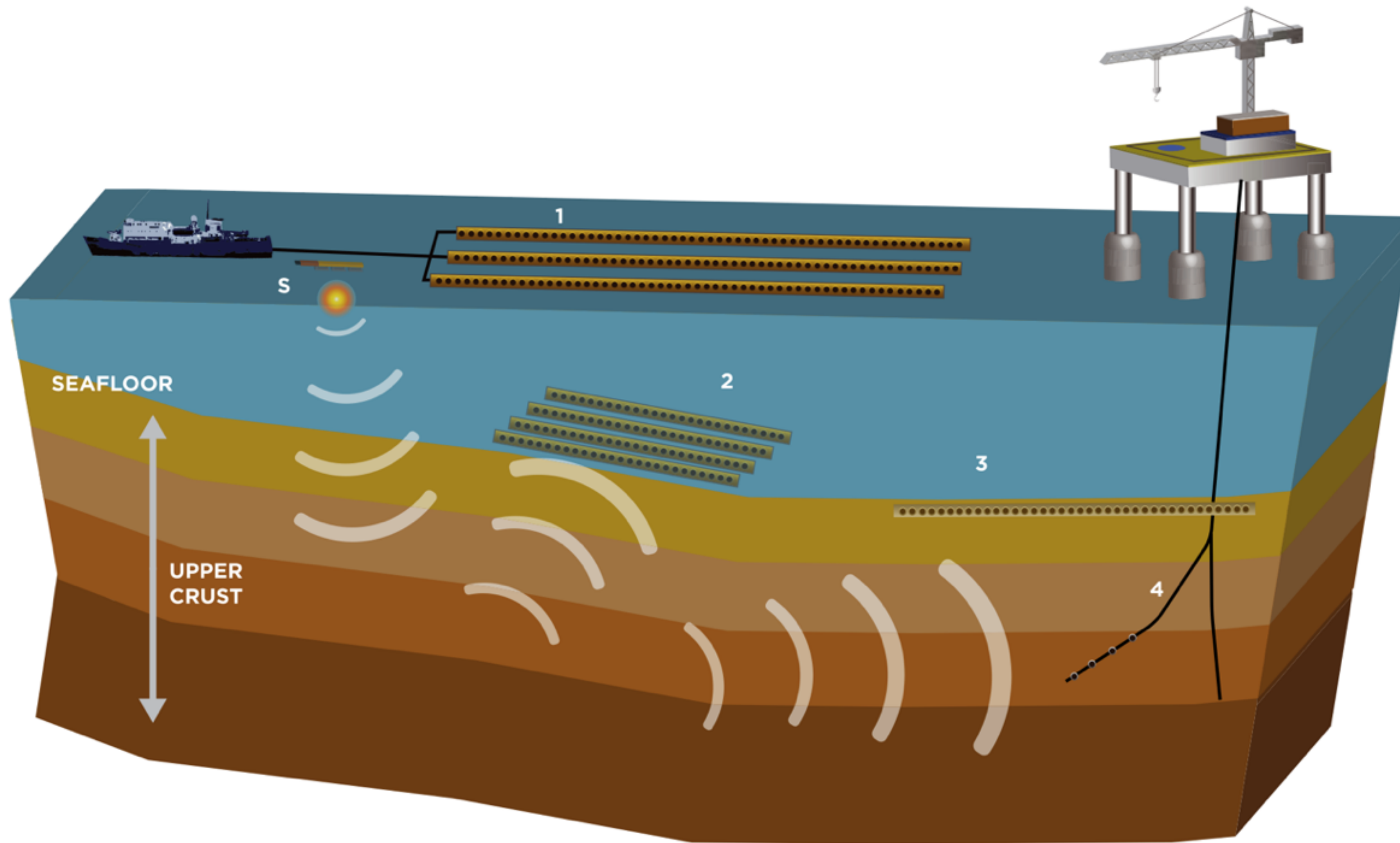
# Large scale high-frequency seismic wavefield reconstruction, acquisition via rank minimization and sparsity-promoting source estimation

Shashin Sharan  
Ph.D. Defense of Dissertation  
October 27, 2020



Georgia Institute of Technology

# Seismic data acquisition



## Objective

► Acquire Dense seismic data for high-resolution subsurface imaging

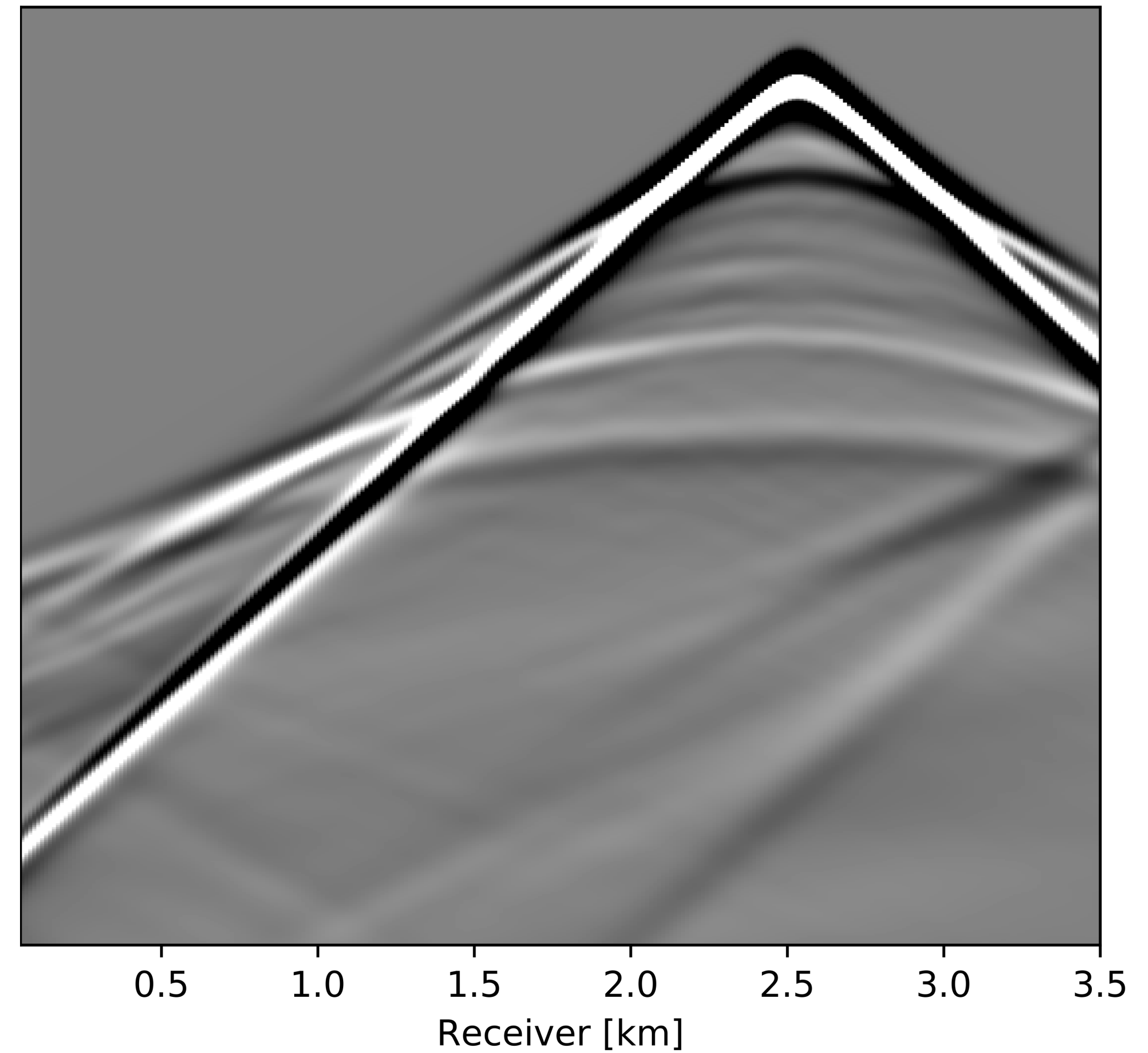
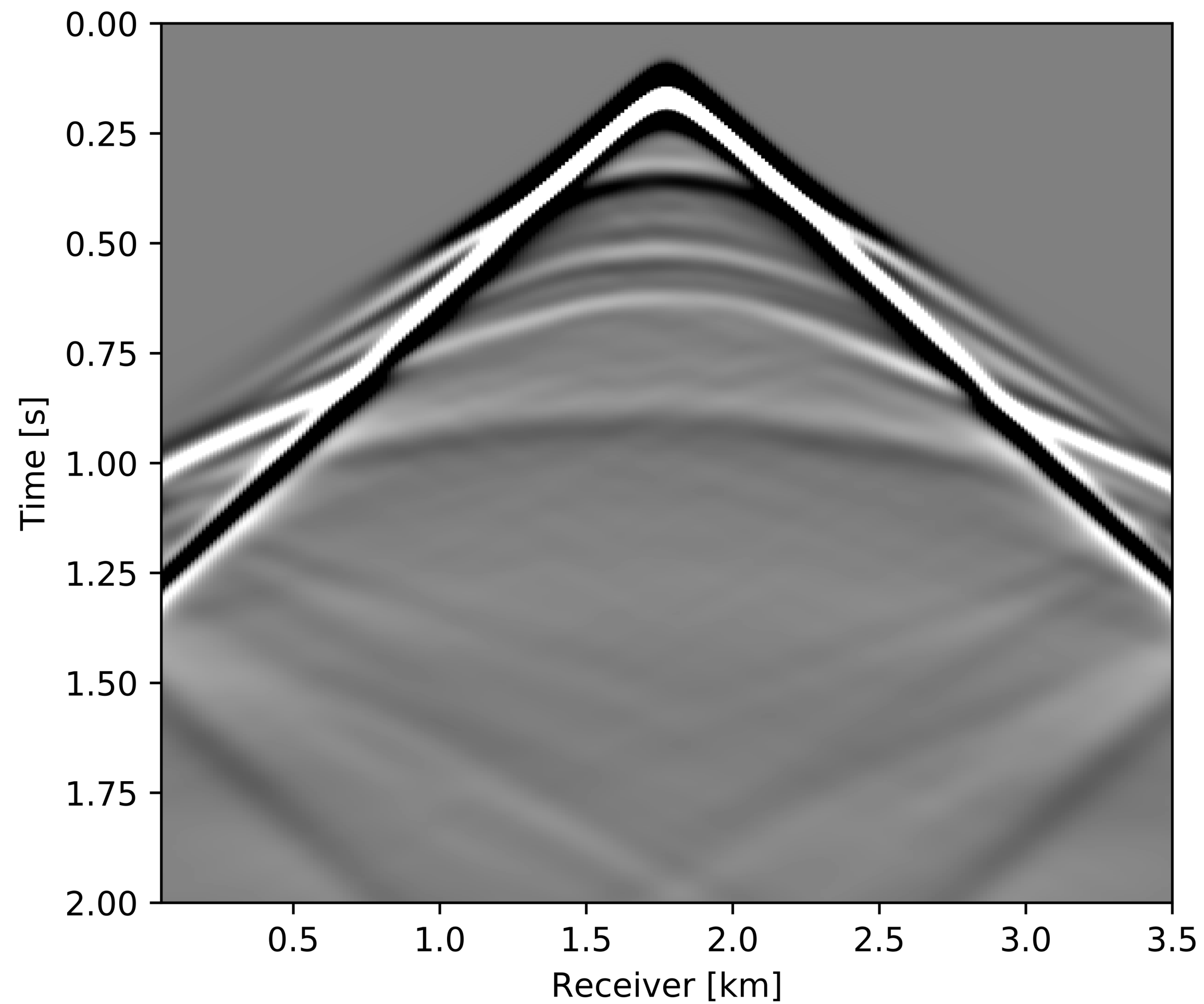
## Challenge

► Operationally complex to acquire dense data

## Solution

► Acquisition on coarse grid followed by data reconstruction on periodic fine grid

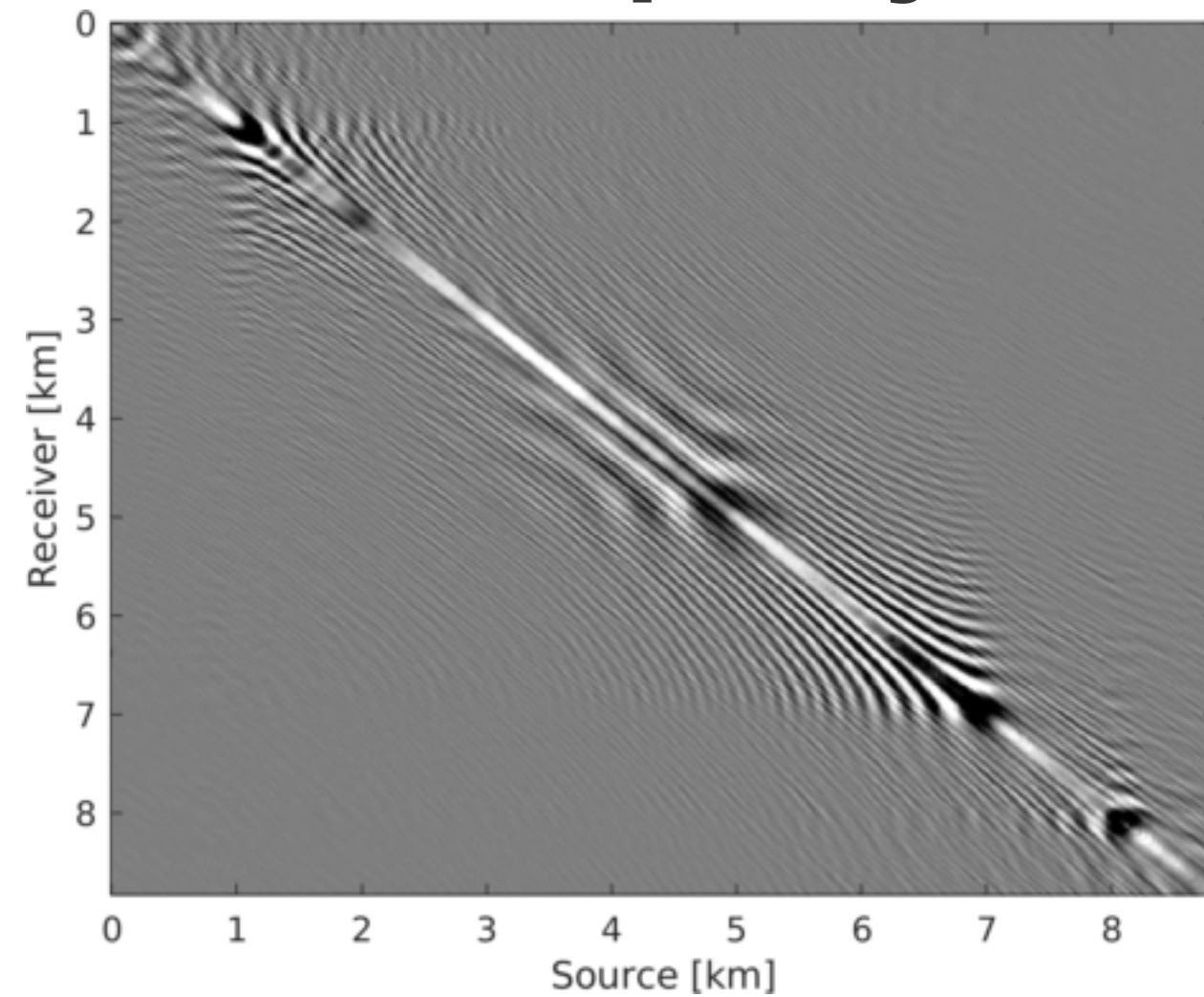
# Common Shot Gather Visualization



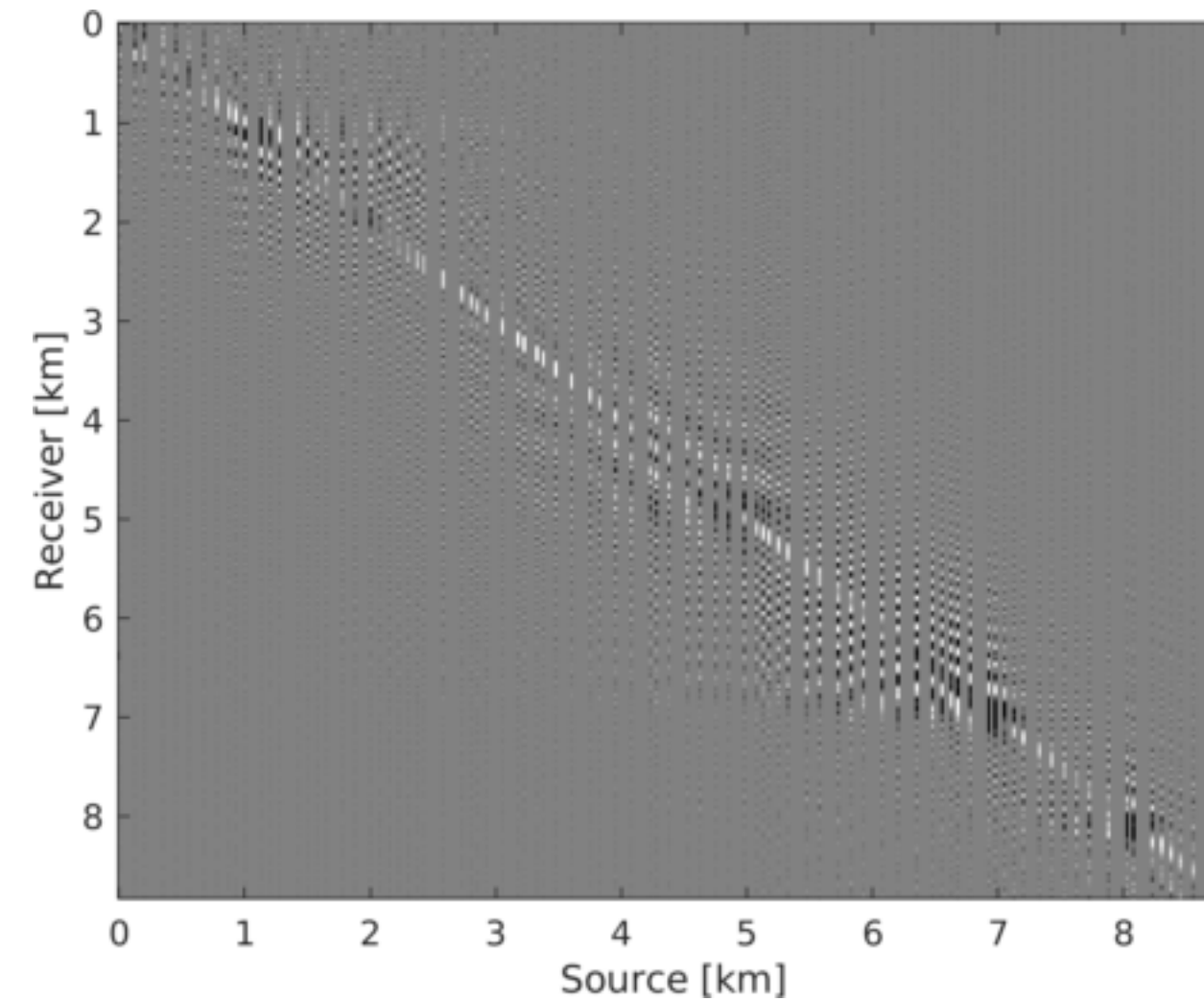


# Seismic data reconstruction w/ Low-rank

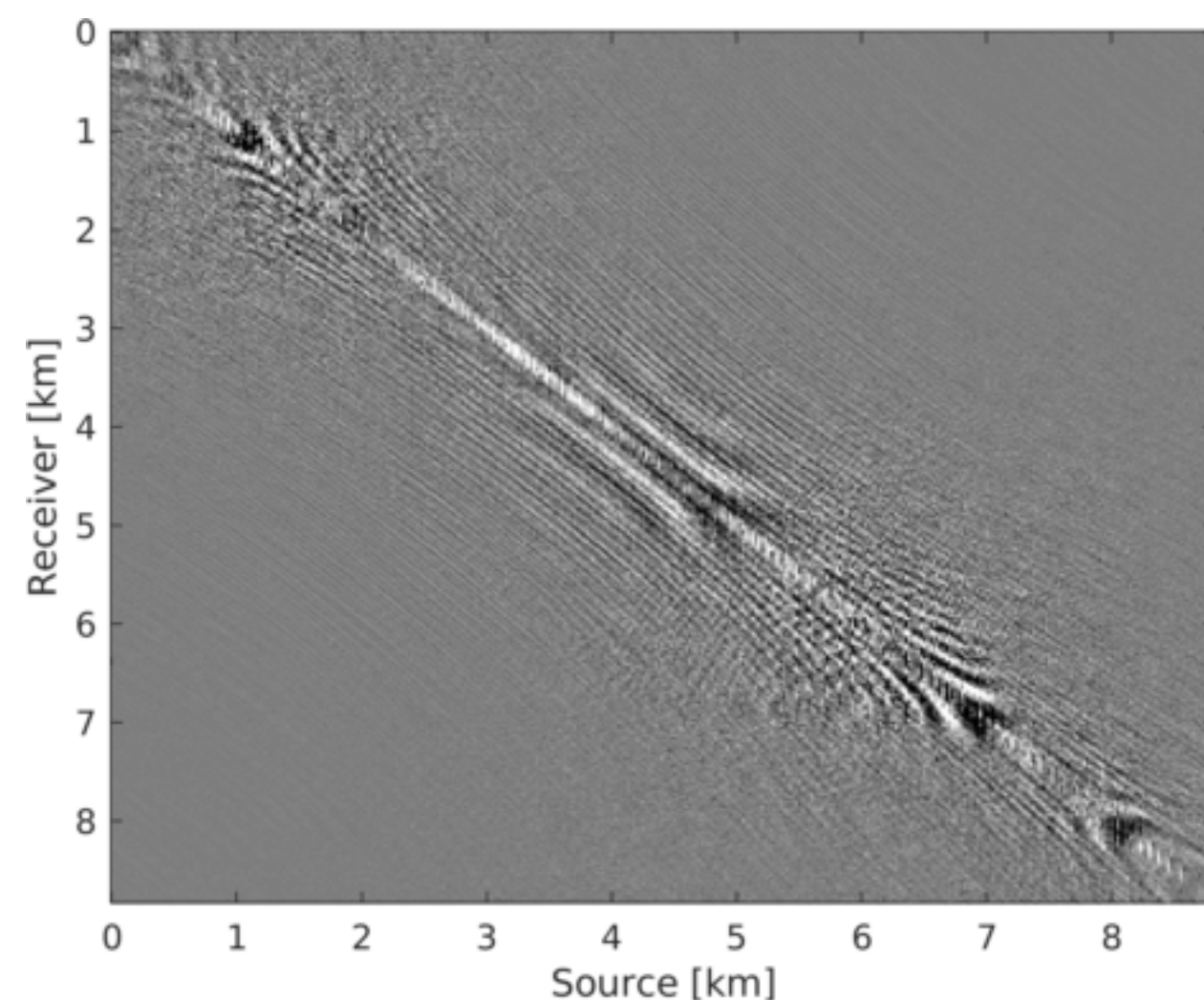
**60 Hz Frequency slice**



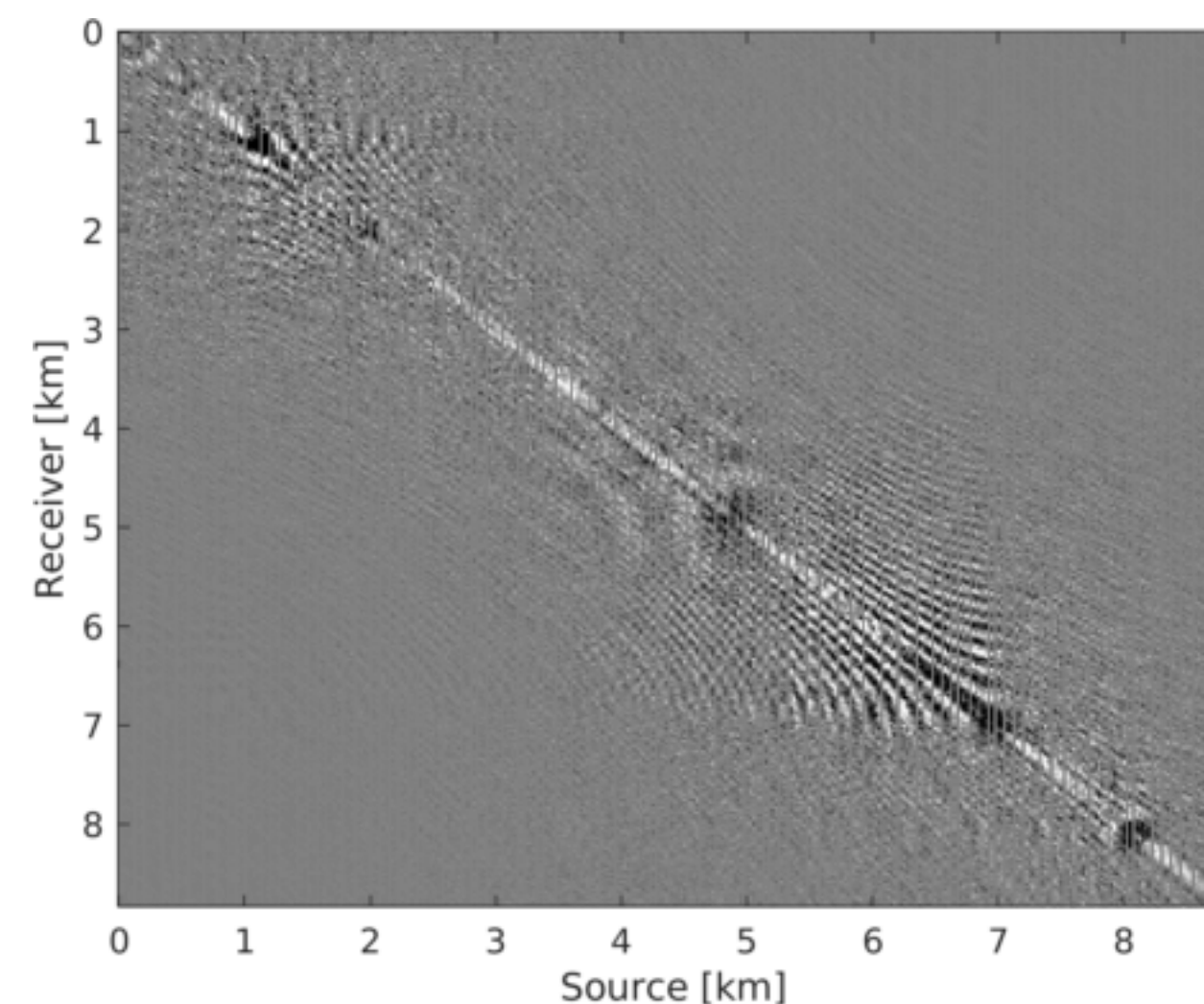
**Observed data**



**Reconstructed data**



**Data residual**



## Advantages

- Scalable for large scale 3D data
- Performs well at lower frequencies

## Limitations

- Performs poorly at higher frequencies



## Key Contributions: Chapters 2 & 3

### Recursively Weighted Matrix Completion Framework

- ▶ Improved data reconstruction at high frequency
- ▶ Scalable for large scale 3D data
- ▶ Computationally faster weighted method in comparison to traditional weighted method

### 5D Time-Jittered Marine Acquisition

- ▶ Simultaneous separation and reconstruction of sources from blended data
- ▶ Scalable for large scale 3D data

## Matrix completion

### Successful reconstruction scheme

- ▶ exploit *structure*
  - *low-rank* / *fast decay* of singular values
- ▶ sampling
  - randomness *increases* rank in “transform domain”
- ▶ optimization
  - via *rank-minimization* (*nuclear norm-minimization*)



# Nuclear-norm minimization

*convex relaxation of rank-minimization*

$$\underset{\mathbf{X} \in \mathbb{C}^{m \times n}}{\text{minimize}} \underbrace{\|\mathbf{X}\|_*}_{\text{Sum of singular values of } \mathbf{X}} \quad \text{subject to} \quad \|\mathcal{A}(\mathbf{X}) - \mathbf{B}\|_F \leq \epsilon$$

**Sum of singular values of  $\mathbf{X}$**

\*where  $\|\cdot\|_F$  is the Frobenius norm

$\mathcal{A}$  is the Measurement operator

$\mathbf{B}$  is the observed data

$\epsilon$  is the noise level

# Weighted Nuclear-norm minimization

*expensive projection operators*

$$\underset{\mathbf{X}}{\text{minimize}} \|\mathbf{Q}\mathbf{X}\mathbf{W}\|_* \quad \text{subject to} \quad \|\mathcal{A}(\mathbf{X}) - \mathbf{B}\|_F \leq \epsilon$$

\*where  $\mathbf{Q} = w_1 \mathbf{U}\mathbf{U}^H + \mathbf{U}^\perp \mathbf{U}^{\perp H}$  and  $\mathbf{W} = w_2 \mathbf{V}\mathbf{V}^H + \mathbf{V}^\perp \mathbf{V}^{\perp H}$

$\mathbf{U}, \mathbf{V}$  are row and column subspaces of adjacent frequency slice

$w_1, w_2$  are weights

# Efficient Weighted Matrix Completion

$$\underset{\bar{\mathbf{X}}}{\text{minimize}} \quad \|\bar{\mathbf{X}}\|_* \quad \text{subject to} \quad \|\mathcal{A}(\mathbf{Q}^{-1}\bar{\mathbf{X}}\mathbf{W}^{-1}) - \mathbf{B}\|_F \leq \epsilon$$

\*where  $\bar{\mathbf{X}} = \mathbf{Q}\mathbf{X}\mathbf{W}$

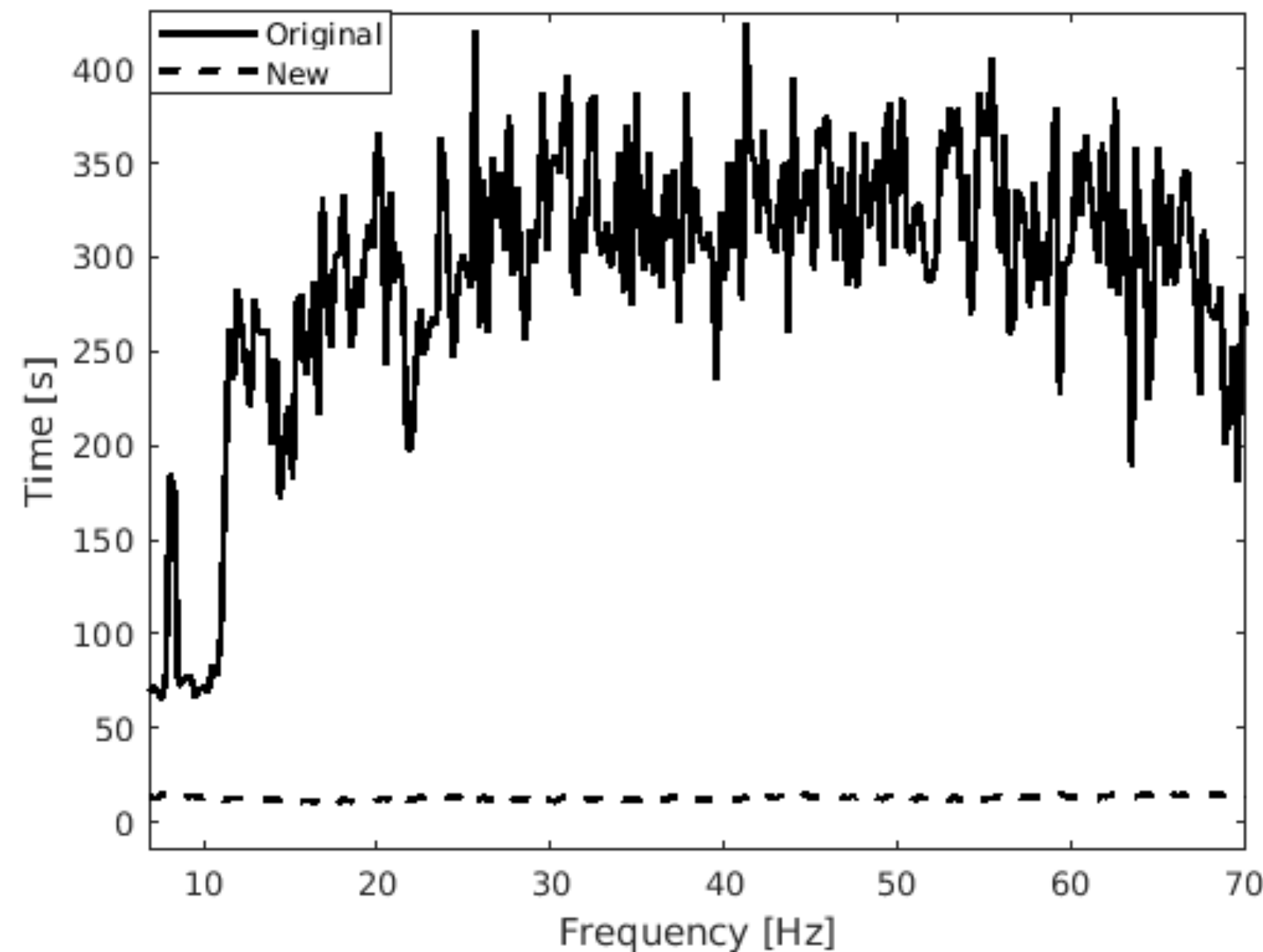
$$\underset{\bar{\mathbf{L}}, \bar{\mathbf{R}}}{\text{minimize}} \quad \frac{1}{2} \left\| \begin{bmatrix} \bar{\mathbf{L}} \\ \bar{\mathbf{R}} \end{bmatrix} \right\|_F^2$$

\*where  $\bar{\mathbf{X}} = \bar{\mathbf{L}}\bar{\mathbf{R}}^H$

with  $\bar{\mathbf{L}} \in \mathbb{C}^{m \times k}$  and  $\bar{\mathbf{R}} \in \mathbb{C}^{n \times k}$   
and  $k \ll m, n$

**Factorized Form**

$$\text{subject to} \quad \|\mathcal{A}(\mathbf{Q}^{-1}\bar{\mathbf{L}}\bar{\mathbf{R}}^H\mathbf{W}^{-1}) - \mathbf{B}\|_F \leq \epsilon$$

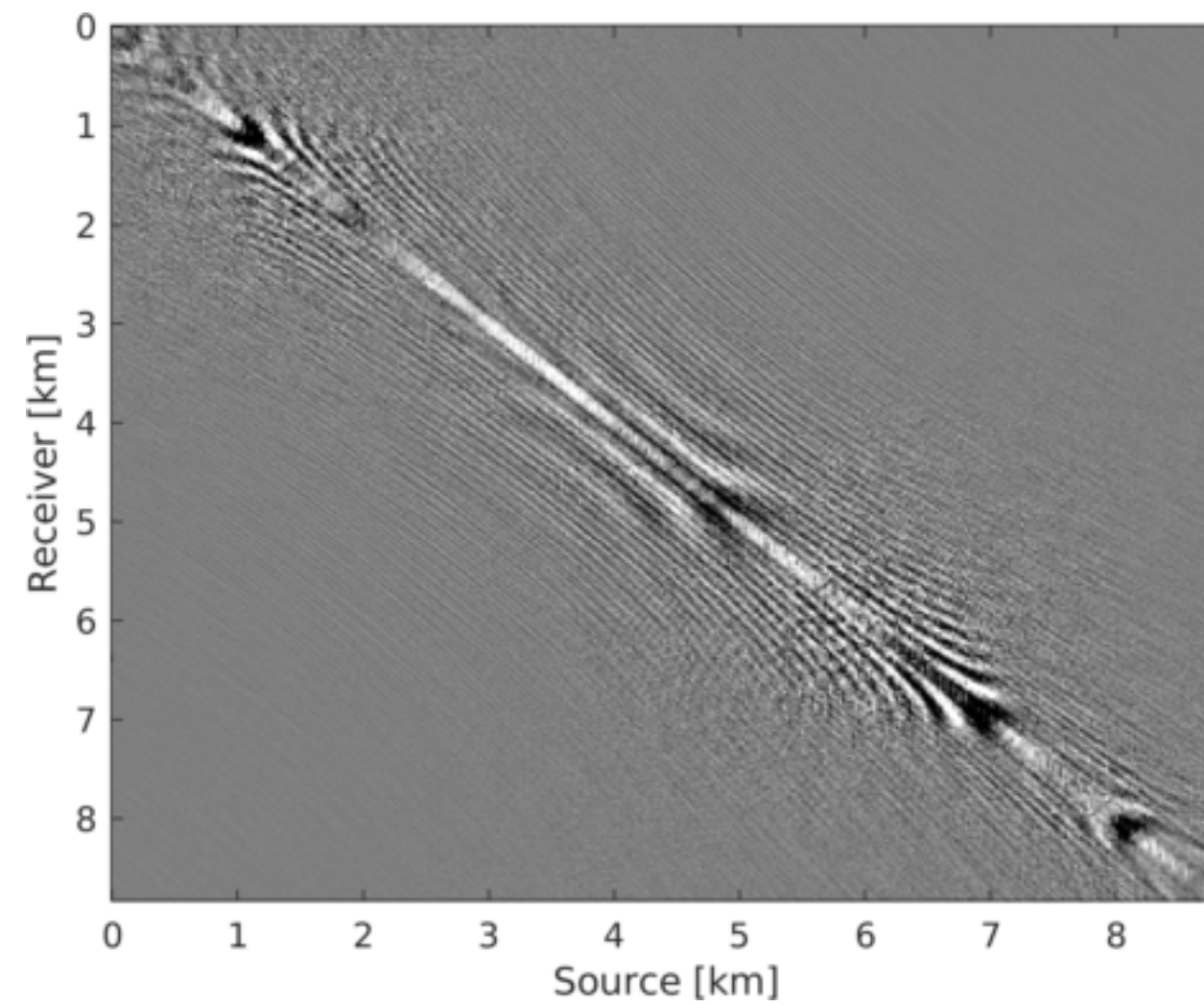


**Runtime Comparison**

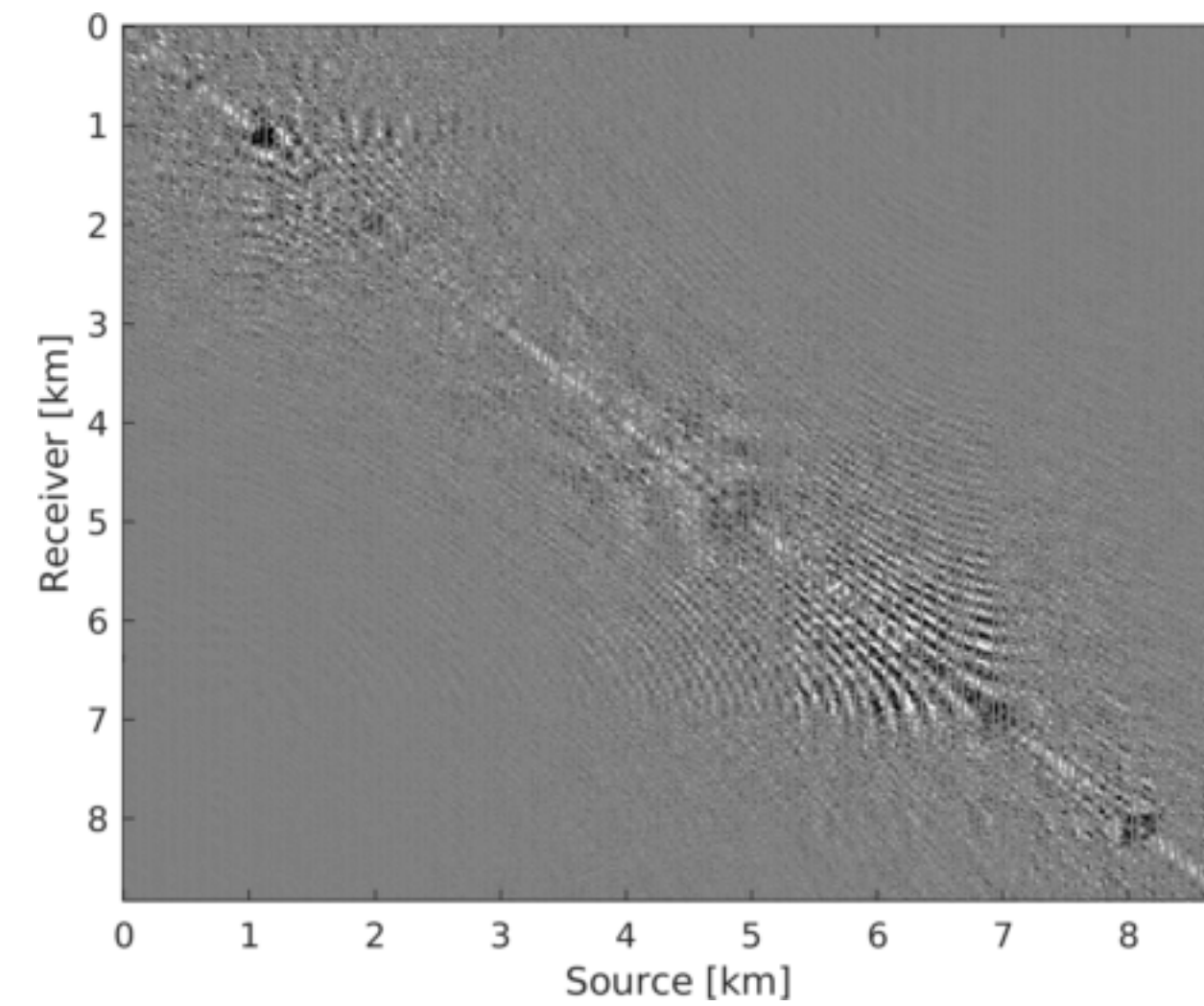


# Recursively Weighted vs Pair Weighted

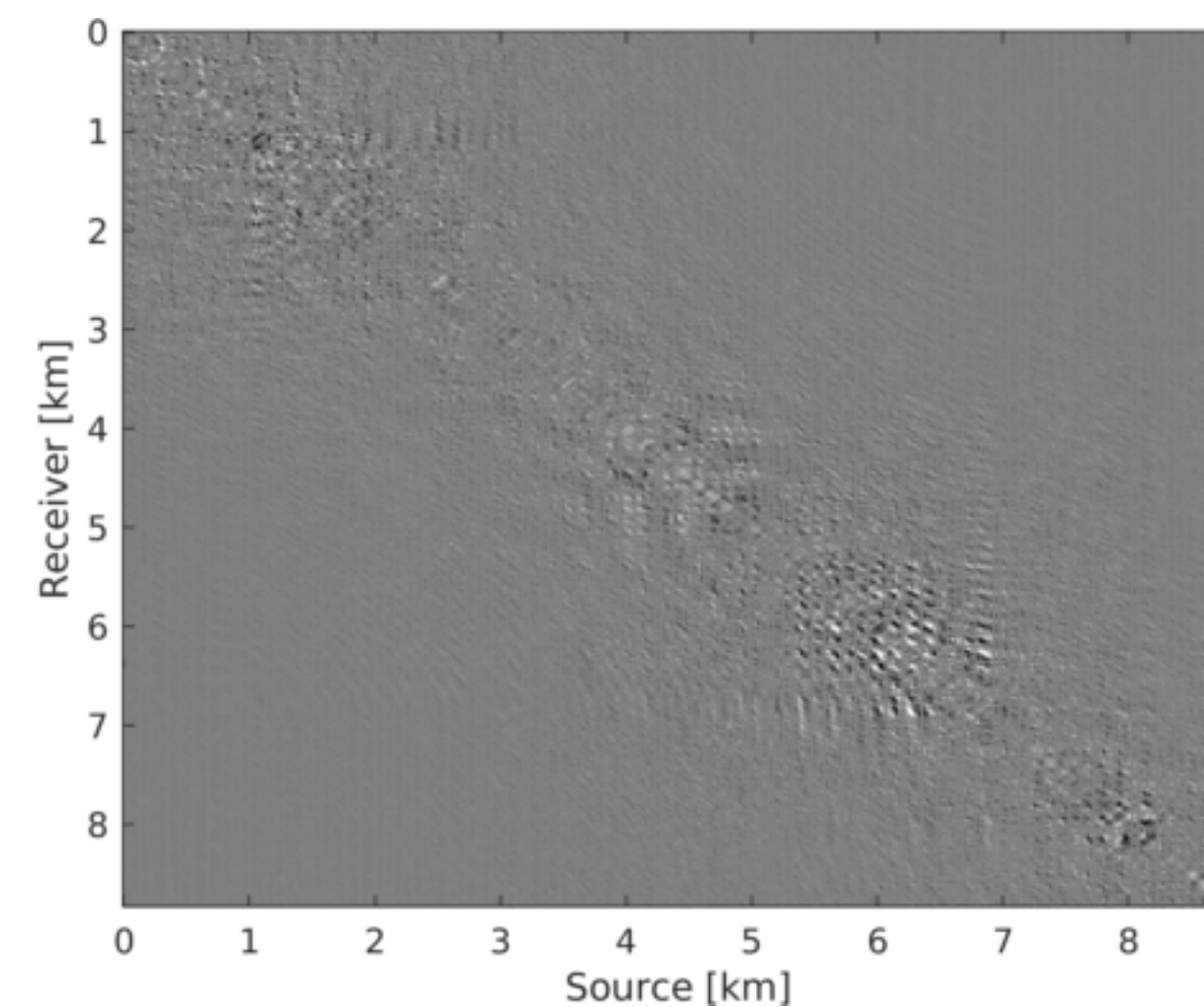
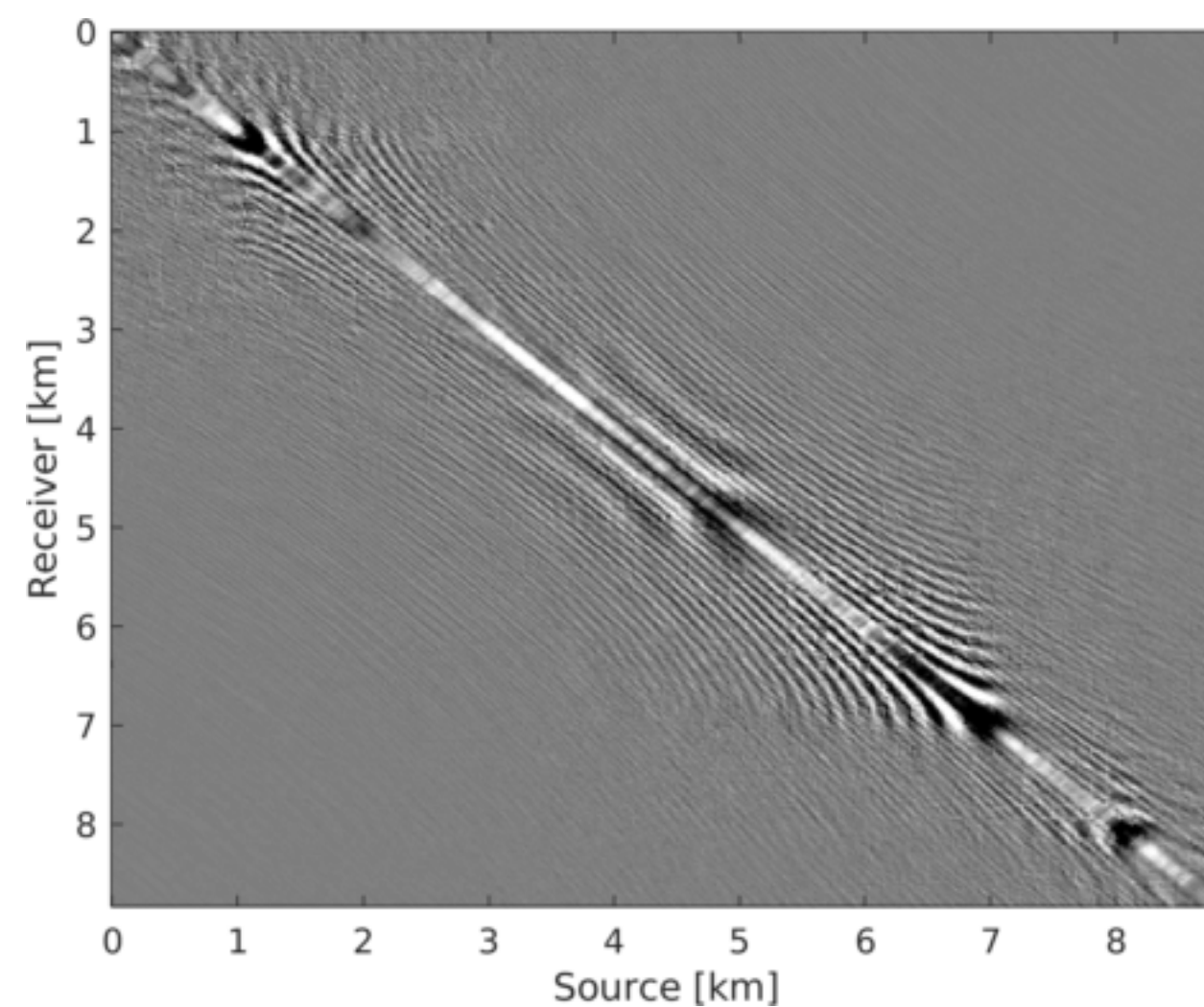
## Reconstructed data



## Data residual



**Pair Weighted, SNR = 5.08 dB**



**Recursively Weighted, SNR = 8.72 dB**



# Parallel Implementation

## Recursively weighted method challenges

- ▶ need to wait for reconstruction of previous frequencies
- ▶ computationally demanding for large scale 3D data

## Alternating minimization and decoupling strategies enable

- ▶ recursively framework scalable for large 3D data
- ▶ parallelized framework

## Inclusion of weight matrices pose

- ▶ challenges in parallelizing
- ▶ unlike in conventional method without weights



# Parallelization w/o weights

$$\mathbf{R}(l_1, :)^H := \arg \min_{\mathbf{v}} \frac{1}{2} \|\mathbf{v}\|^2 \quad \text{subject to} \quad \|\mathcal{A}_{l_1}(\mathbf{L}\mathbf{v}) - \mathbf{B}(:, l_1)\| \leq \gamma$$

for  $l_1 = 1, 2, \dots, n$

$$\mathbf{L}(l_2, :)^H := \arg \min_{\mathbf{u}} \frac{1}{2} \|\mathbf{u}\|^2 \quad \text{subject to} \quad \|\mathcal{A}_{l_2}((\mathbf{R}\mathbf{u})^H) - \mathbf{B}(l_2, :)\| \leq \gamma$$

for  $l_2 = 1, 2, \dots, m$

\* where  $\mathcal{A}_{l_1}$  is acquisition mask for  $l_1^{th}$  row of  $\mathbf{B}$

and  $\mathcal{A}_{l_2}$  is acquisition mask for  $l_2^{th}$  column of  $\mathbf{B}$

***Inclusion of weight matrices poses challenge in parallelizing***

# Parallelization w/ weights

For large weights:

$$\mathbf{Q}\mathcal{A}(\mathbf{Q}^{-1}\bar{\mathbf{X}}\mathbf{W}^{-1}) \approx \mathcal{A}(\bar{\mathbf{X}}\mathbf{W}^{-1}) \quad \text{and} \quad \mathcal{A}(\mathbf{Q}^{-1}\bar{\mathbf{X}}\mathbf{W}^{-1})\mathbf{W} \approx \mathcal{A}(\mathbf{Q}^{-1}\bar{\mathbf{X}})$$

This commutation property allows parallelization

$$\bar{\mathbf{R}}(l_1, :)^H := \arg \min_{\bar{\mathbf{v}}} \frac{1}{2} \|\bar{\mathbf{v}}\|^2 \quad \text{subject to} \quad \|\mathcal{A}_{l_1}(\hat{\mathbf{Q}}\bar{\mathbf{L}}\bar{\mathbf{v}}) - w_1 w_2 \mathbf{B}(:, l_1)\| \leq w_1 w_2 \gamma$$

$$\bar{\mathbf{L}}(l_2, :)^H := \arg \min_{\bar{\mathbf{u}}} \frac{1}{2} \|\bar{\mathbf{u}}\|^2 \quad \text{subject to} \quad \|\mathcal{A}_{l_2}((\bar{\mathbf{R}}\bar{\mathbf{u}})^H \hat{\mathbf{W}}) - w_1 w_2 \mathbf{B}(l_2, :)\| \leq w_1 w_2 \gamma$$

\*where  $\hat{\mathbf{Q}} = \mathbf{U}\mathbf{U}^H + w_1 \mathbf{U}^\perp \mathbf{U}^{\perp H} = w_1 \mathbf{Q}^{-1}$

and  $\hat{\mathbf{W}} = \mathbf{V}\mathbf{V}^H + w_2 \mathbf{V}^\perp \mathbf{V}^{\perp H} = w_2 \mathbf{W}^{-1}$



# Case Study: BG Synthetic 3D Data

**Data dimension:** 501 x 201 x 201 x 41 x 41 (nt x nrx x nry x nsx x nsy)

**Time sampling interval:** 10 ms

**Source sampling interval (x and y):** 150 m

**Receiver sampling interval (x and y):** 25 m

**Velocity model:** BG Compass

**Observed data:** 90 % missing receivers

# Optimization Information

**Number of alternations per frequency: 4**

**Number of inner iterations per alternation: 40**

**Rank parameter: 228**

**Weight: 0.75**

**Computational resource: AWS cloud**

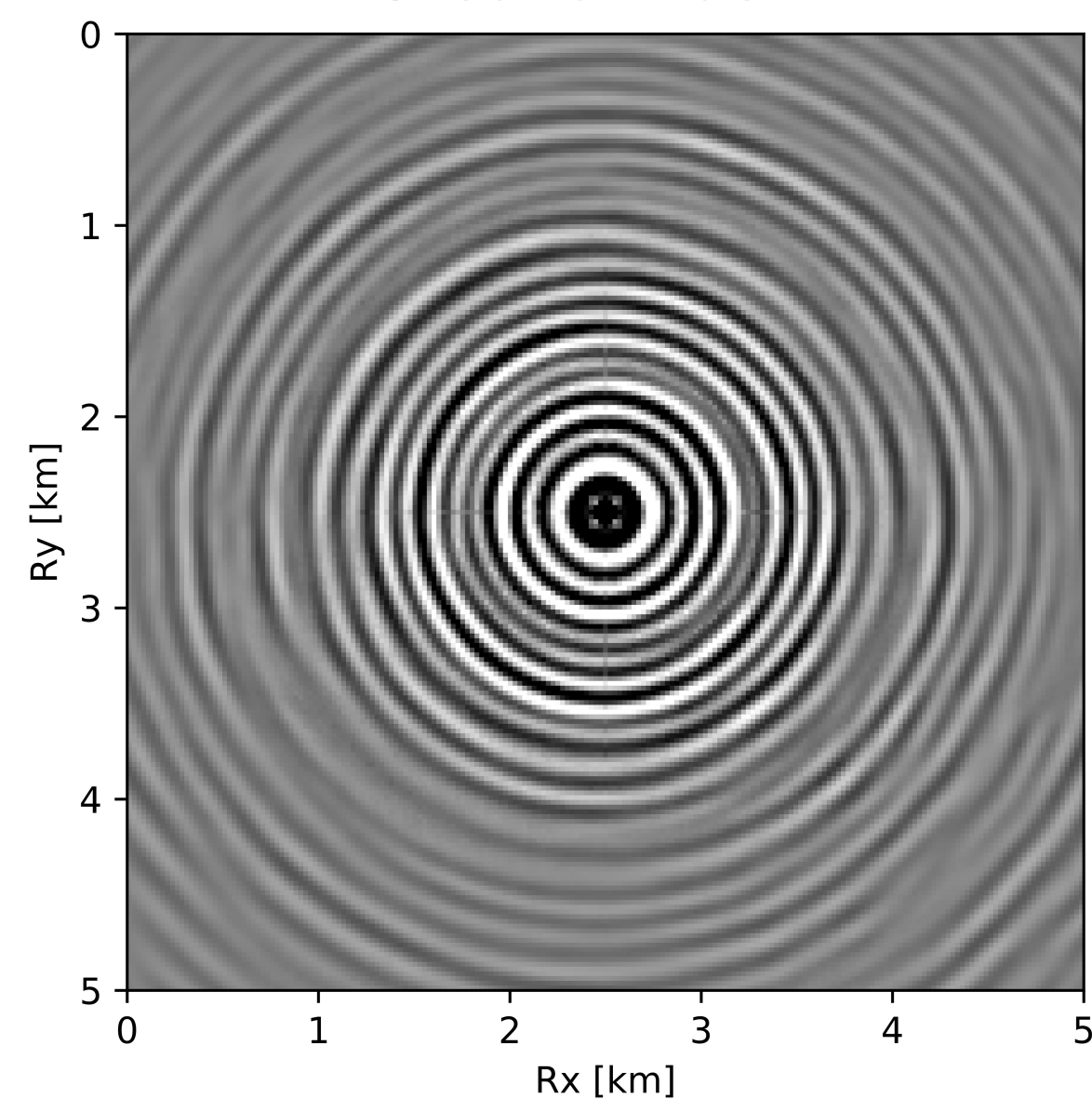
**Time per frequency: 8 minutes**

**Final volume: 7 GB (95% compressed)**

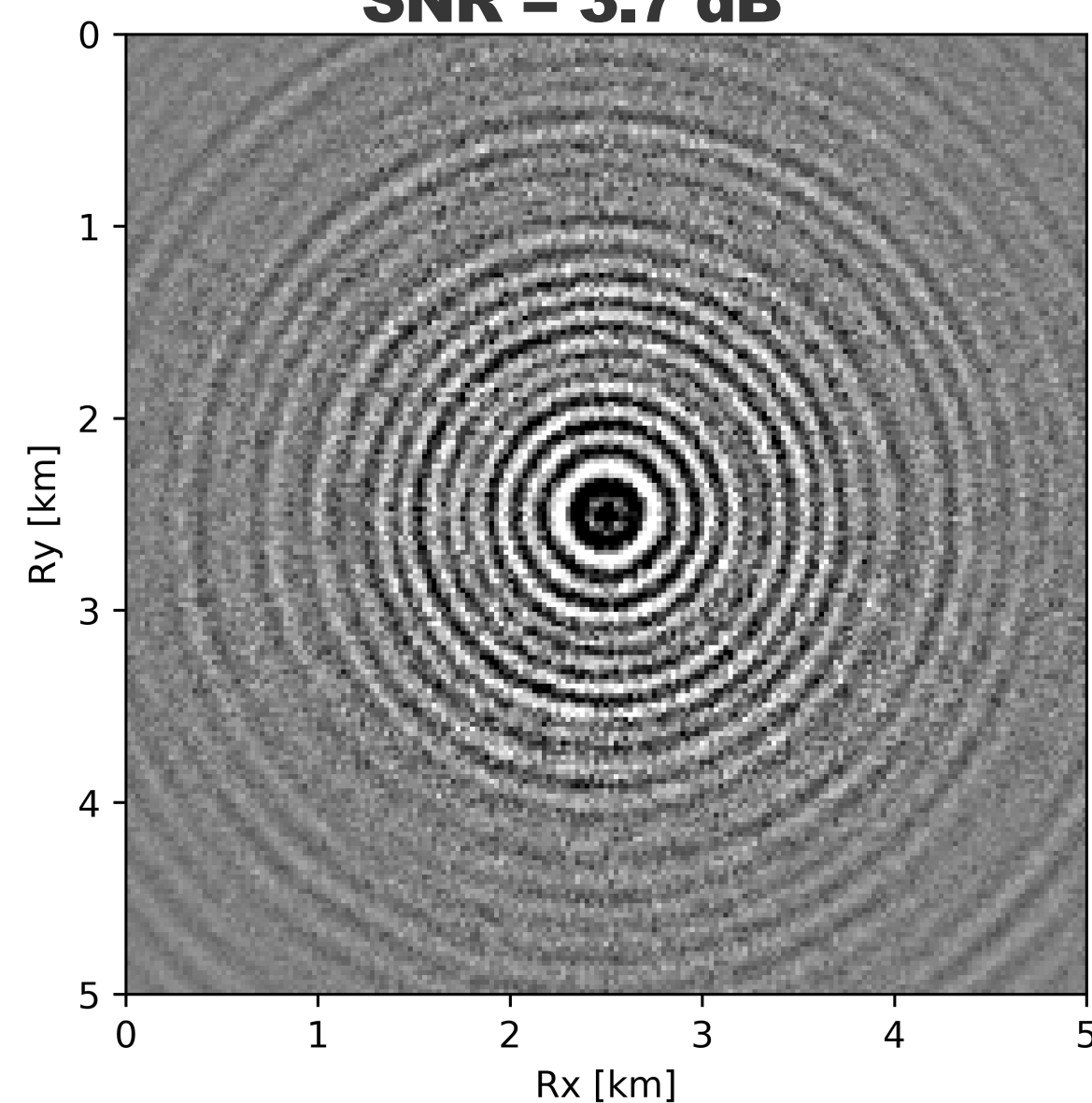


# 15 Hz Frequency Slice

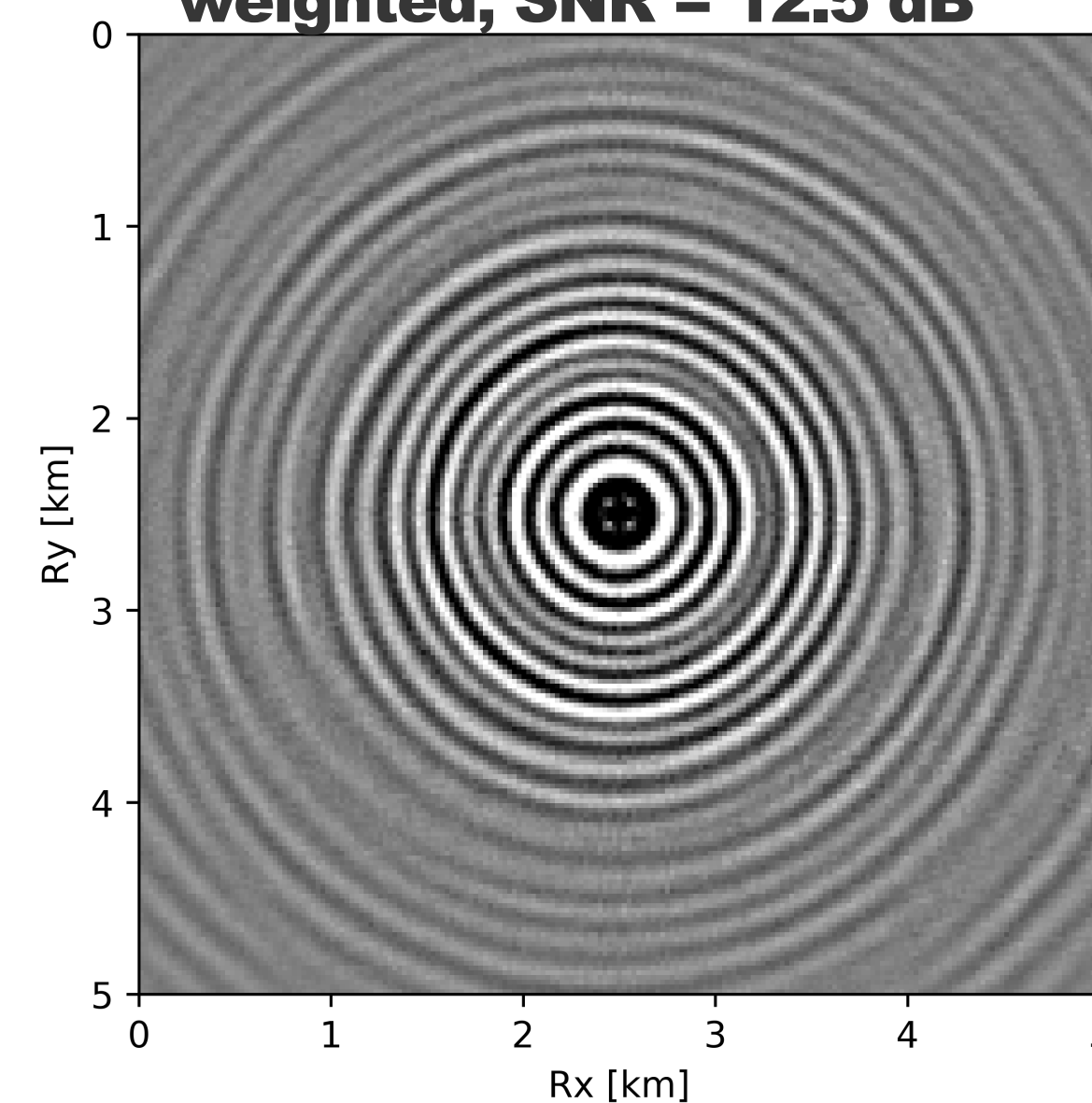
**Ground Truth**



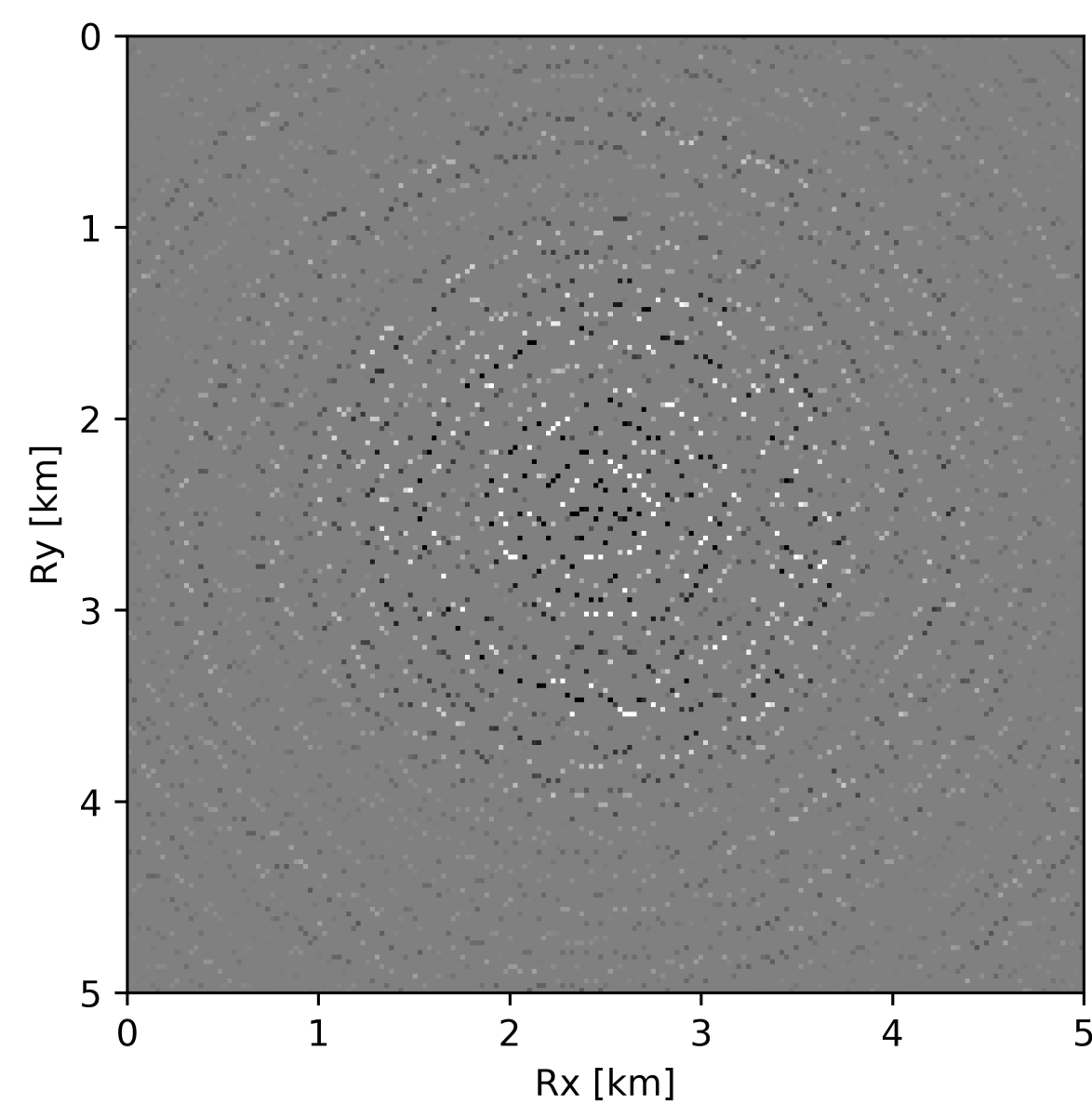
**Reconstruction w/ conventional,  
SNR = 3.7 dB**



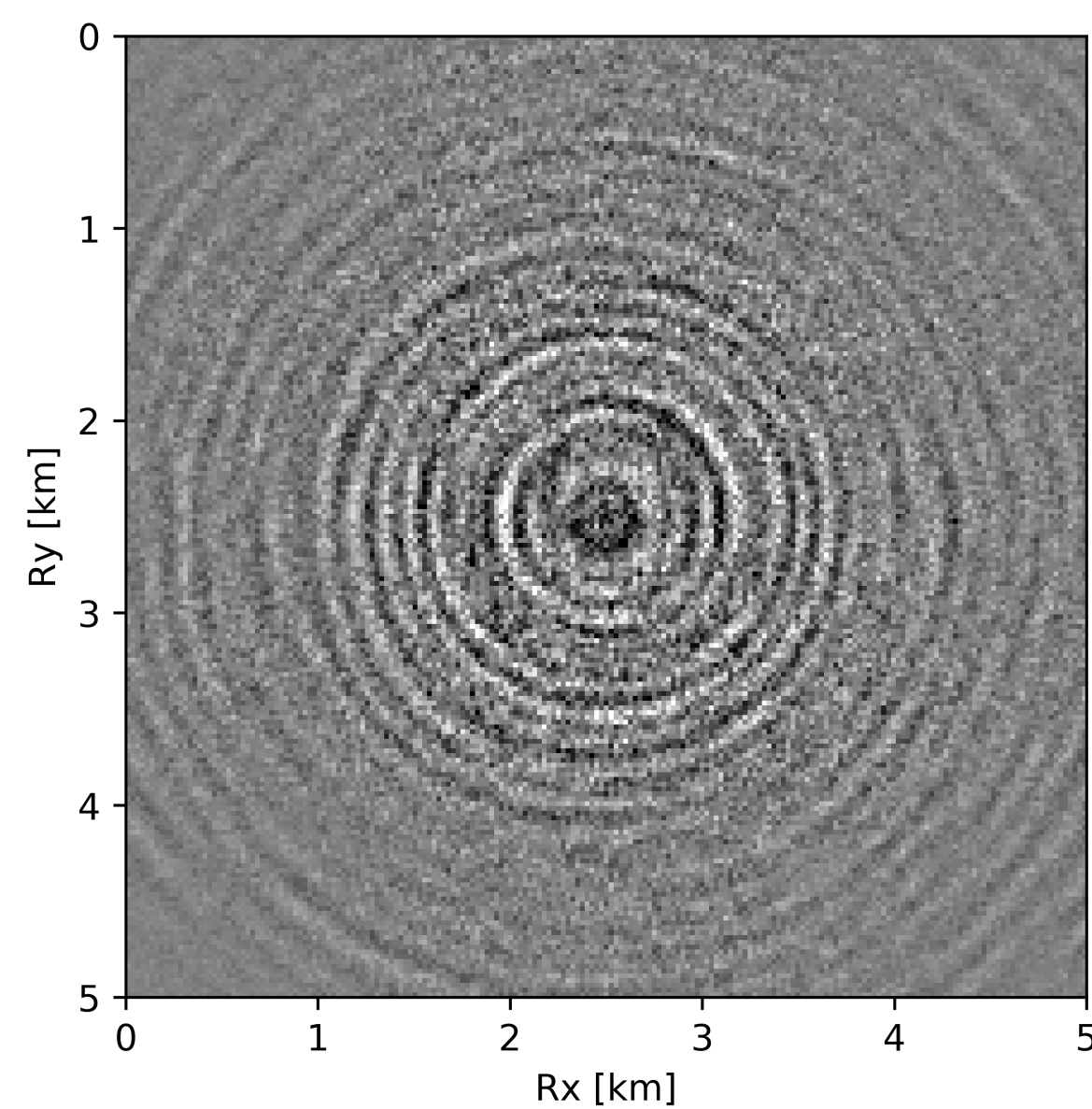
**Reconstruction w/ recursively  
weighted, SNR = 12.5 dB**



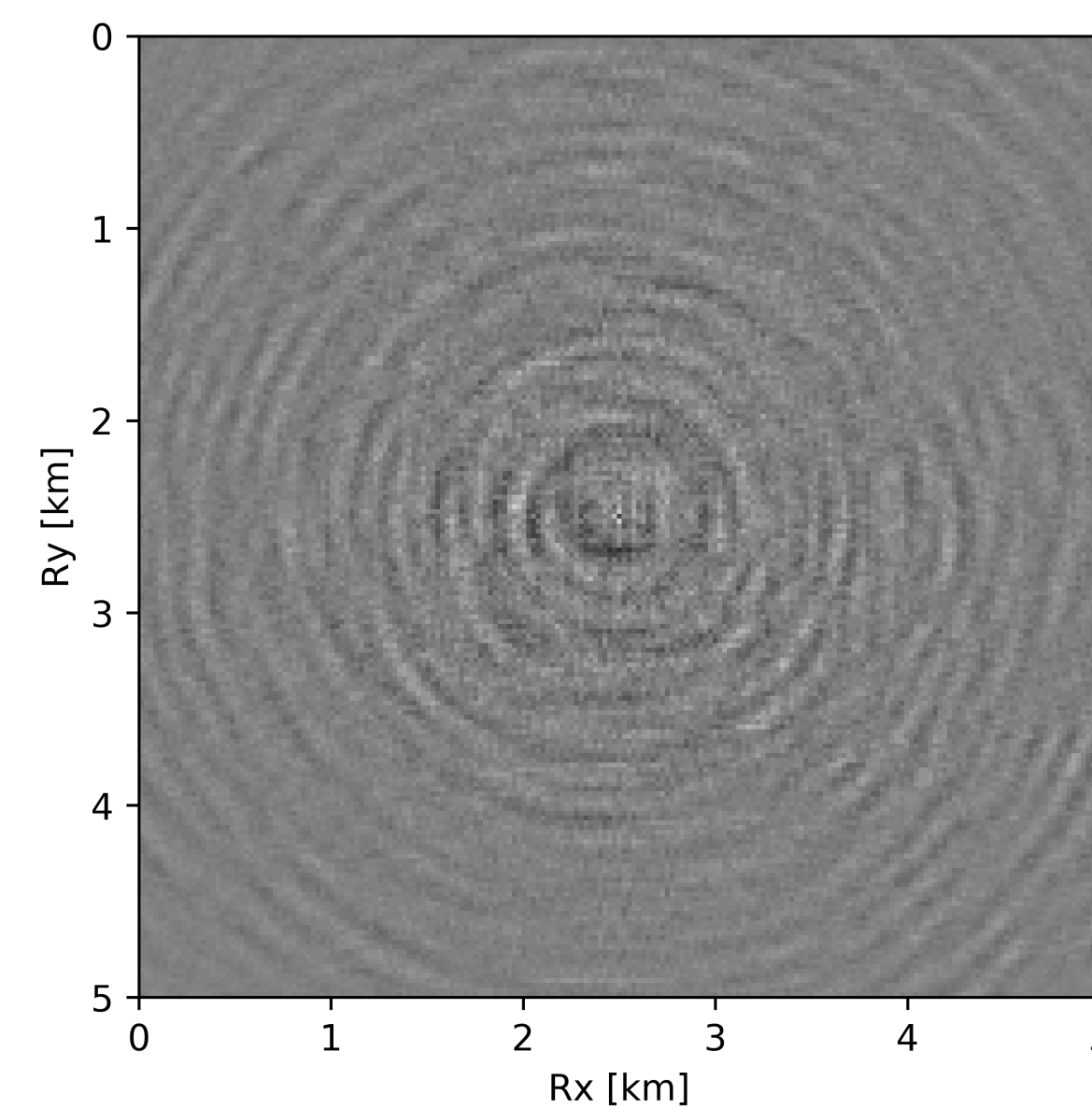
**Observed w/ 90% missing receivers**



**Data Residual w/ conventional**

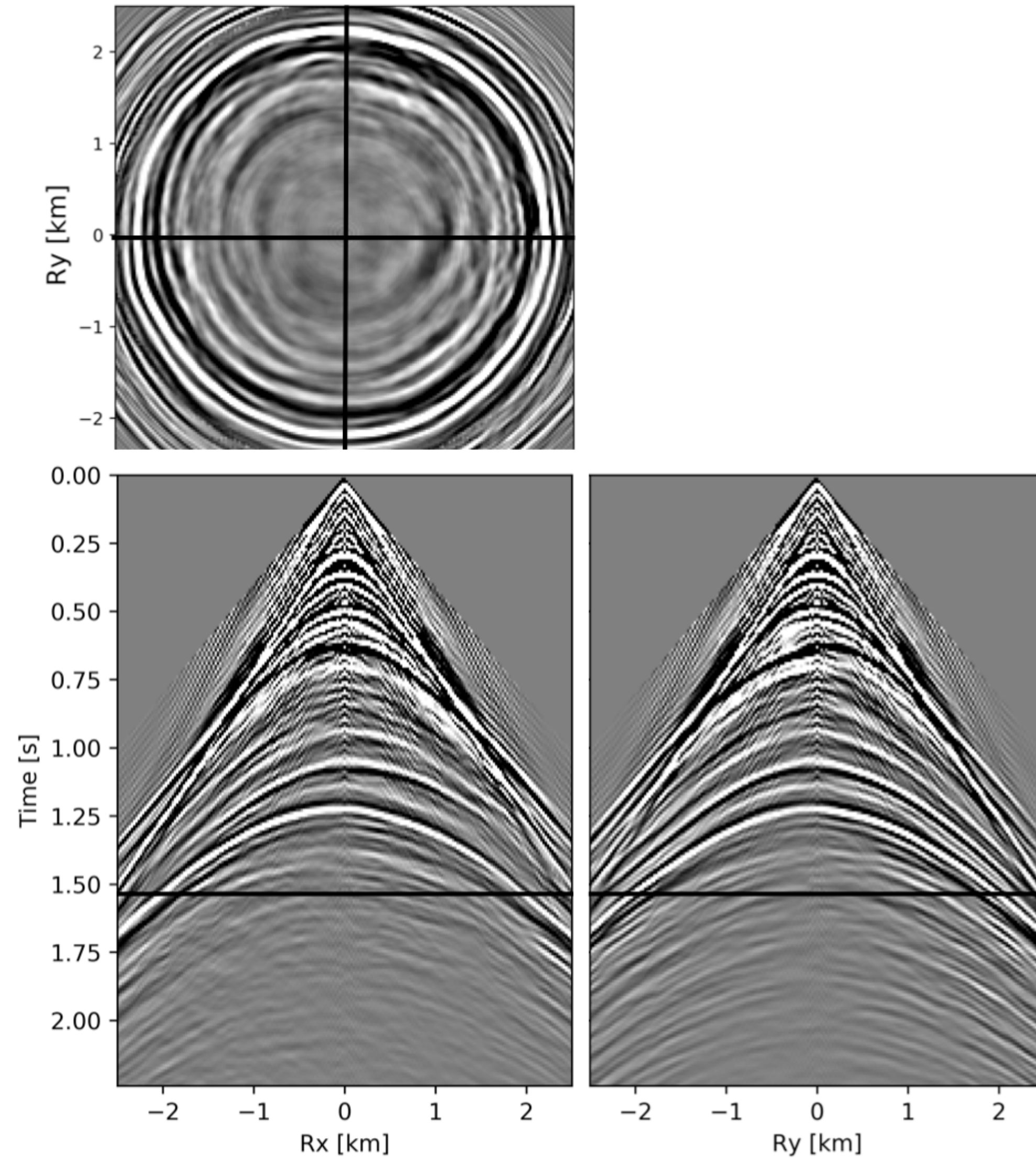


**Data Residual w/ recursively weighted**

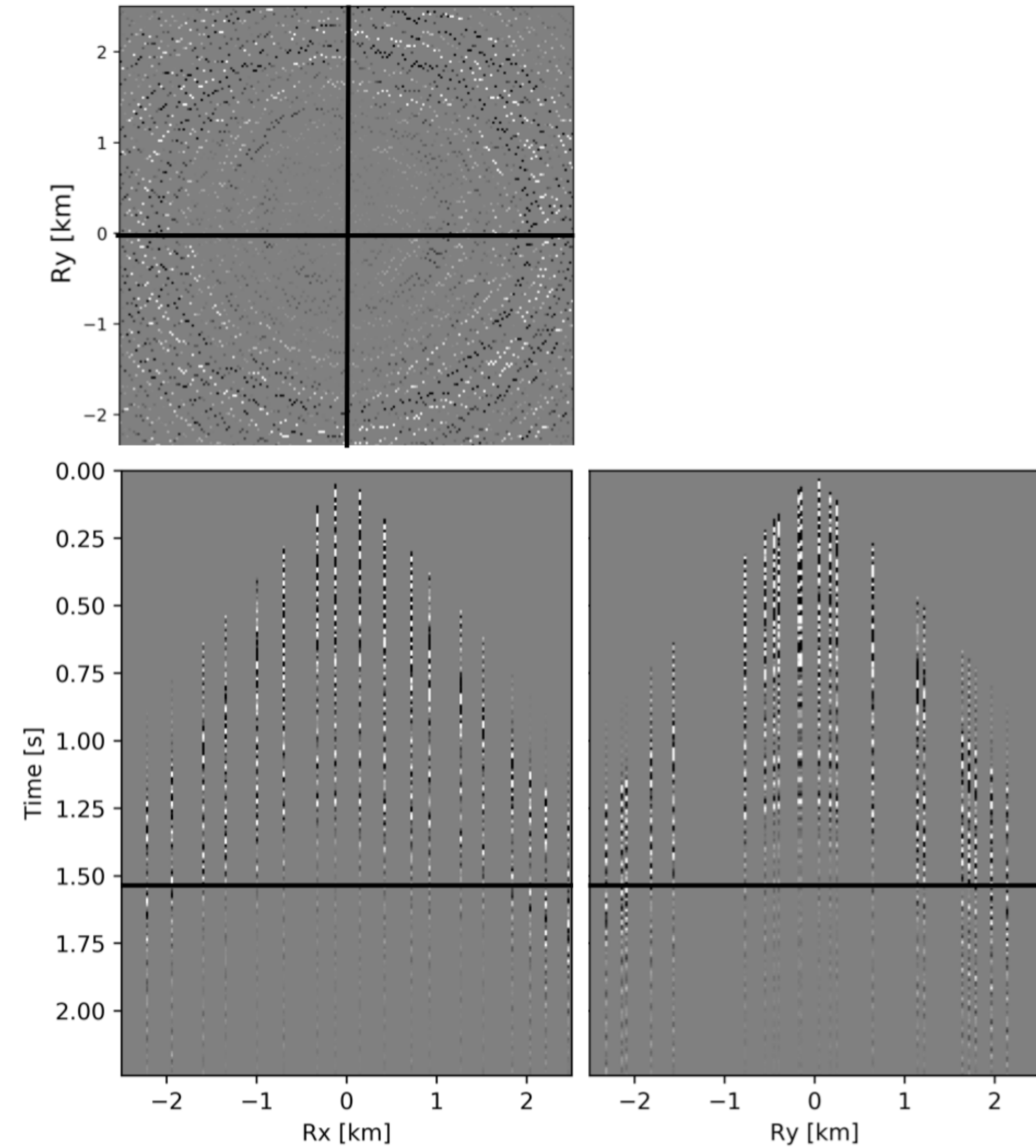




# Time Domain Results



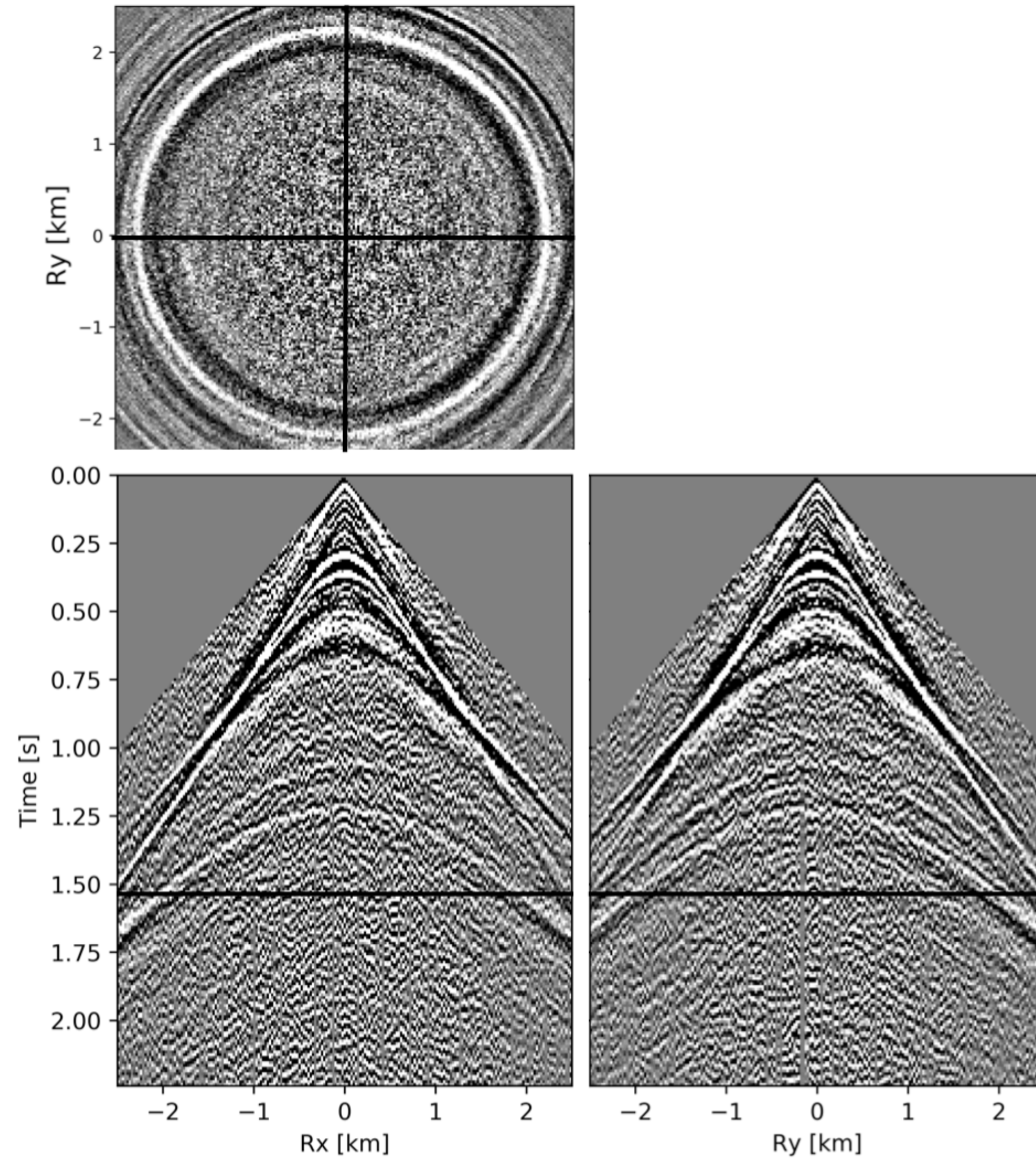
**Ground Truth**



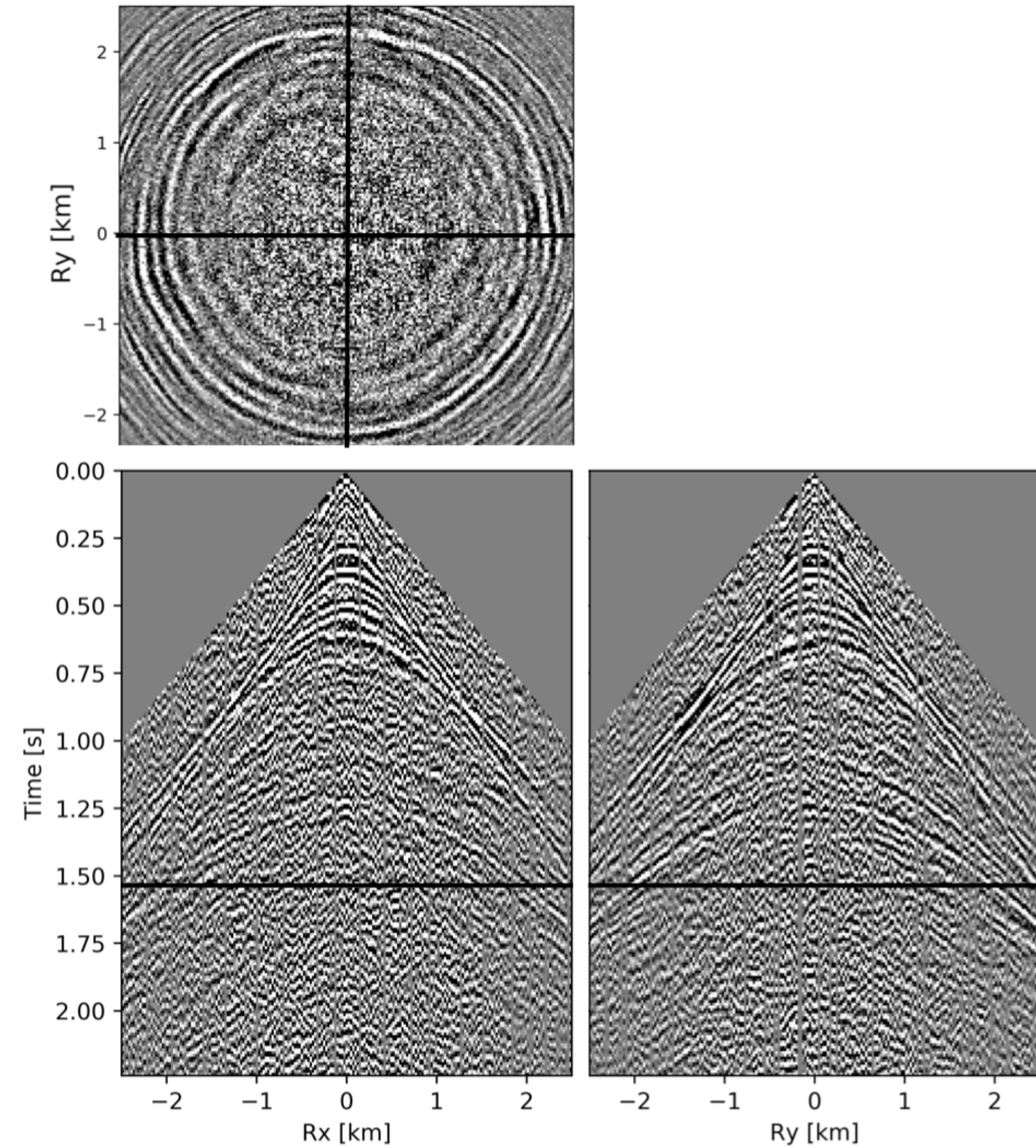
**Observed Data w/ 90% missing receivers**



# Time Domain Results



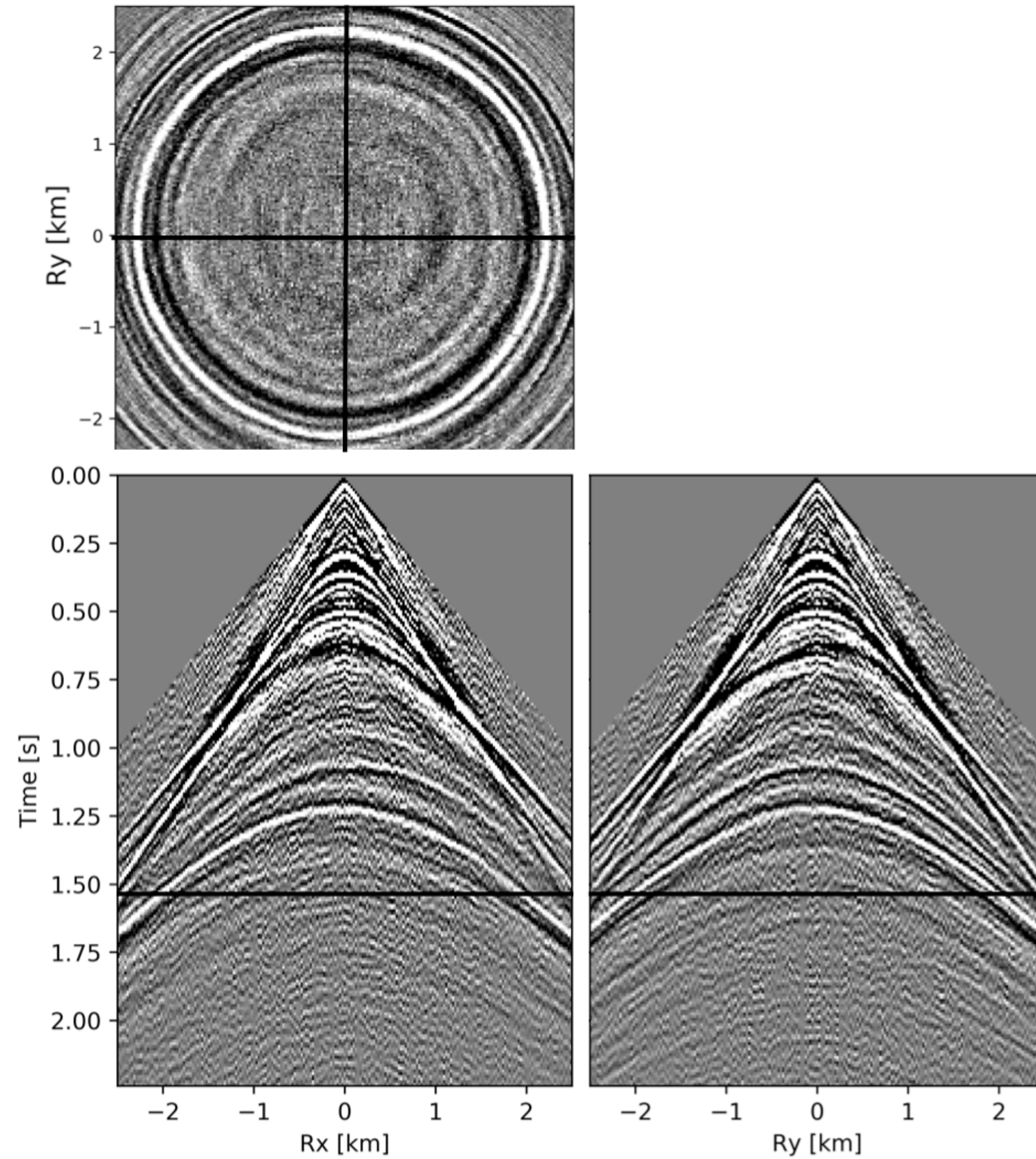
**Reconstruction w/ conventional**



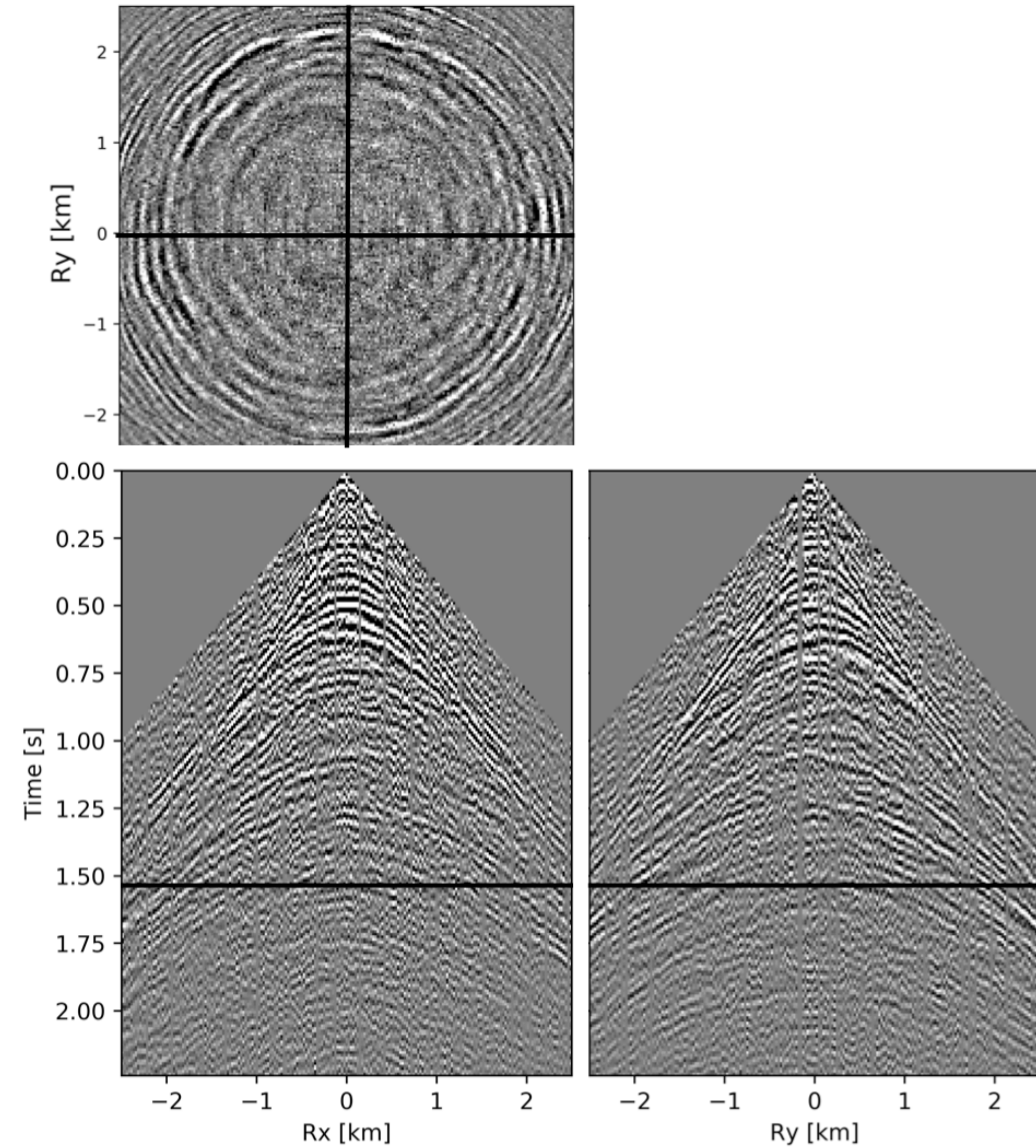
**Data residual**



# Time Domain Results



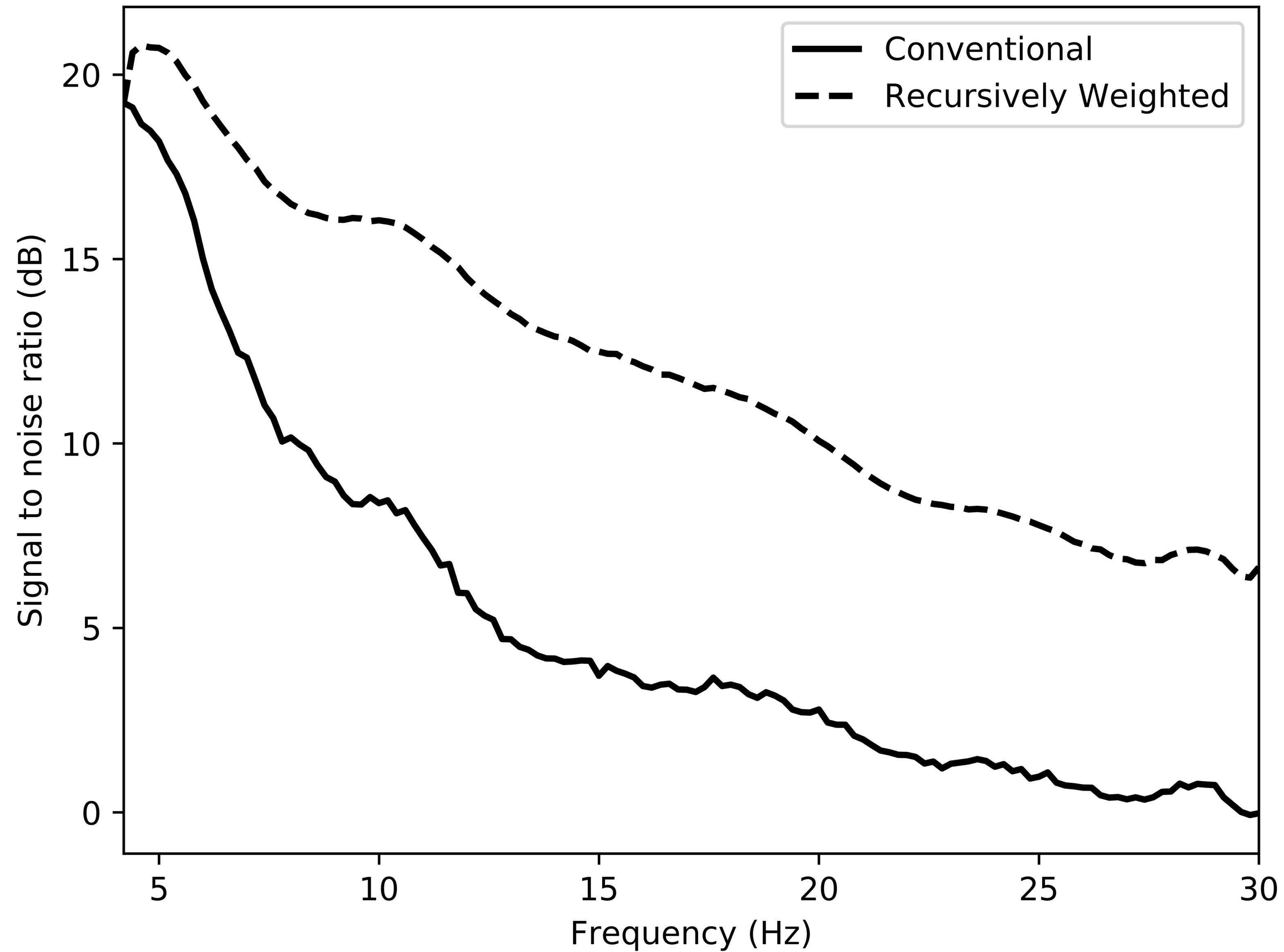
**Reconstruction w/ recursively weighted**



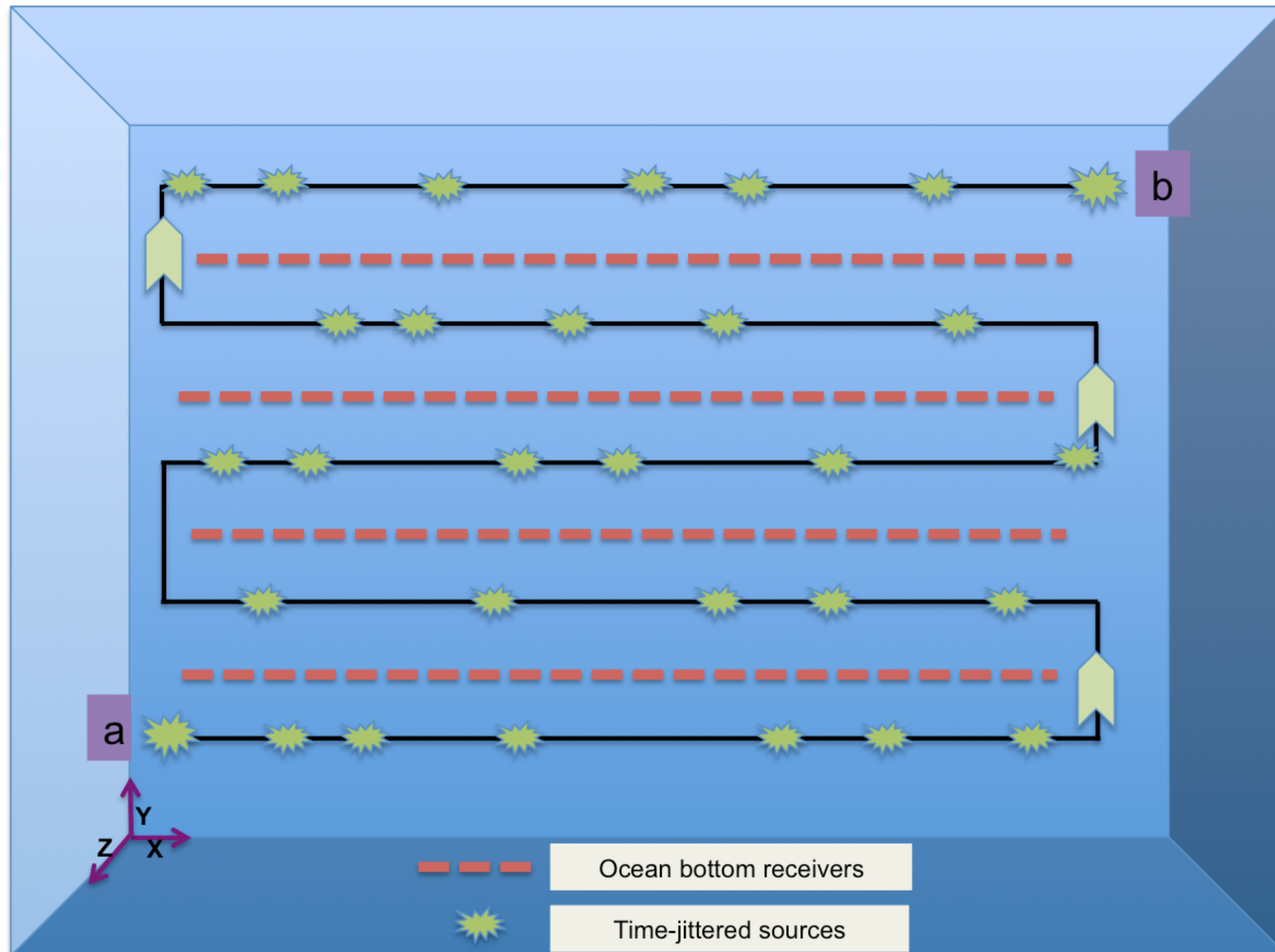
**Data residual**



# Signal to noise ratio comparison



# 5D Time-Jittered marine acquisition



## Objective

- ▶ Acquire blended seismic data using multiple sources
- ▶ Simultaneous separation and reconstruction of sources on dense grid

## Benefits

- ▶ Reduction in overall cost of acquiring dense seismic data



# Low-rank formulation

Restriction operator is non-separable

- ▶ combination of time-shifting and shot-jittered operator

$$\mathcal{A}(\cdot) = \mathbf{M}\mathbf{F}^H \mathcal{S}^H(\cdot)$$

$\mathbf{M}$  time-jittered operator

$\mathbf{F}^H$  inverse Fourier transform along frequency axis

$\mathcal{S}^H$  rank-revealing transform domain

Can't perform matrix-completion over independent frequencies

- ▶ reformulate low-rank factorization over temporal-frequency domain

$$\underset{\mathbf{L}, \mathbf{R}}{\text{minimize}} \quad \sum_j^{n_f} \frac{1}{2} \left\| \begin{bmatrix} \mathbf{L}_j \\ \mathbf{R}_j \end{bmatrix} \right\|_F^2 \quad \text{subject to} \quad \|\mathcal{A}(\mathbf{L}\mathbf{R}^H) - \mathbf{b}\|_2 \leq \epsilon$$

## Case Study: 3D BG Compass model

Temporal length

- ▶ 65 minutes

25 m flip-flop shooting

- ▶ source-sampling ranges from 25 m to 175 m
- ▶ effective 50 m source sampling for each airgun array
- ▶ acquired 400 sources

101 x 101 receivers (nr<sub>x</sub> x nr<sub>y</sub>)

Ricker wavelet with central frequency 15 Hz

Dimensions of deblended/interpolated data volume on 6.25 m grid

- ▶ 2501 x 101 x 101 x 40 x 40 (nt x nr<sub>x</sub> x nr<sub>y</sub> x ns<sub>x</sub> x ns<sub>y</sub>)



# Optimization Information

## Computational environment

- ▶ SENAI Yemoja cluster

## Parallelized over

- ▶ receivers and frequencies

## Computational information

- ▶ 200 iterations, 42 hours

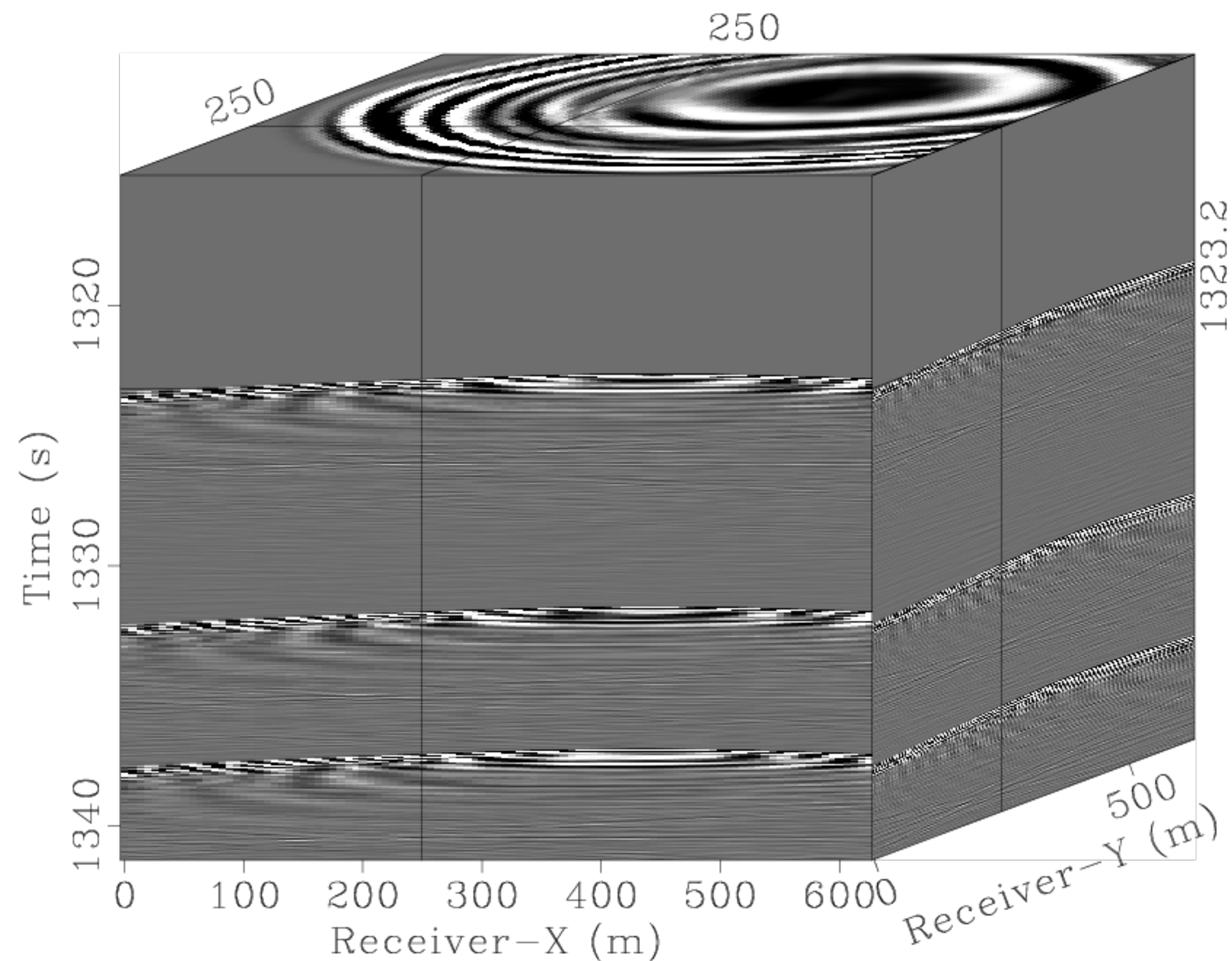
## Final volume

- ▶ 13 GB (98% compression)



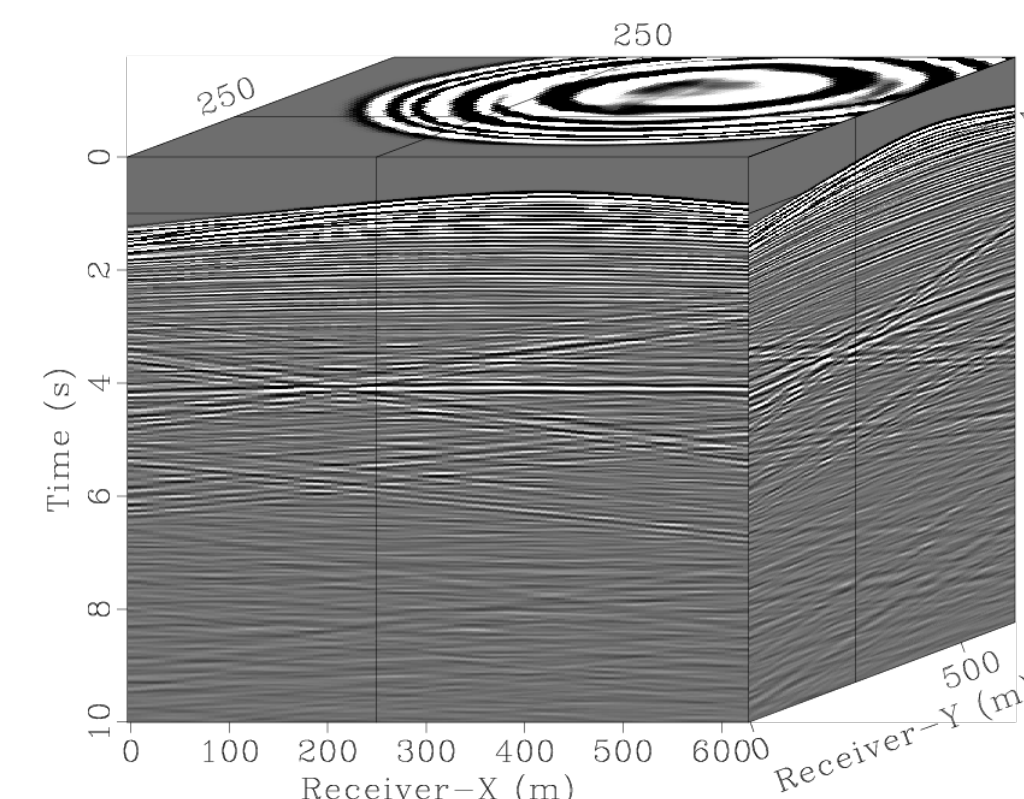
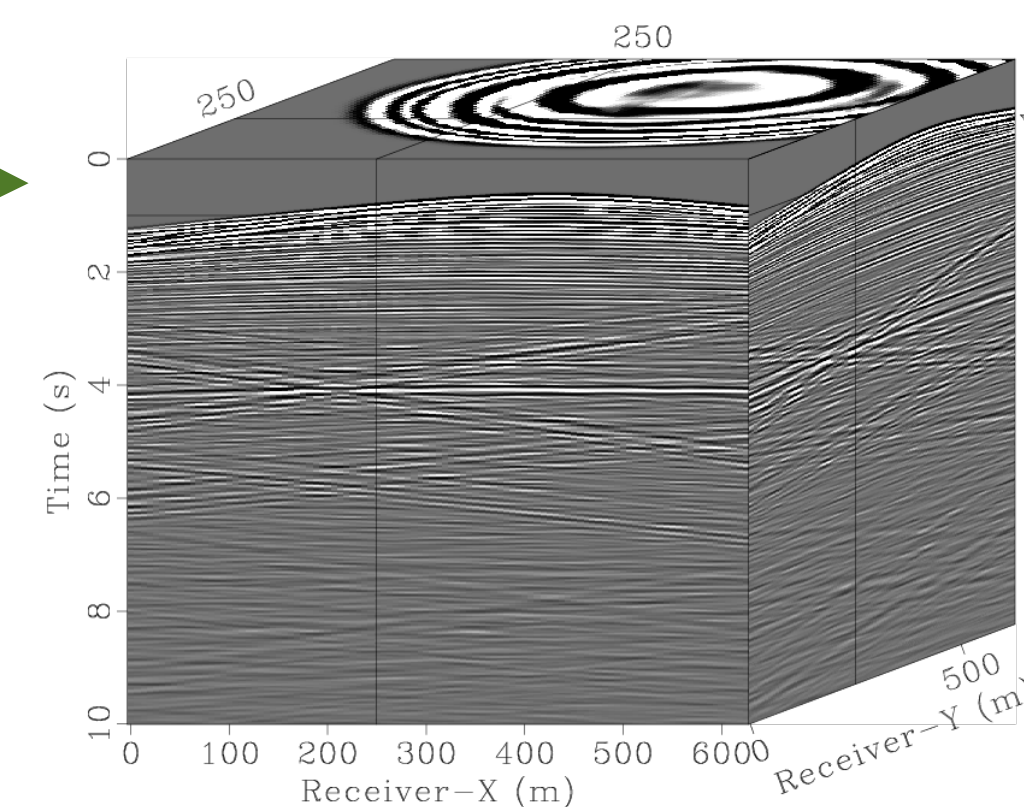
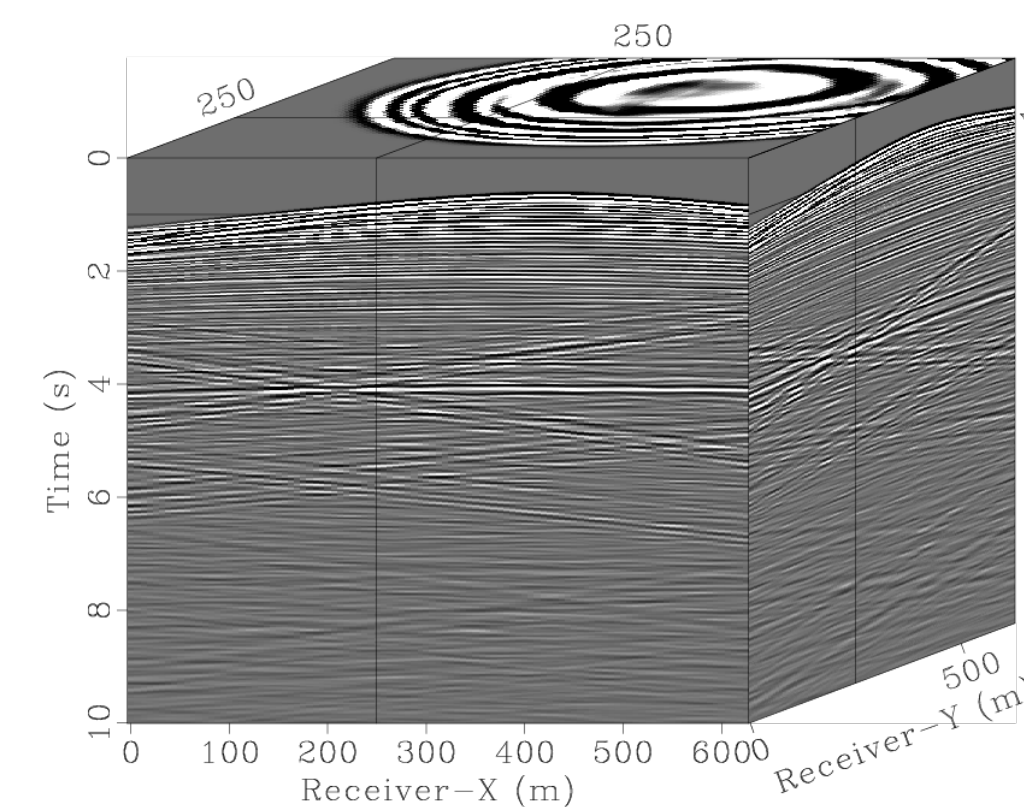
# 5D Time-Jittered marine acquisition

Blended data @ 25 m flip-flop  
(overlapping & missing shots)



Recovery  
→  
SNR = 21 dB

Separation + Interpolation  
(recovered grid @ 6.25m)





## Conclusions

Low-rank matrix factorization based wavefield reconstruction method

- ▶ performs poorly at higher frequencies
- ▶ recursively weighted method improves reconstruction at higher frequencies
- ▶ by including prior information from lower frequencies

Scaling for full azimuth industry-size data is achieved via

- ▶ shifting the weights from objective to data-misfit to avoid expensive projections
- ▶ using strategies of alternating minimization and decoupling
- ▶ parallelizing over rows of low-rank factors
- ▶ using low-rank factors avoiding expensive SVD of full data

Factorized based time-jittered acquisition

- ▶ scalable for large scale 5D data
- ▶ by using parallel computation
- ▶ achieves data compression by saving low-rank factors

## Future work

In recursively weighted framework

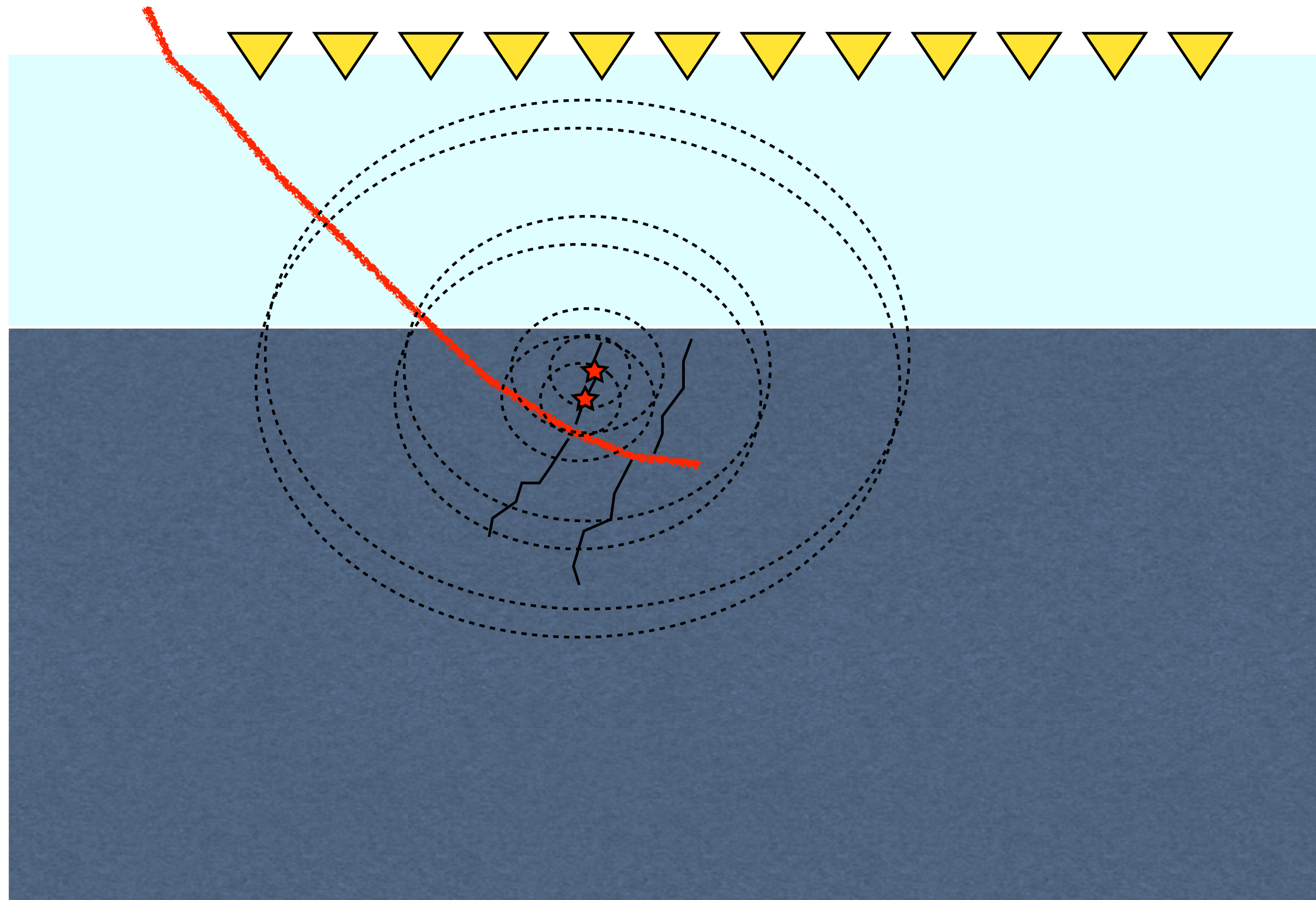
- ▶ include smaller weights
- ▶ for large scale data

In time-jittered acquisition

- ▶ include weights
- ▶ to further improve reconstruction quality



# Unconventional Reservoir



## Objectives

- ▶ detection of microseismic events in space and time
- ▶ estimation of source-time function

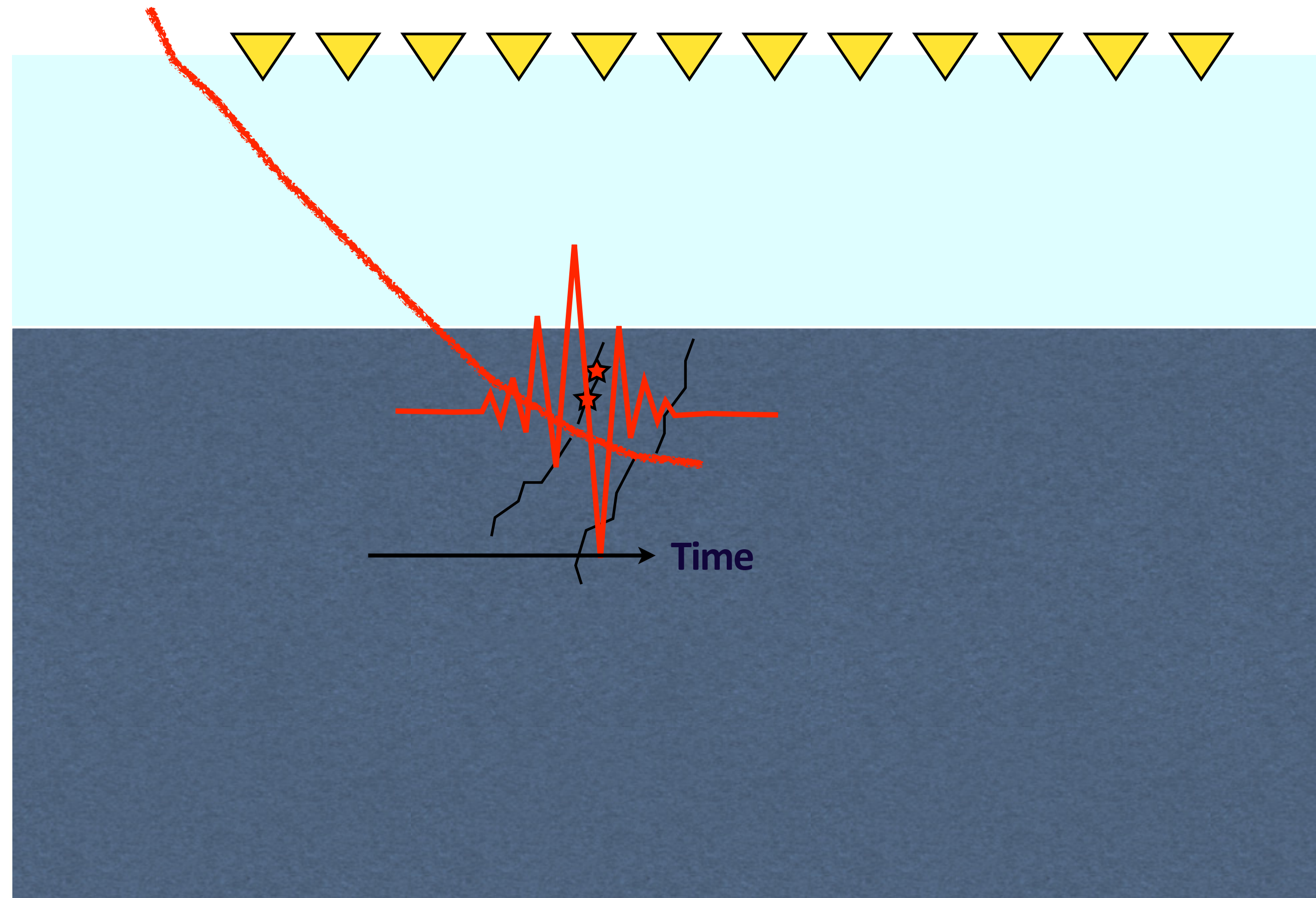
## Key Contributions: Chapters 4 & 5

### Sparsity-promoting microseismic estimation

- ▶ Detection of closely spaced microseismic sources from noisy data
- ▶ Estimation of associated source-time function with correct amplitude



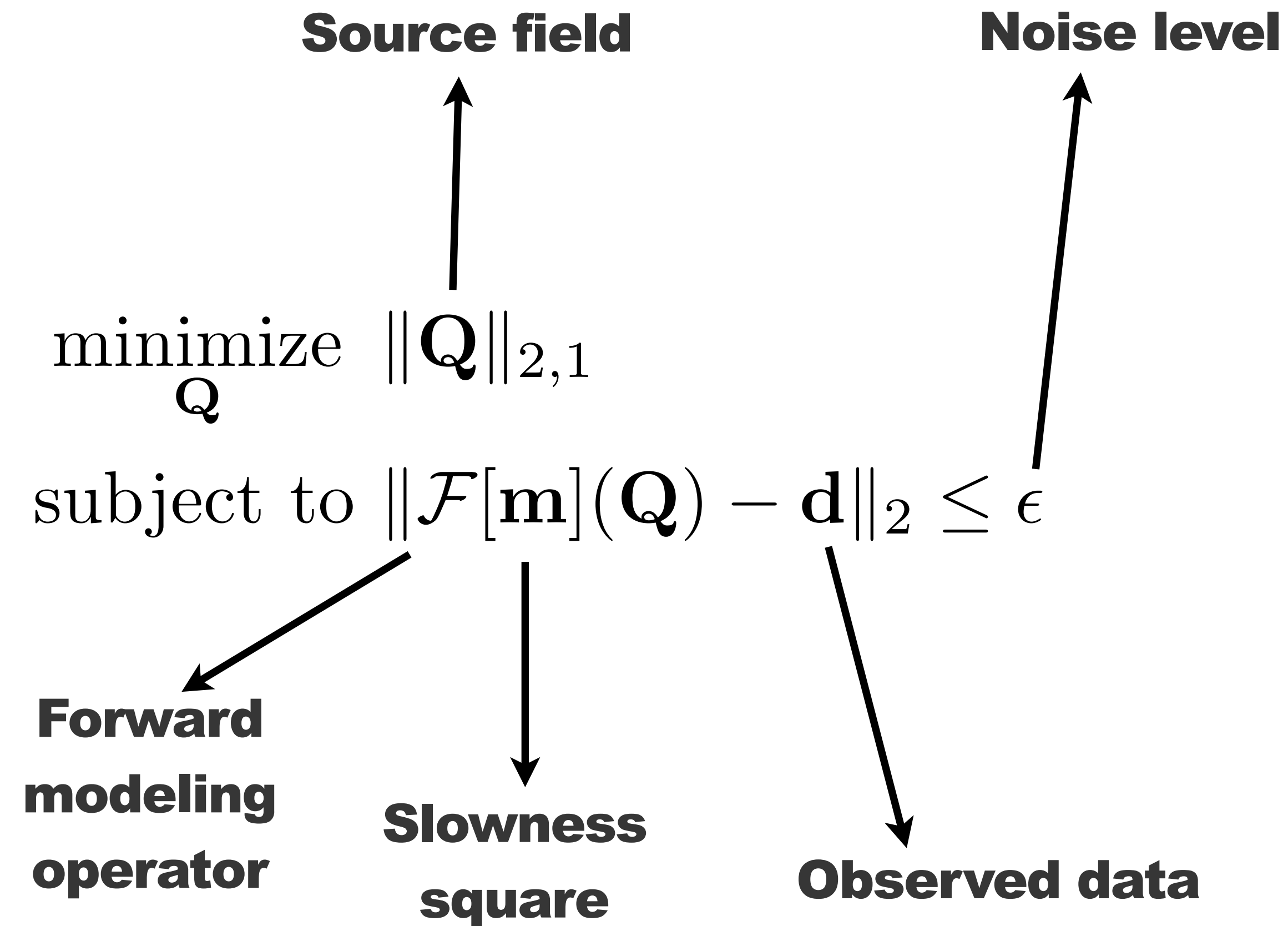
# Proposed method w/ sparsity promotion



## Assumptions

- ▶ localized in space
- ▶ finite energy along time

## Proposed method w/ sparsity promotion



$$Q \in \mathbb{R}^{n_x \times n_t}$$

$n_x$ : number of grid points

$n_t$ : number of time samples

Similar to classic Basis pursuit denoising (BPDN)



## Solving w/ Linearized Bregman

$$\begin{aligned} & \underset{\mathbf{Q}}{\text{minimize}} \quad \|\mathbf{Q}\|_{2,1} + \frac{1}{2\mu} \|\mathbf{Q}\|_F^2 \\ & \text{subject to} \quad \|\mathcal{F}[\mathbf{m}](\mathbf{Q}) - \mathbf{d}\|_2 \leq \epsilon \end{aligned}$$

\*where  $\|\cdot\|_F$  is the Frobenius norm

- ▶ Recent successful application to seismic imaging problem
- ▶ Three-step algorithm simple to implement
- ▶ Choice of  $\mu$  controls the trade off between sparsity and the Frobenius norm
- ▶  $\mu \uparrow \infty$  corresponds to solving original BPDN problem

# Linearized Bregman algorithm

1. **Data  $\mathbf{d}$ , slowness square  $\mathbf{m}$**  //Input
2. **for**  $k = 0, 1, \dots$
3.  $\mathbf{V}_k = \mathcal{F}^\top[\mathbf{m}](\Pi_\epsilon(\mathcal{F}[\mathbf{m}](\mathbf{Q}_k) - \mathbf{d}))$  //adjoint solve
4.  $\mathbf{Z}_{k+1} = \mathbf{Z}_k - t_k \mathbf{V}_k$  //auxiliary variable update
5.  $\mathbf{Q}_{k+1} = \text{Prox}_{\mu\ell_{2,1}}(\mathbf{Z}_{k+1})$  //sparsity promotion
6. **end**
7.  $\mathbf{I}(\mathbf{x}) = \sum_t |\mathbf{Q}(\mathbf{x}, t)|$  //Intensity plot

\*  $\Pi_\epsilon(\mathbf{x}) = \max\{0, 1 - \frac{\epsilon}{\|\mathbf{x}\|}\} \cdot (\mathbf{x})$  the projection on to  $\ell_2$  norm ball

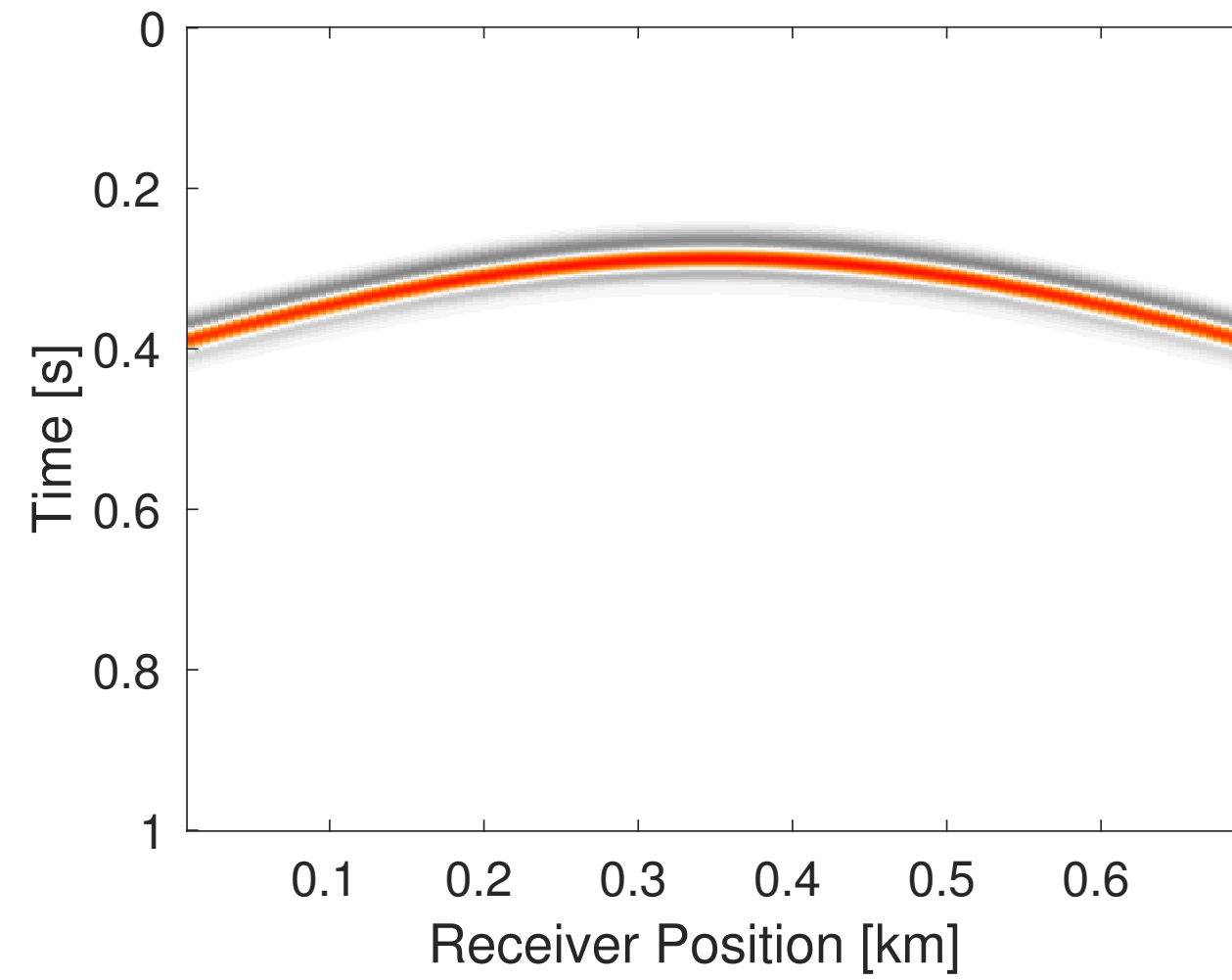
\*where  $t_k = \frac{\|\mathcal{F}[\mathbf{m}](\mathbf{Q}_k) - \mathbf{d}\|^2}{\|\mathcal{F}^\top[\mathbf{m}](\mathcal{F}[\mathbf{m}](\mathbf{Q}_k) - \mathbf{d})\|^2}$  is the dynamic step length

\*  $\text{Prox}_{\mu\ell_{2,1}}(\mathbf{C}) := \arg \min_{\mathbf{B}} \|\mathbf{B}\|_{2,1} + \frac{1}{2\mu} \|\mathbf{C} - \mathbf{B}\|_F^2$  is the proximal mapping of the  $\ell_{2,1}$  norm

► **Source location:** estimated as outlier in intensity plot

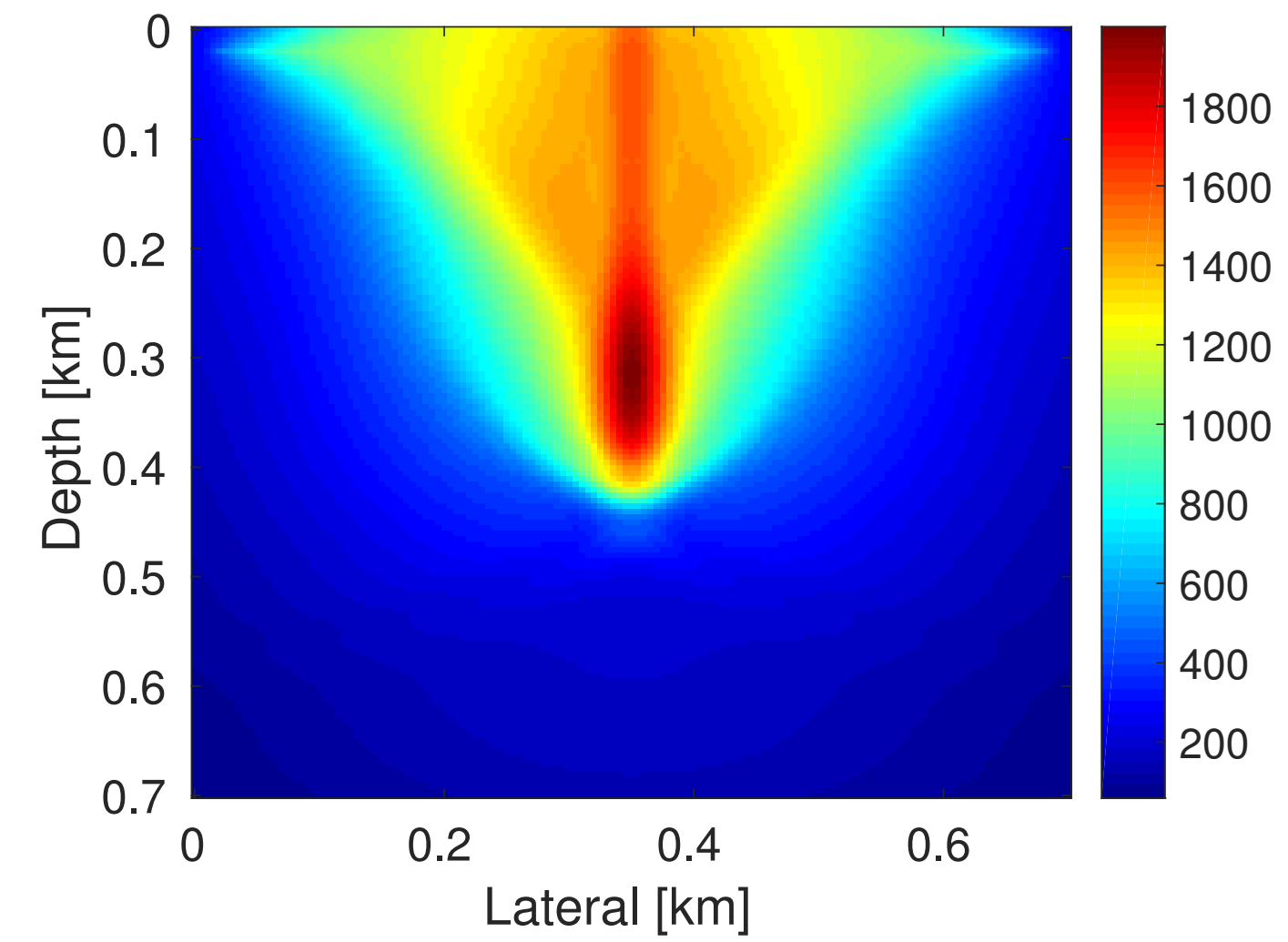
► **Source-time function:** temporal variation of wavefield at estimated source location





$$\mathbf{V}_1 = \mathcal{F}^\top[\mathbf{m}](\Pi_\epsilon(\mathcal{F}[\mathbf{m}](\mathbf{Q}_0) - \mathbf{d}))$$

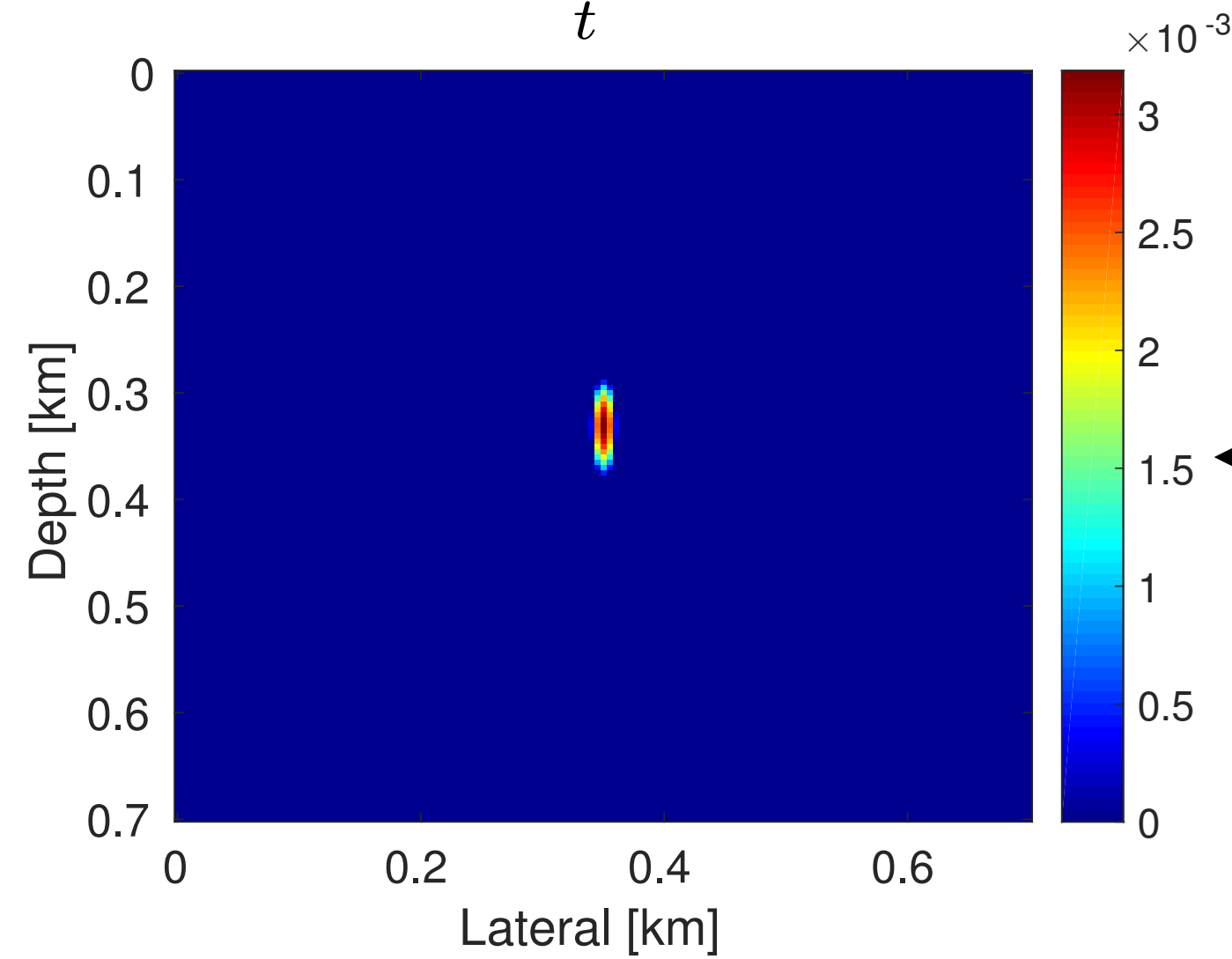
**Adjoint solve**



**Auxiliary variable  
update**

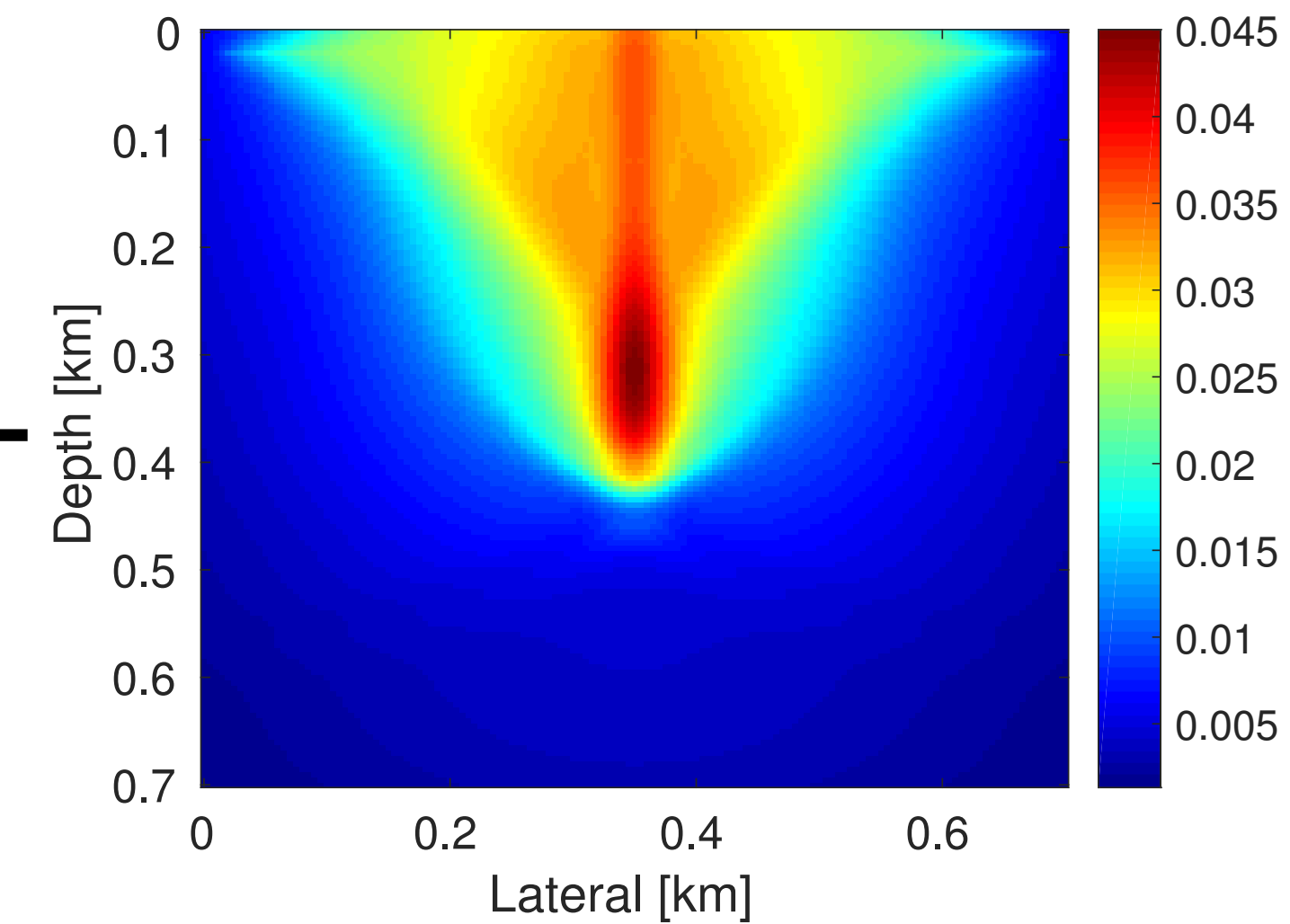
$$\mathbf{Z}_1 = \mathbf{Z}_0 - t_1 \mathbf{V}_1$$

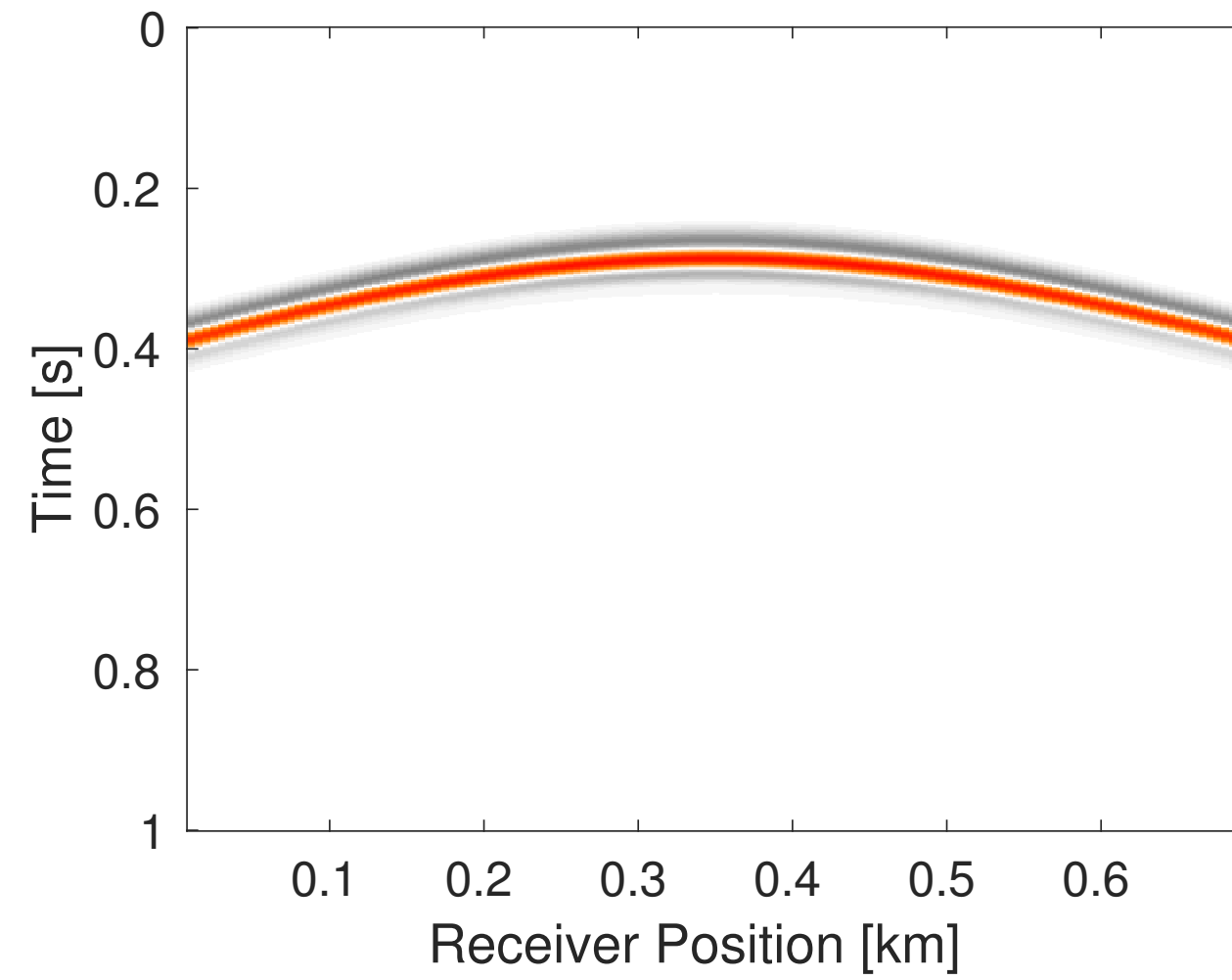
$$\mathbf{I}(\mathbf{x}) = \sum_t | \mathbf{Q}_1(\mathbf{x}, t) |$$



$$\mathbf{Q}_1 = \text{Prox}_{\mu\ell_{2,1}}(\mathbf{Z}_1)$$

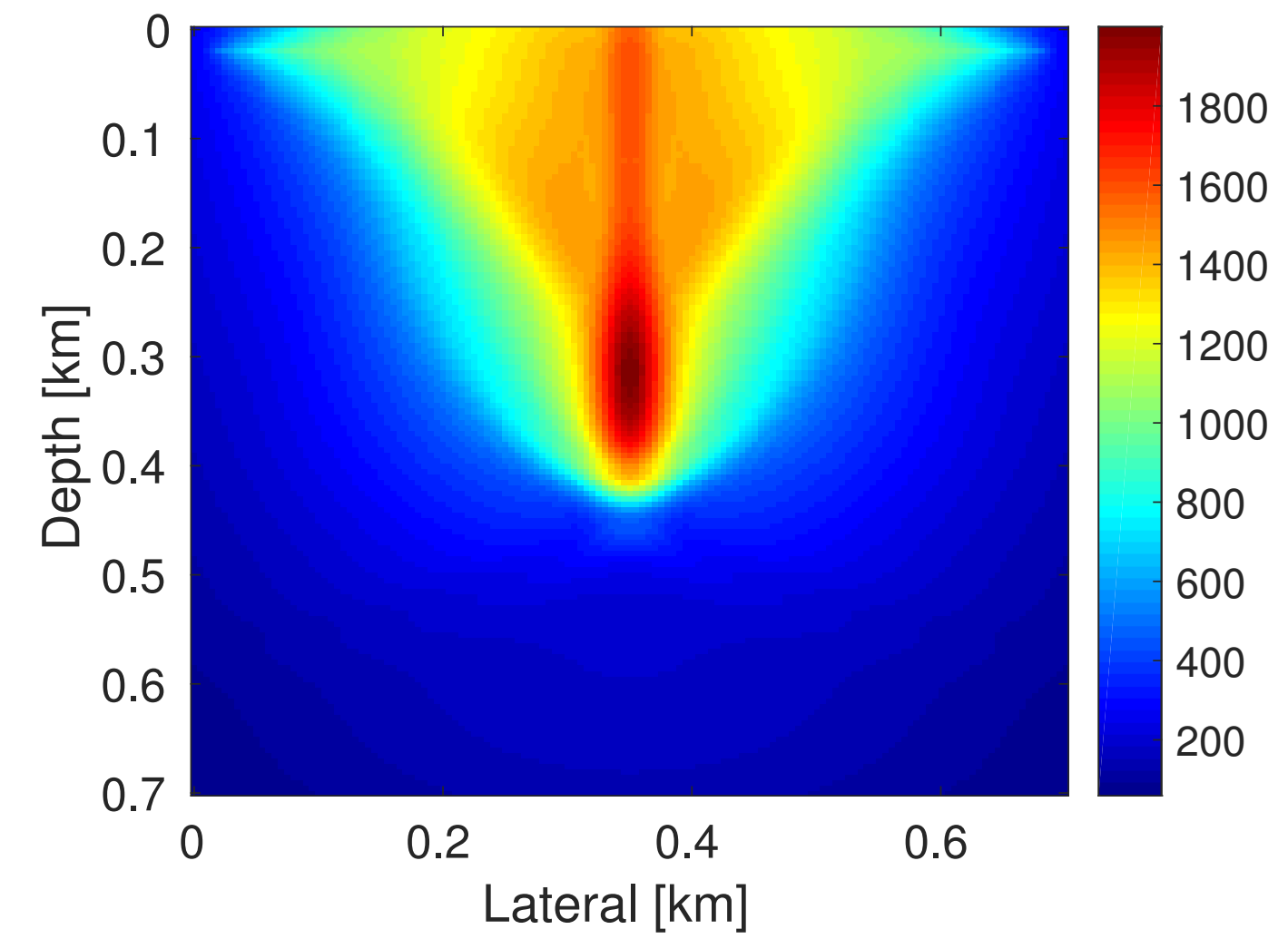
**Sparsity promotion**





$$\mathbf{V}_1 = \mathcal{F}^\top[\mathbf{m}](\Pi_\epsilon(\mathcal{F}[\mathbf{m}](\mathbf{Q}_0) - \mathbf{d}))$$

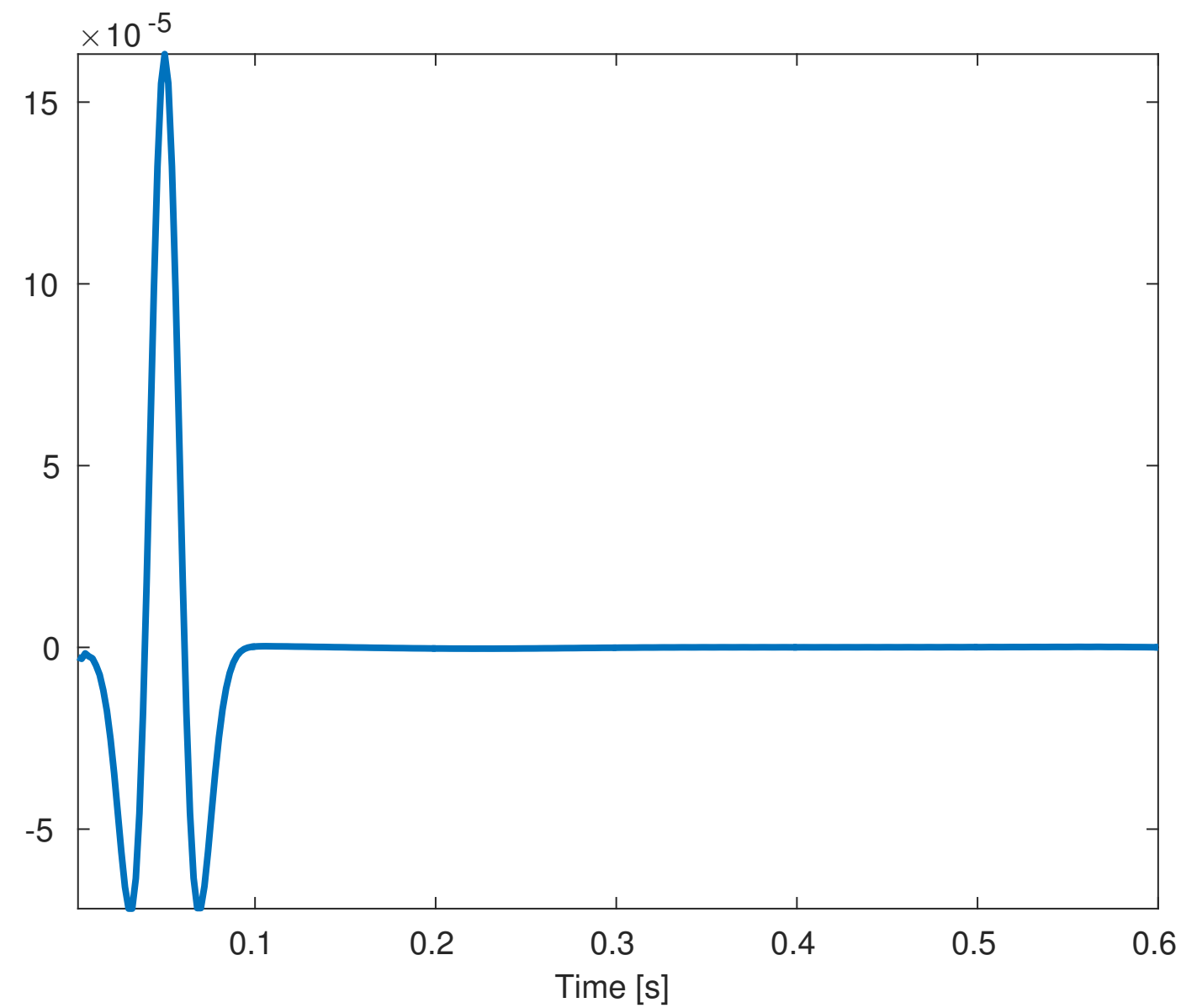
**Adjoint solve**



**Auxiliary variable  
update**

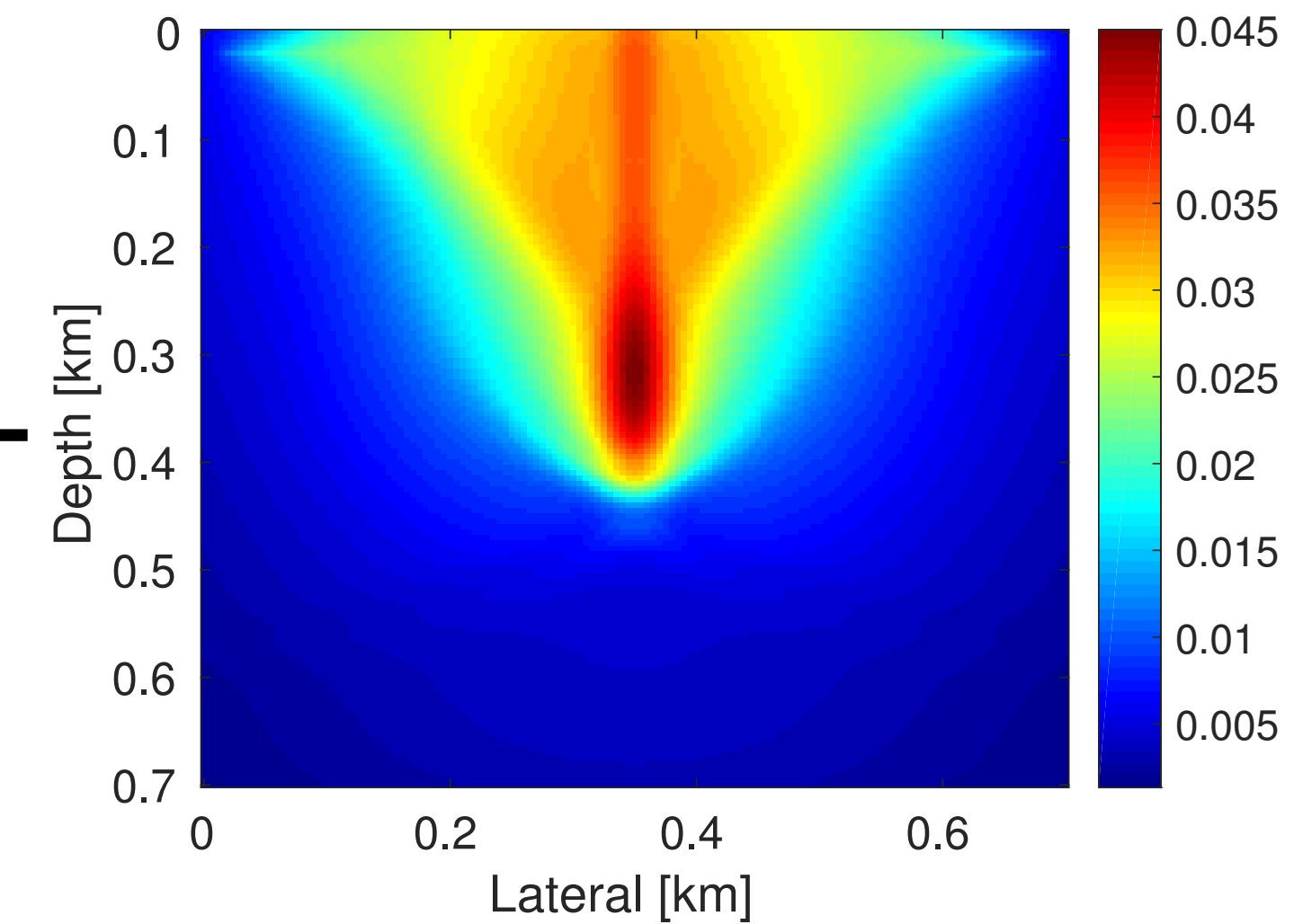
$$\mathbf{Z}_1 = \mathbf{Z}_0 - t_1 \mathbf{V}_1$$

**Source-time function**



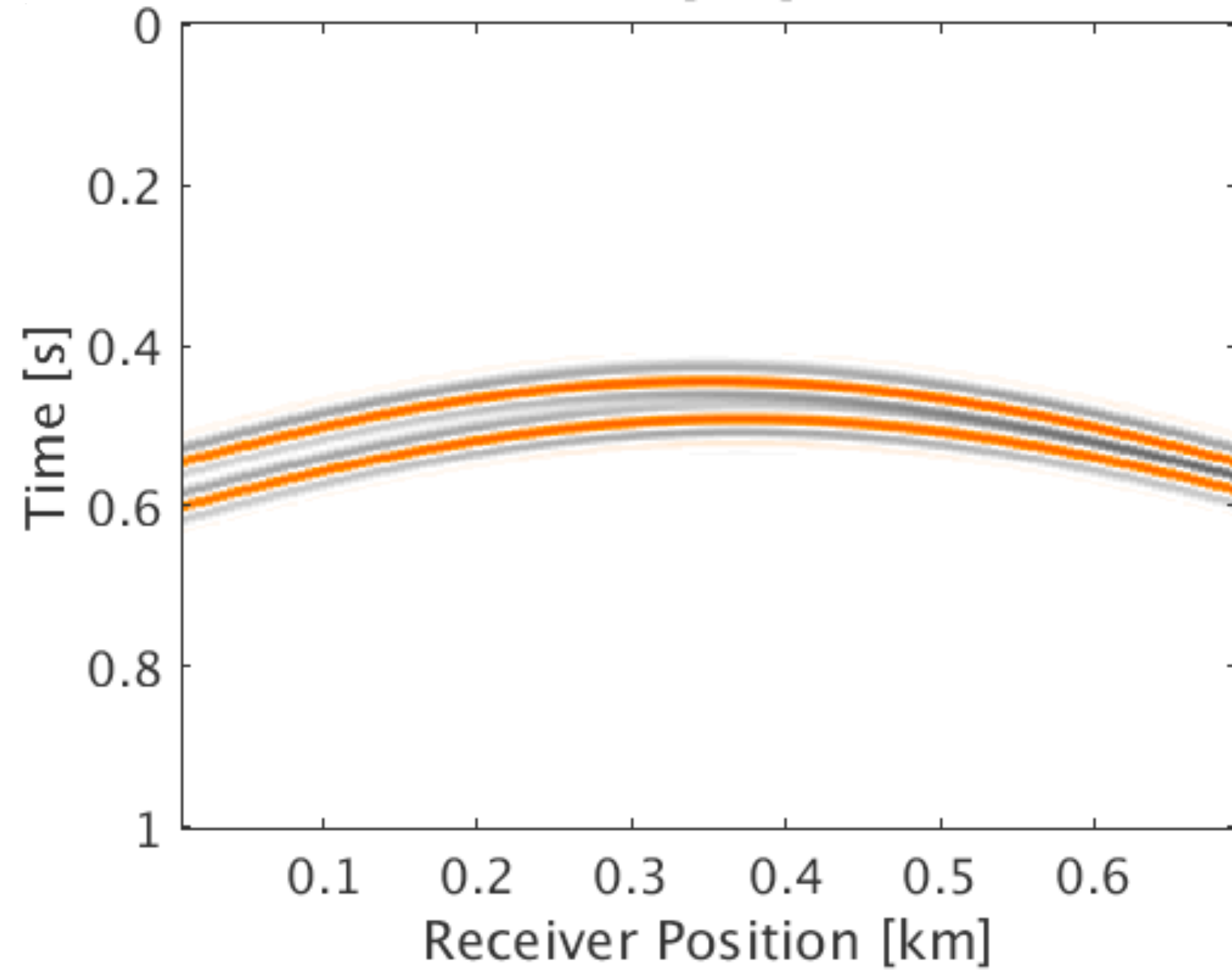
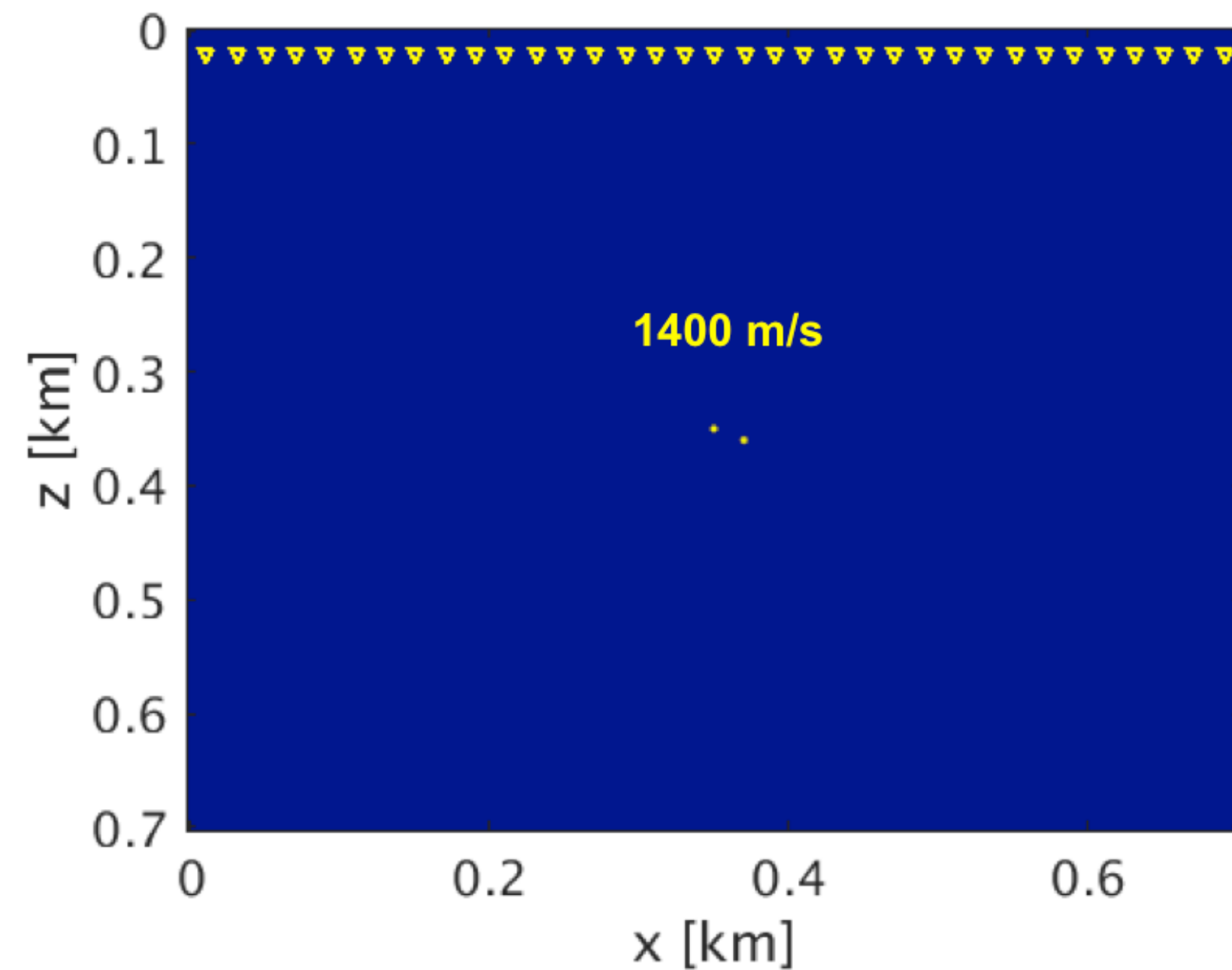
$$\mathbf{Q}_1 = \text{Prox}_{\mu\ell_{2,1}}(\mathbf{Z}_1)$$

**Sparsity promotion**





# Case study: two nearby sources



## Modeling information:

**Model size:** 0.7 km x 0.7 km

**Grid spacing:** 5m

**Receiver spacing:** 10m

**Receiver depth:** 20m

**Fixed spread:** 0.69km

**Sampling interval:** 2 ms

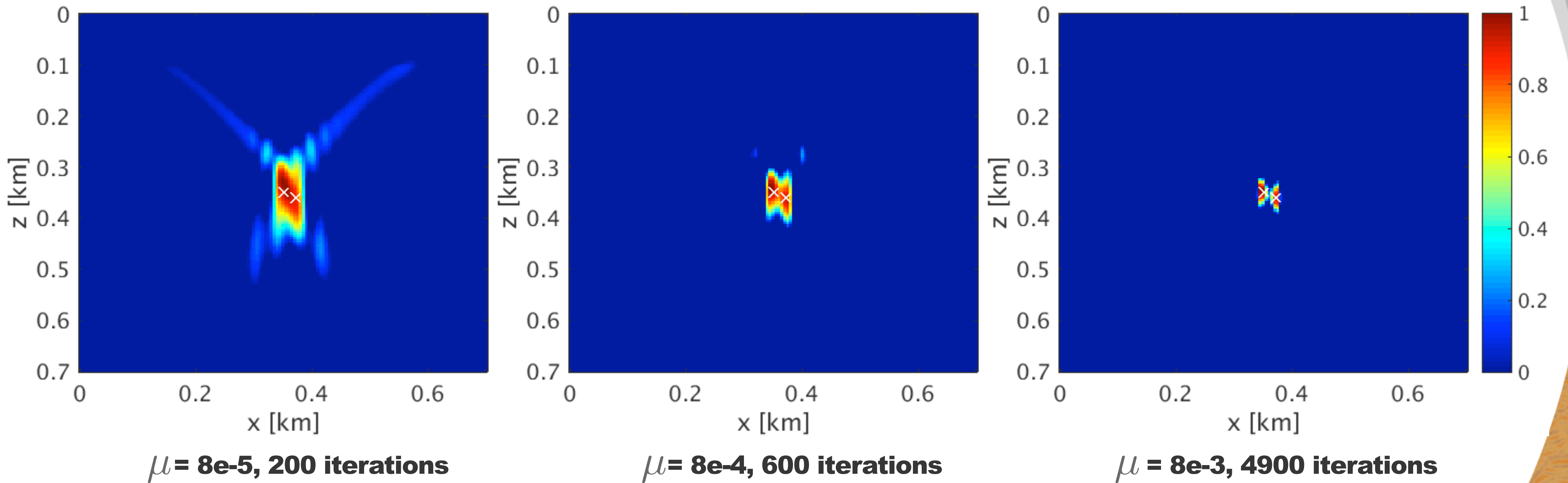
**Recording length:** 1s

**Peak frequency :** 30 Hz

**Dominant wavelength:** 46 m

**Source separation:** 22 m

# Results w/ different threshold parameters





## Acceleration with quasi-Newton: Algorithm

1. **Data  $\mathbf{d}$ , slowness square  $\mathbf{m}$ , number of iterations  $k$**  //Input
  2. **Initialize dual variable  $\mathbf{y} = 10^{-3}\mathbf{d}$**
  3.  $\hat{\mathbf{y}} = \text{L-BFGS}(f(\mathbf{y}), g(\mathbf{y}), \mathbf{y}, k)$  //Dual solution
- where  $f(\mathbf{y}) = \Psi(\mathbf{y}) - \epsilon \|\mathbf{y}\|_2$  //L-BFGS objective  
 and  $g(\mathbf{y}) = \Psi'(\mathbf{y}) - \epsilon \mathbf{y} / \|\mathbf{y}\|_2$  //L-BFGS gradient
4.  $\hat{\mathbf{Q}} = \text{Prox}_{\mu\ell_{2,1}}(\mu\mathcal{F}[\mathbf{m}]^\top(\hat{\mathbf{y}}))$  //Primal solution
  5.  $\mathbf{I}(\mathbf{x}) = \sum_t |\hat{\mathbf{Q}}(\mathbf{x}, t)|$  //Intensity plot
- lives in much smaller space
- ▶ dimensions equals that of observed data
  - ▶ better approximation of inverse Hessian by storing more and more dual variable updates

\*where  $\Psi(\mathbf{y}) = \min_{\mathbf{Q}} \|\mathbf{Q}\|_{2,1} + \frac{1}{2\mu} \|\mathbf{Q}\|_F - \mathbf{y}^\top (\mathcal{F}[\mathbf{m}](\mathbf{Q}) - \mathbf{d})$

\*  $\Psi'(\mathbf{y}) = \mathbf{d} - \mathcal{F}[\mathbf{m}](\text{Prox}_{\mu\ell_{2,1}}(\mu\mathcal{F}[\mathbf{m}]^\top(\mathbf{y})))$  is the gradient of  $\Psi(\mathbf{y})$

## Further acceleration w/ 2D Preconditioning

Each iteration of L-BFGS requires solving at least one

- ▶ wave equation and
- ▶ its adjoint

Requires further reduction in the total number of iterations due to:

- ▶ the problem size and
- ▶ computational costs

Left preconditioner:

- ▶ reduces the condition number of 2D forward modeling operator  $\mathcal{F}$
- ▶ accelerates the convergence



## Further acceleration w/ 2D Preconditioning

In 2D, a point source implicitly assumes

- ▶ a line source
- ▶ extending infinitely in the out of plane direction

This causes wavefields to have:

- ▶ amplitude and
- ▶ phase differ from the wavefields of a true point source

We introduce:

- ▶ a symmetric half differentiation correction along time
- ▶ corrects for the amplitude and phase of 2D wavefield
- ▶ which acts as a left preconditioner

## Modified problem w/ 2D Preconditioning

$$\begin{aligned} & \underset{\mathbf{Q}}{\text{minimize}} \quad \|\mathbf{Q}\|_{2,1} + \frac{1}{2\mu} \|\mathbf{Q}\|_F^2 \\ & \text{subject to} \quad \|\mathcal{M}_L \mathcal{F}[\mathbf{m}](\mathbf{Q}) - \mathcal{M}_L \mathbf{d}\|_2 \leq \gamma \end{aligned}$$

\*with  $\mathcal{M}_L := \partial_{|t|}^{1/2}$  is the half differentiation correction

\*where  $\partial_{|t|}^{1/2} = \mathbf{F}^{-1} |\omega|^{1/2} \mathbf{F}$

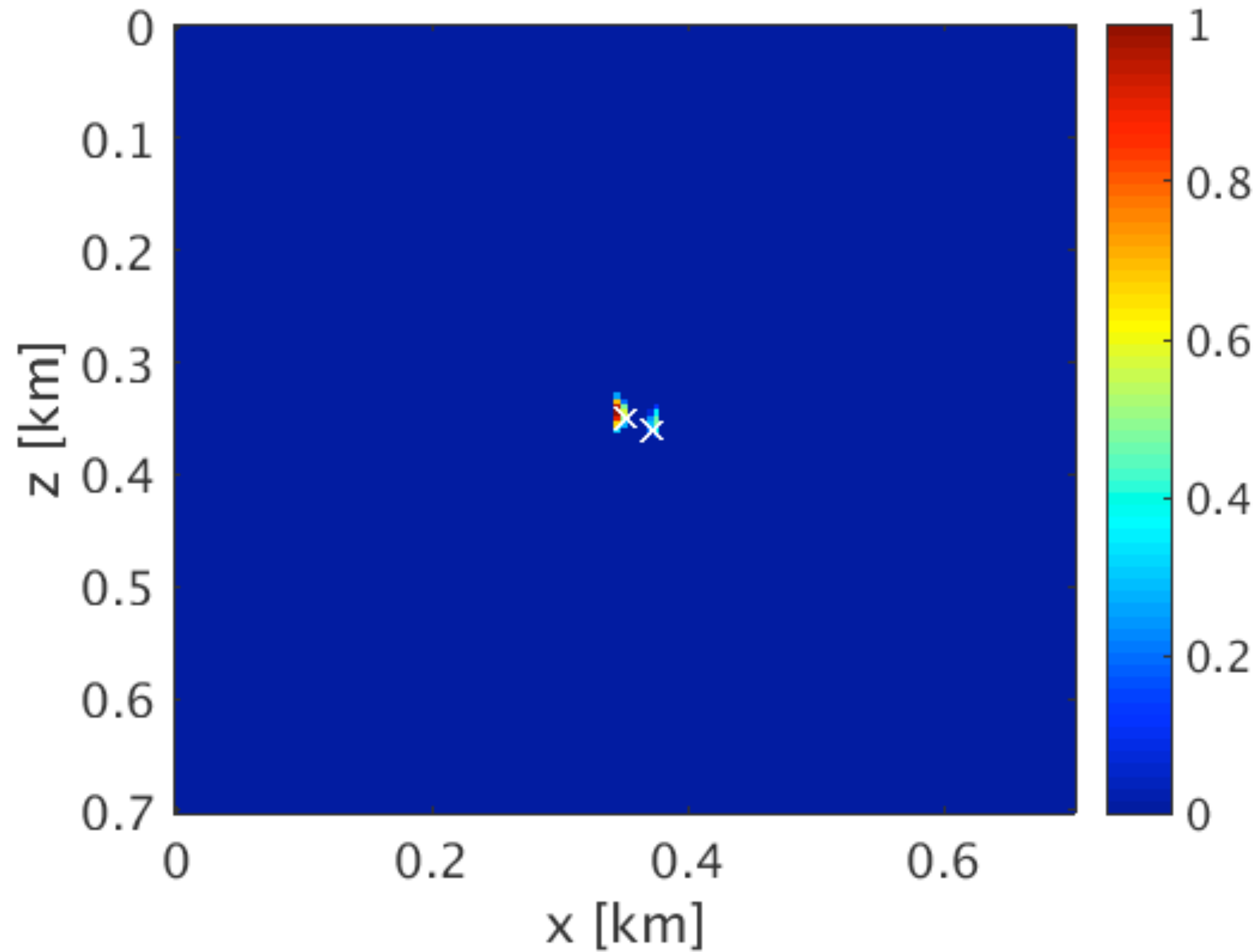
\* $\mathbf{F}$  is the Fourier transform and  $\omega$  is the frequency

\* $\gamma$  is the noise level

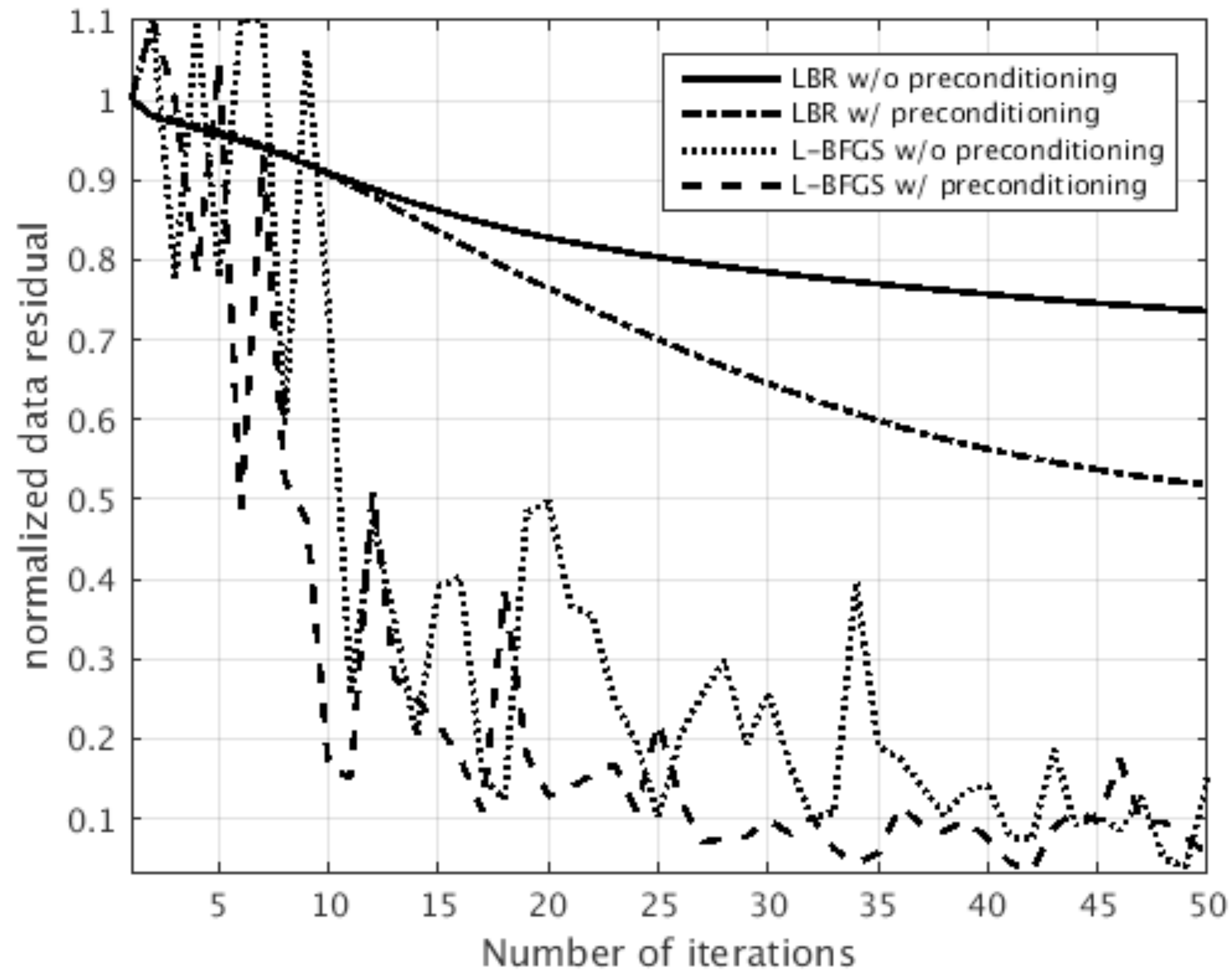


# Estimated location

$w/\mu = 8e-2$  and 10 iterations



# Convergence comparison: LBR vs L-BFGS



Convergence comparison

► Using same value of  $\mu$

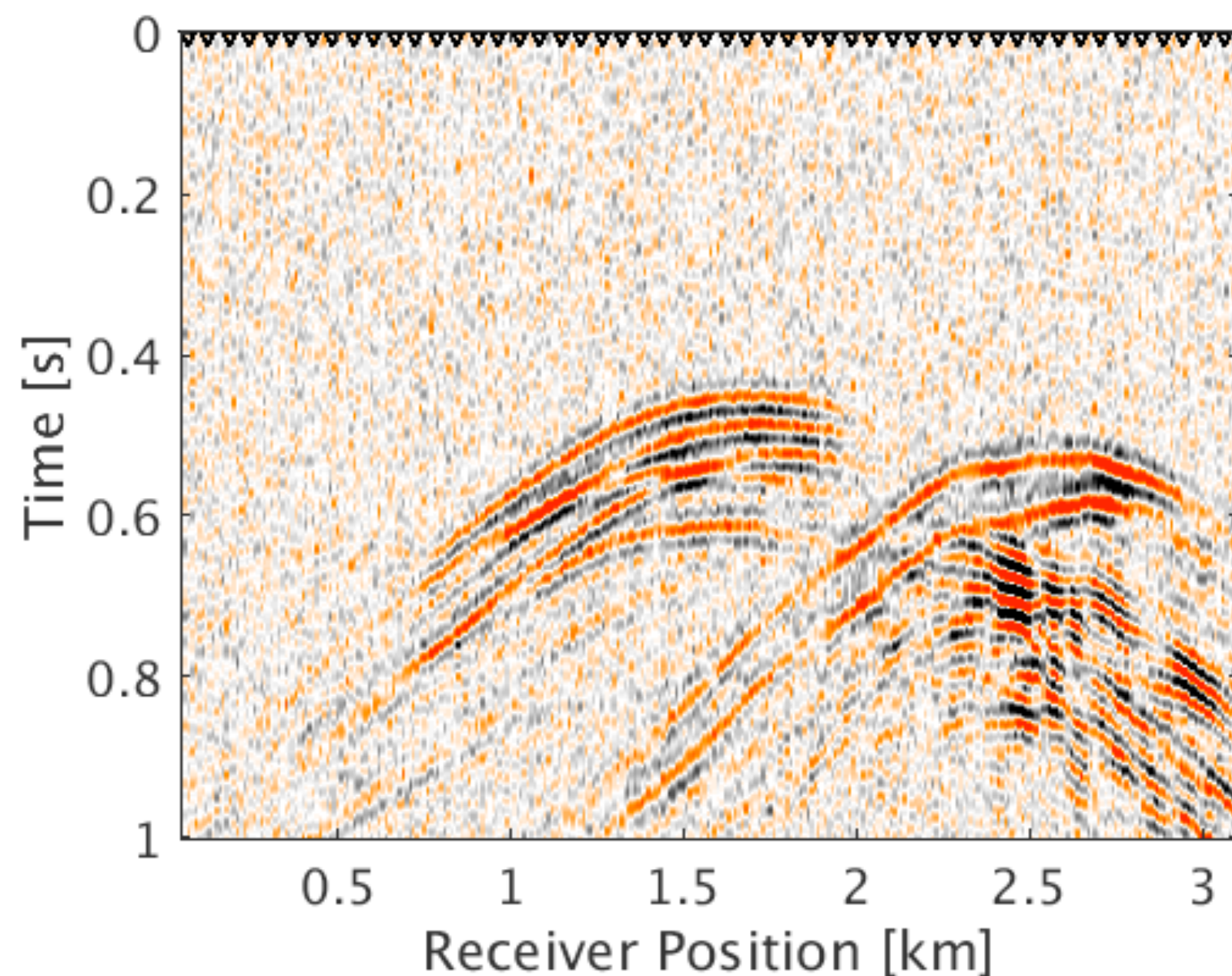
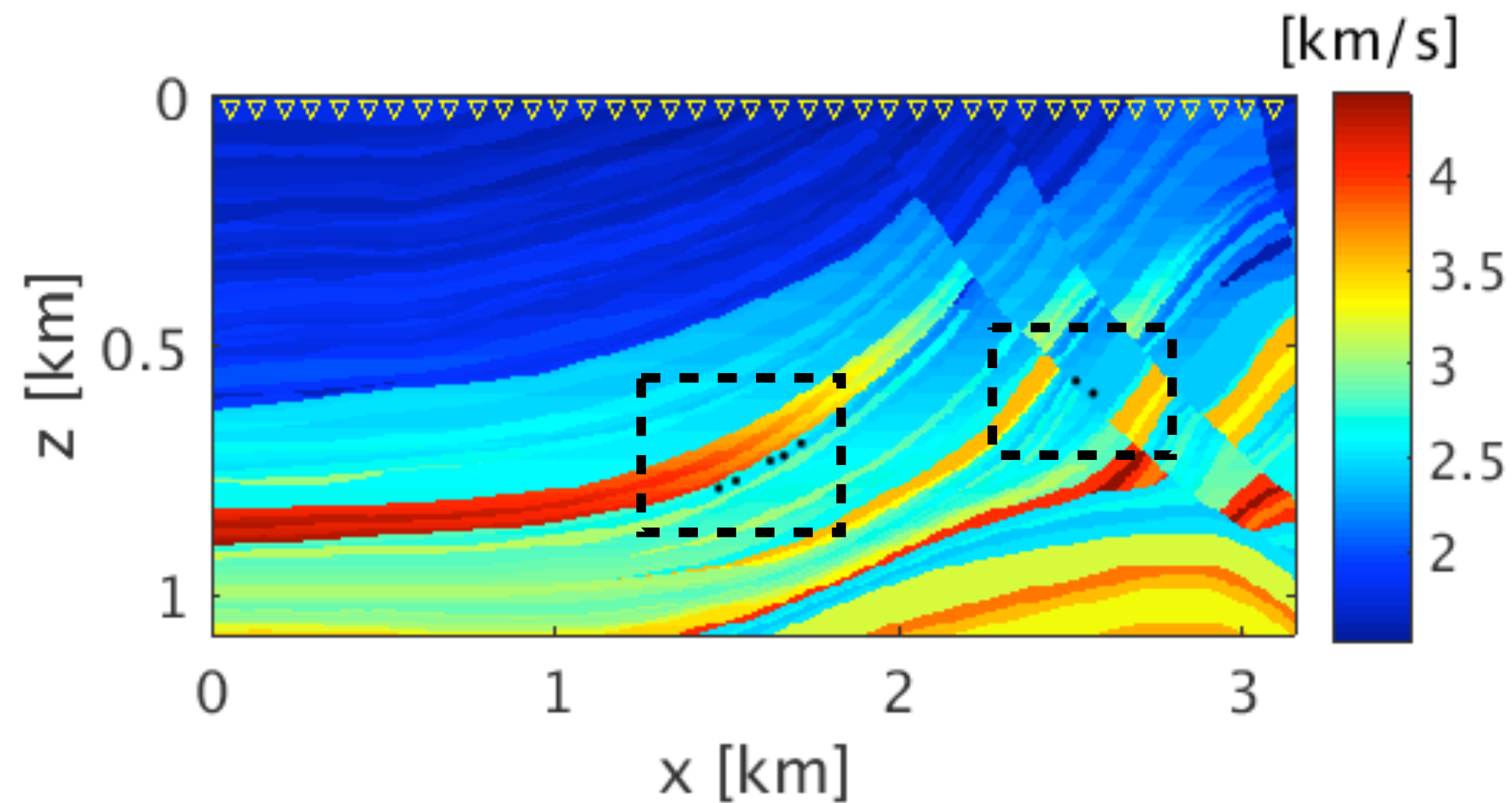
Improvement in convergence with

► Dual formulation and

► 2D Preconditioning



# Multiple source cluster experiment in Marmousi model



► Contaminated with 5 to 45 Hz random noise

► SNR = 3.5 dB

## Modeling information:

**Model size:** 3.15 km x 1.08 km

**Grid spacing:** 5 m

**Total number of sources:** 7

**Peak frequency :** 22 Hz, 25 Hz & 30 Hz

**Receiver spacing:** 10m

**Receiver depth:** 20m

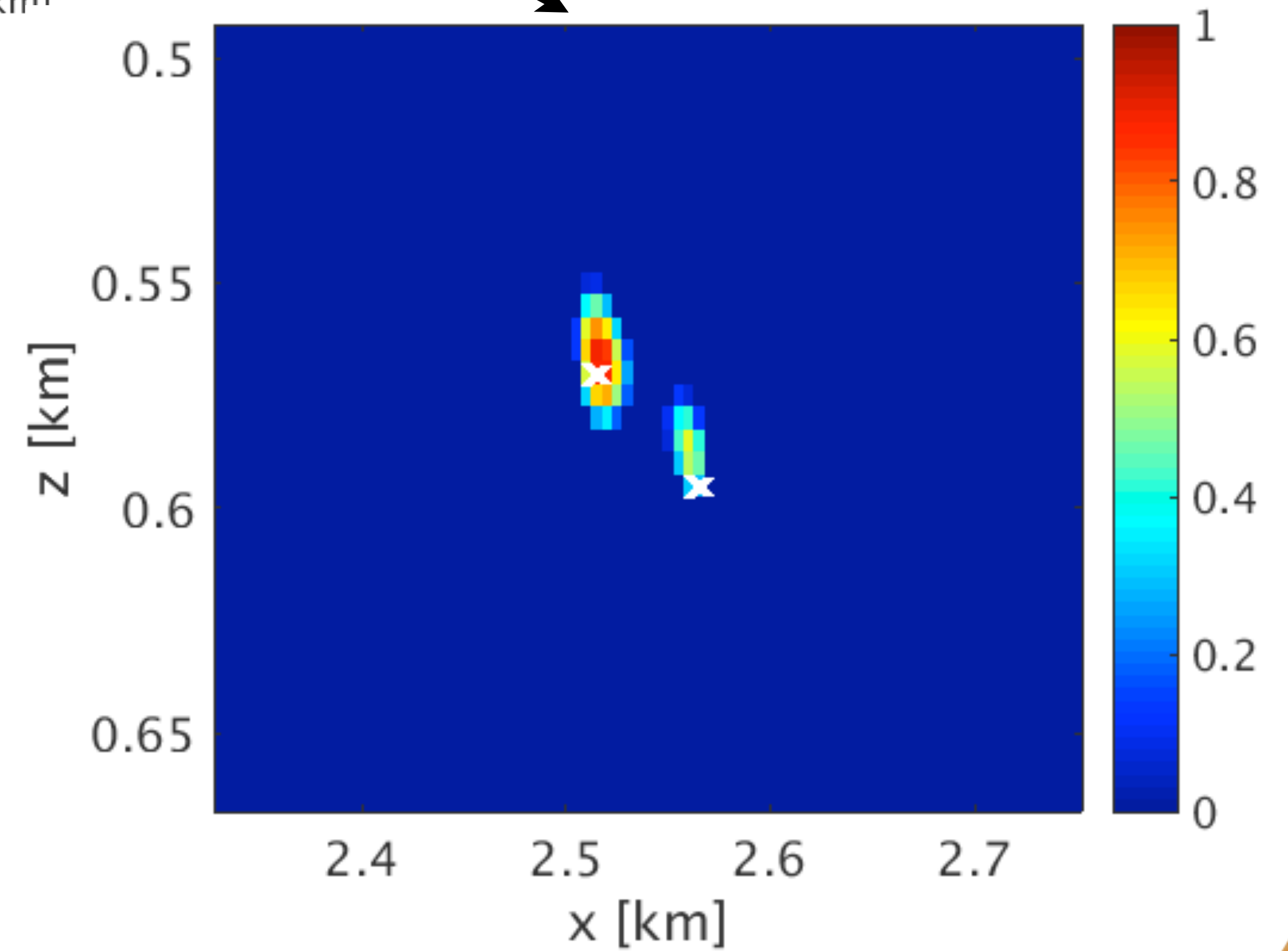
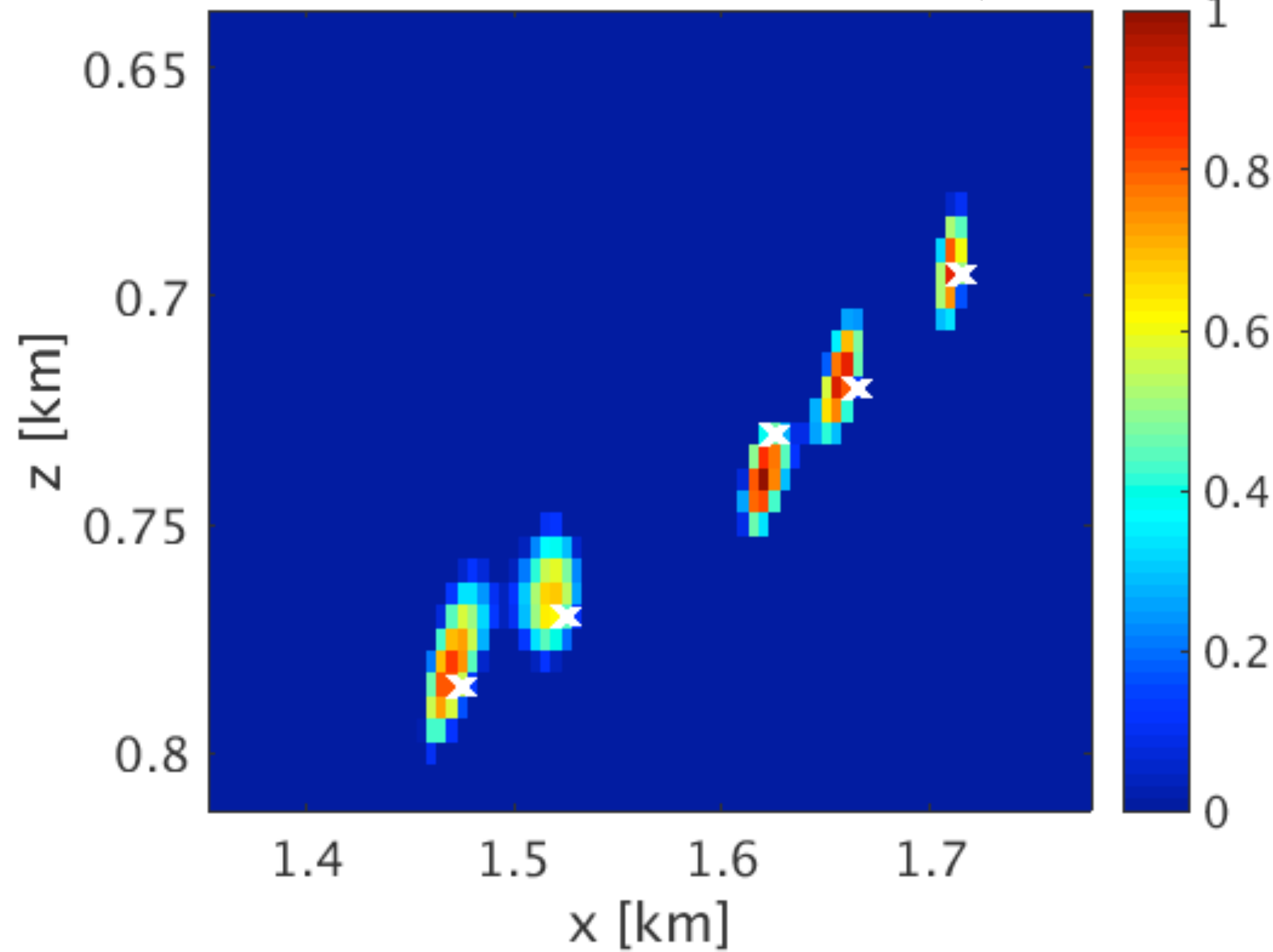
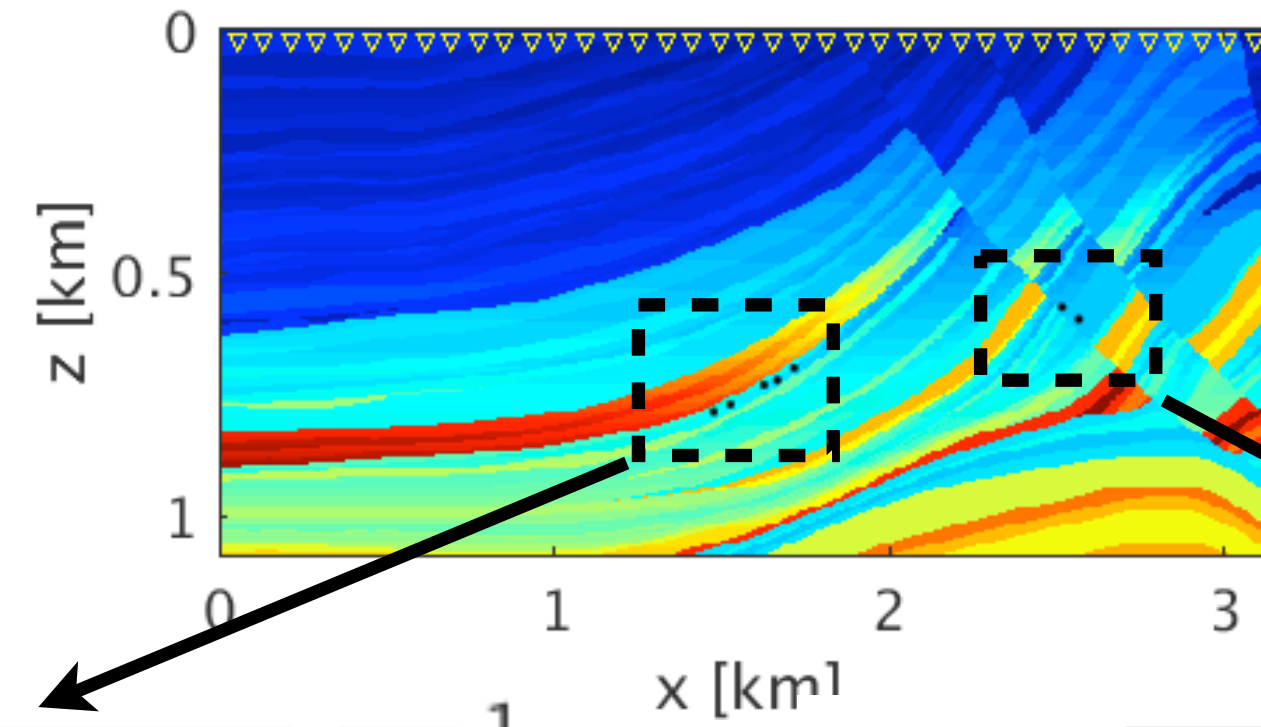
**Sampling interval:** 0.5 ms

**Recording length:** 1 s

**Free surface:** No

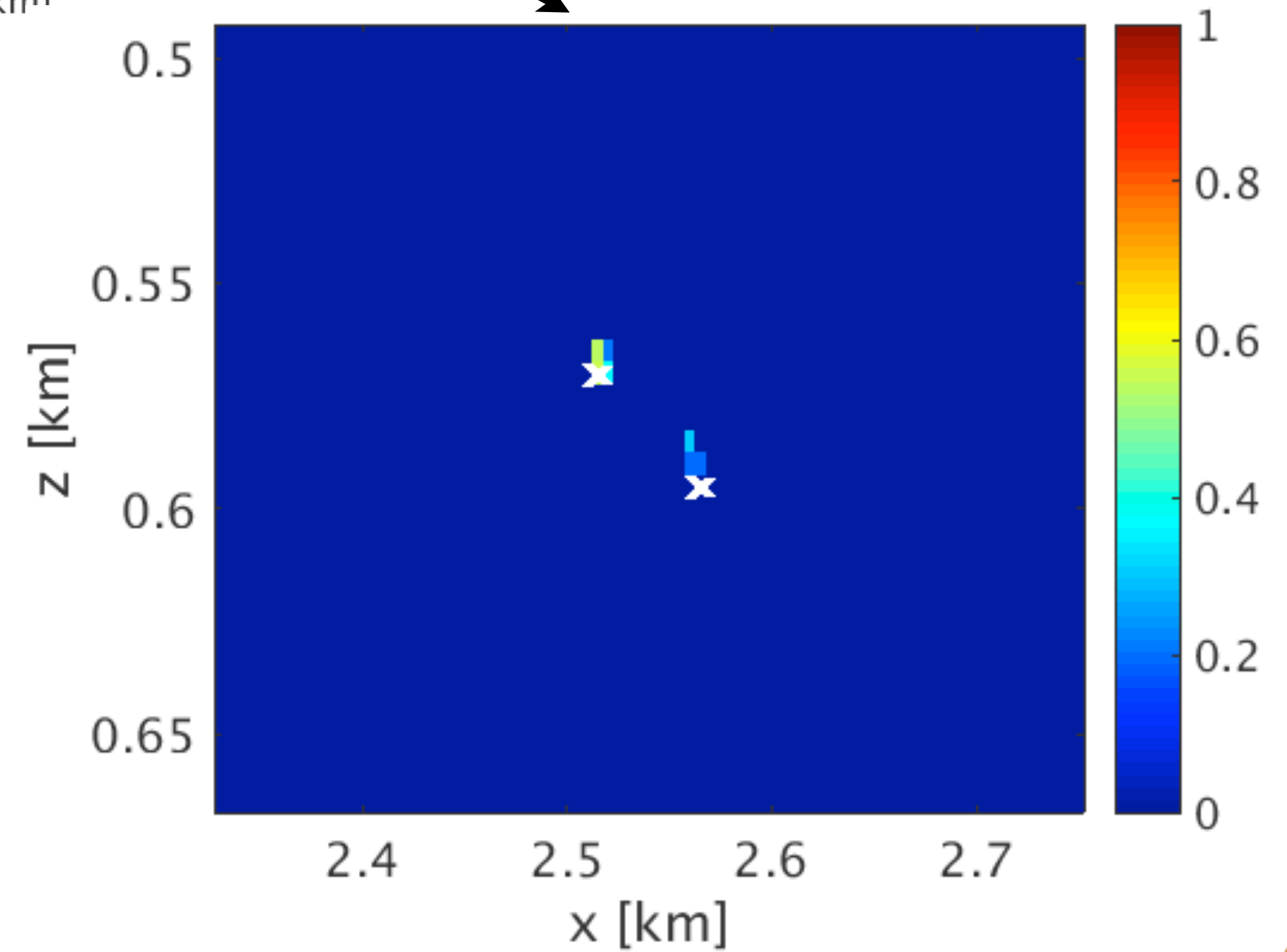
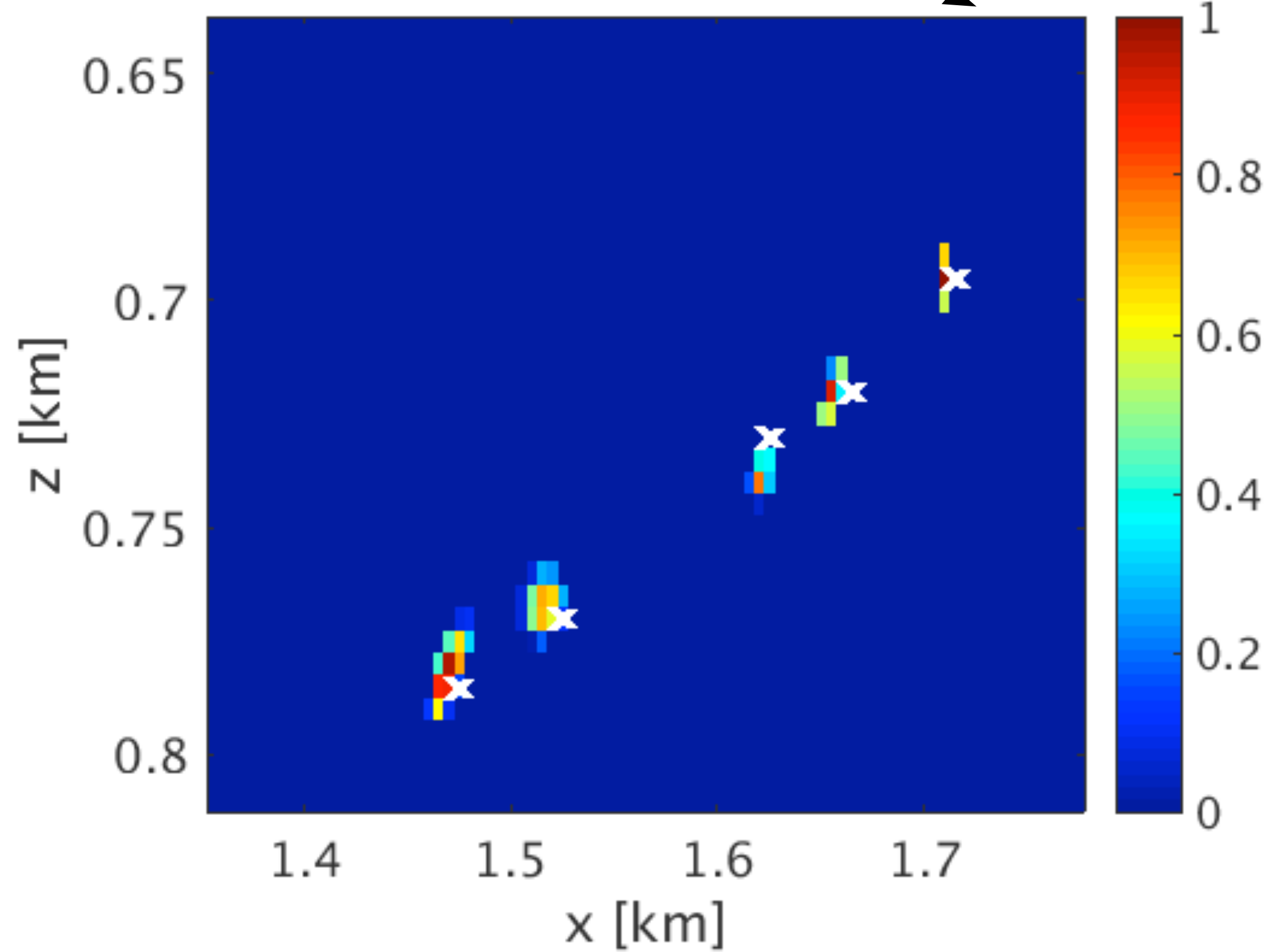
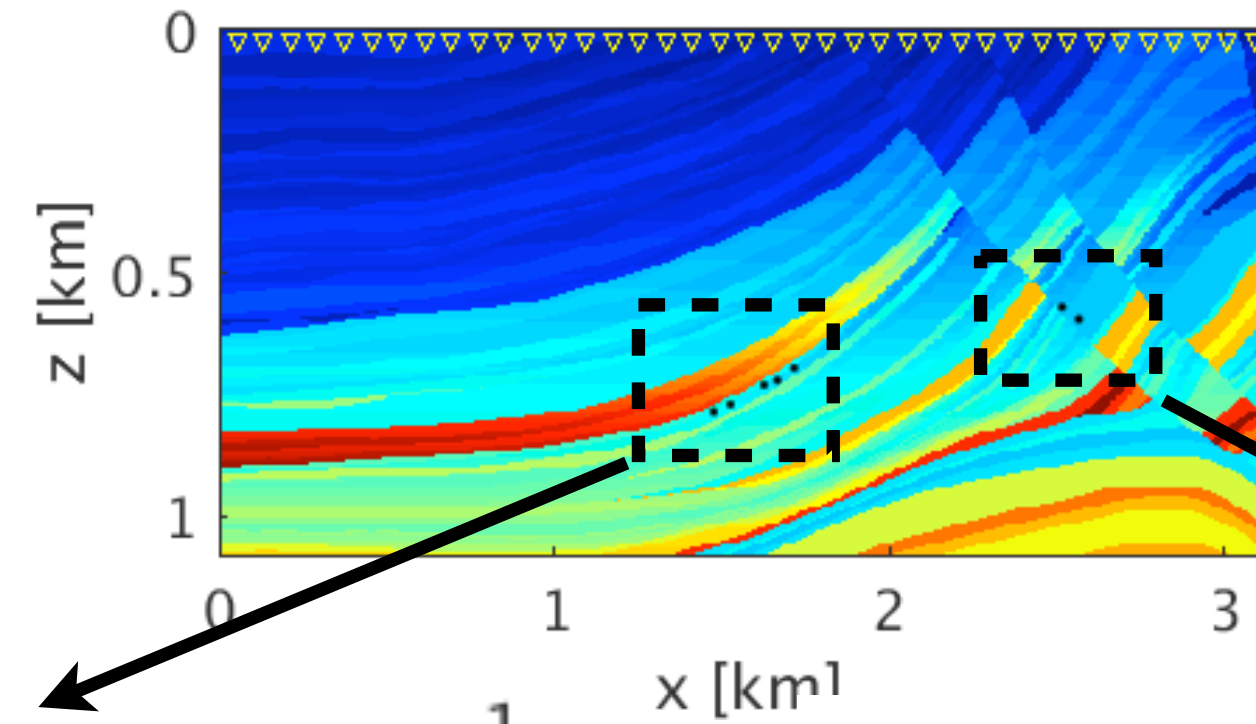


# Estimated location $w/\mu = 9e-4$ and 10 iterations

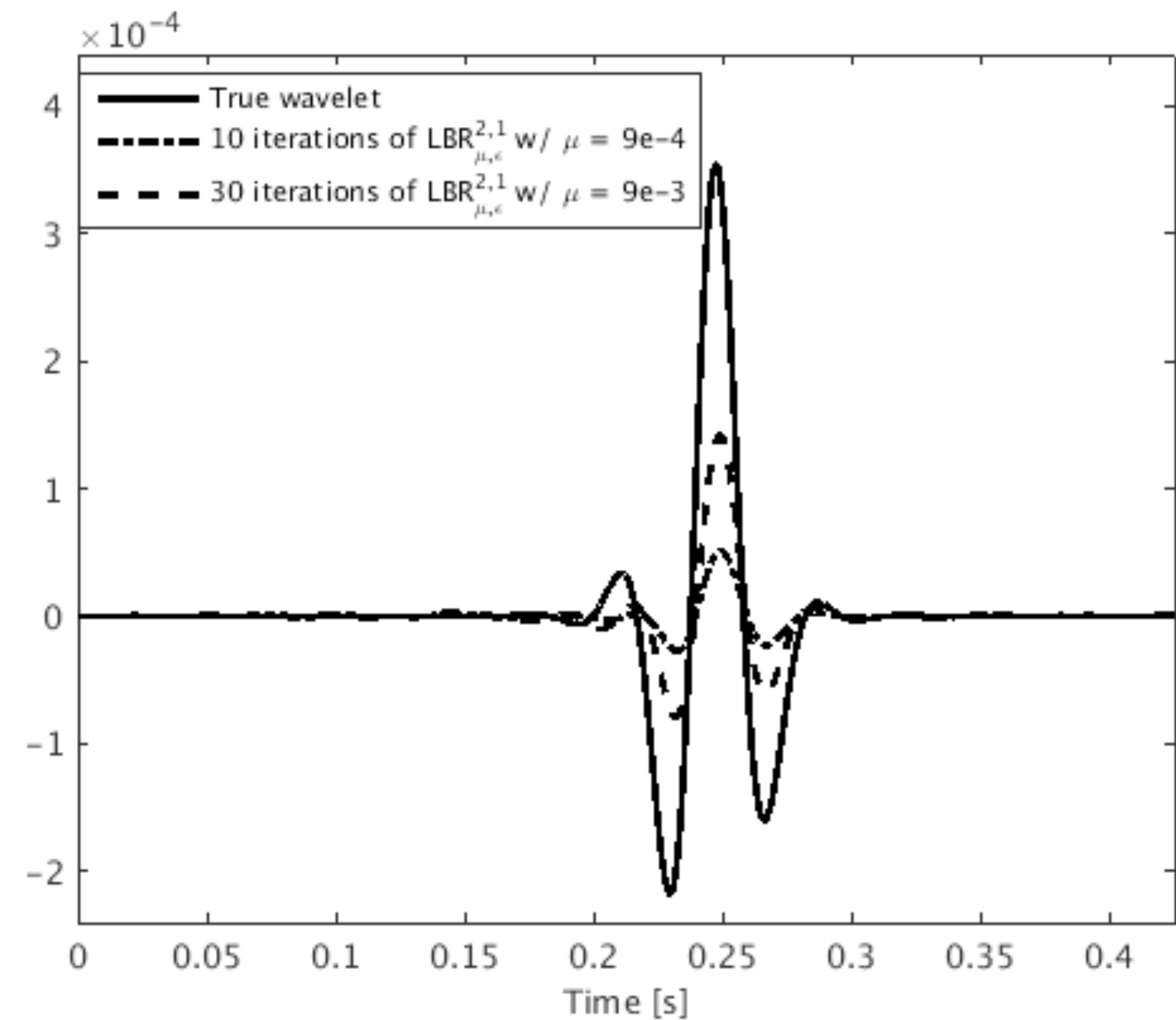
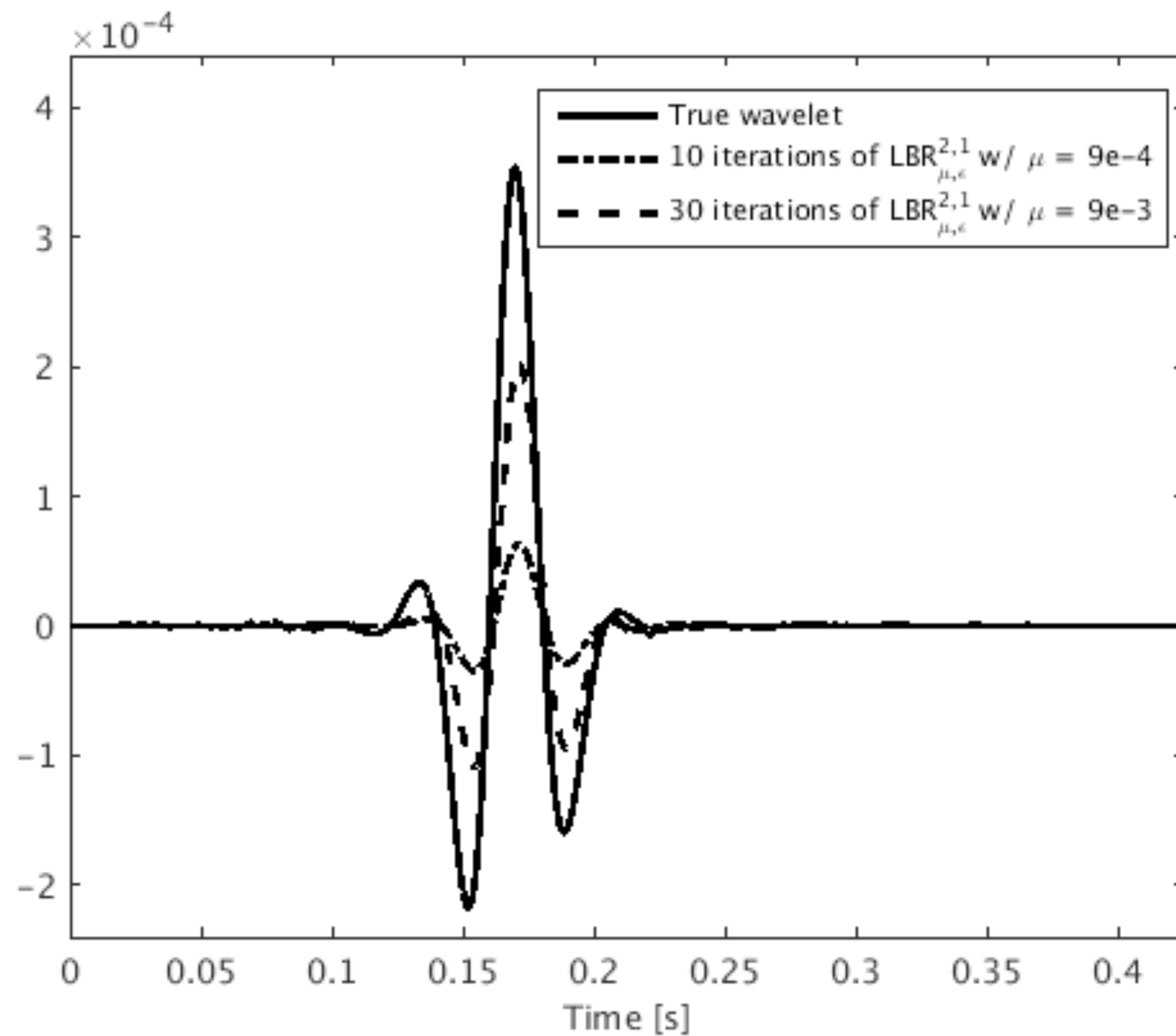
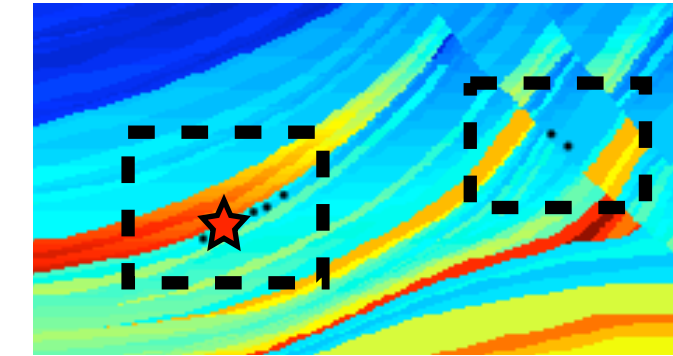
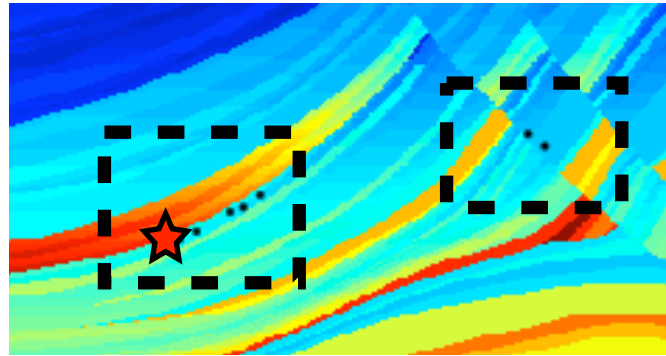




# Estimated location $w/\mu = 9e-3$ and 30 iterations

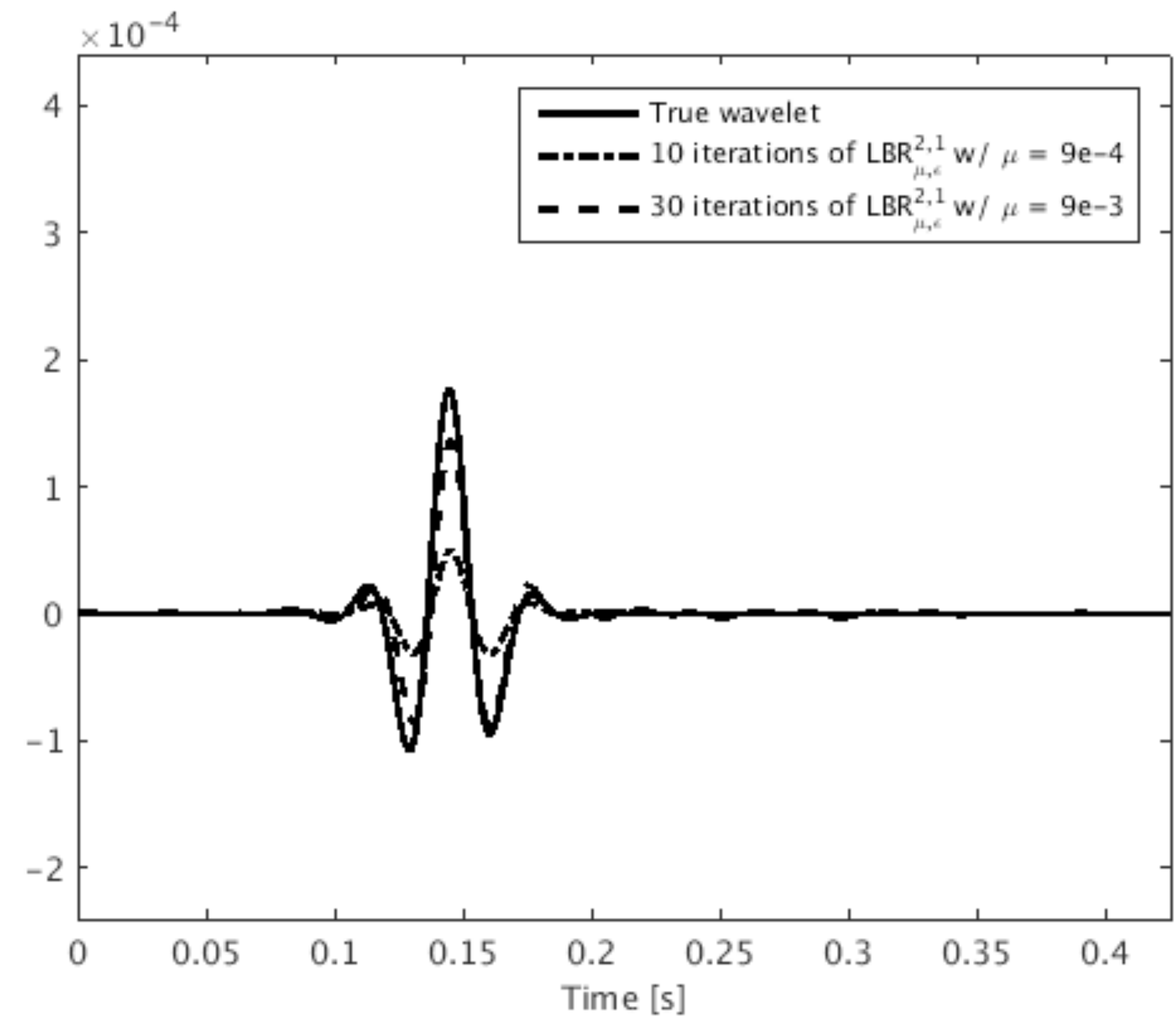
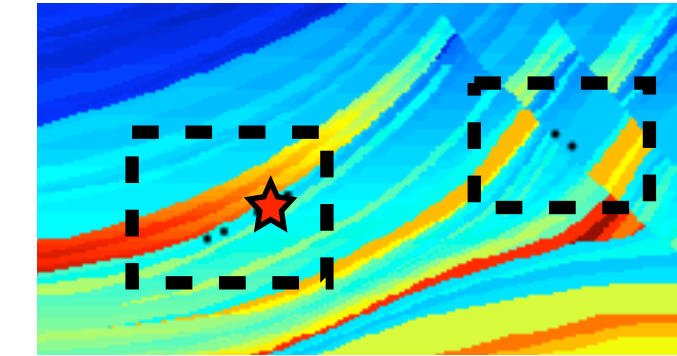
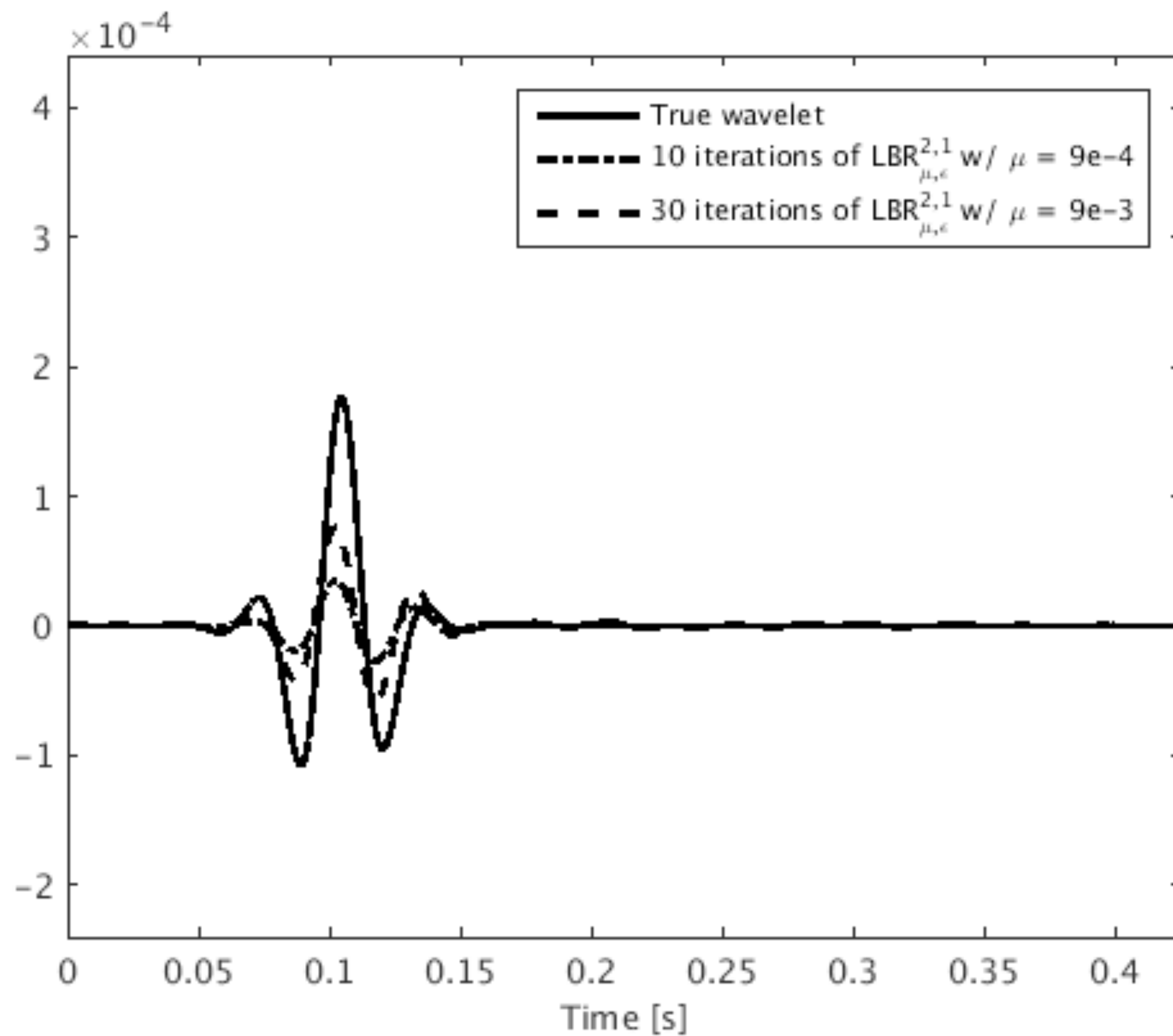
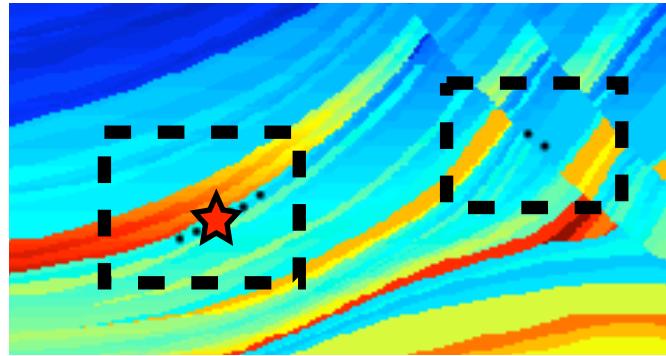


# Wavelet comparison

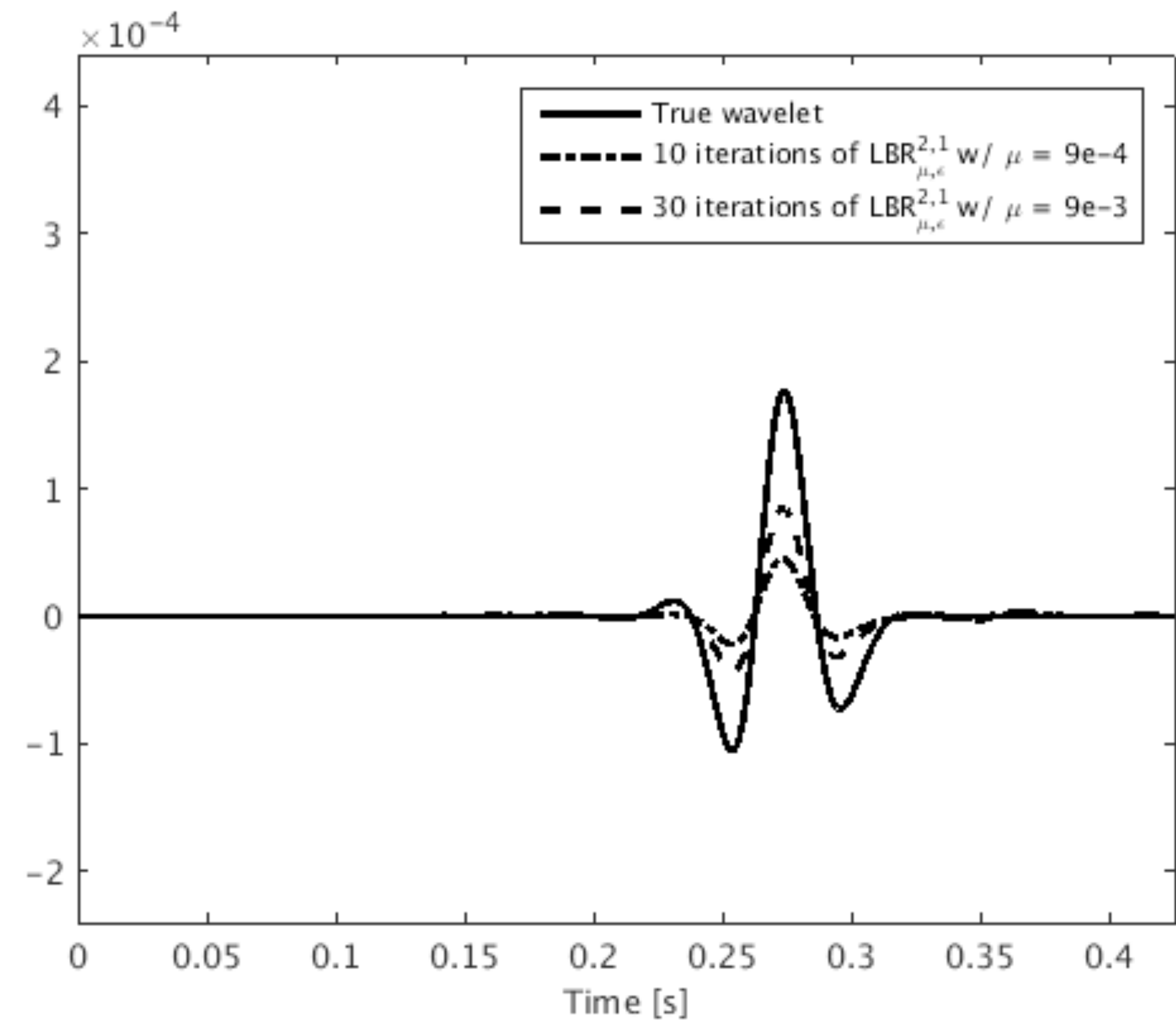
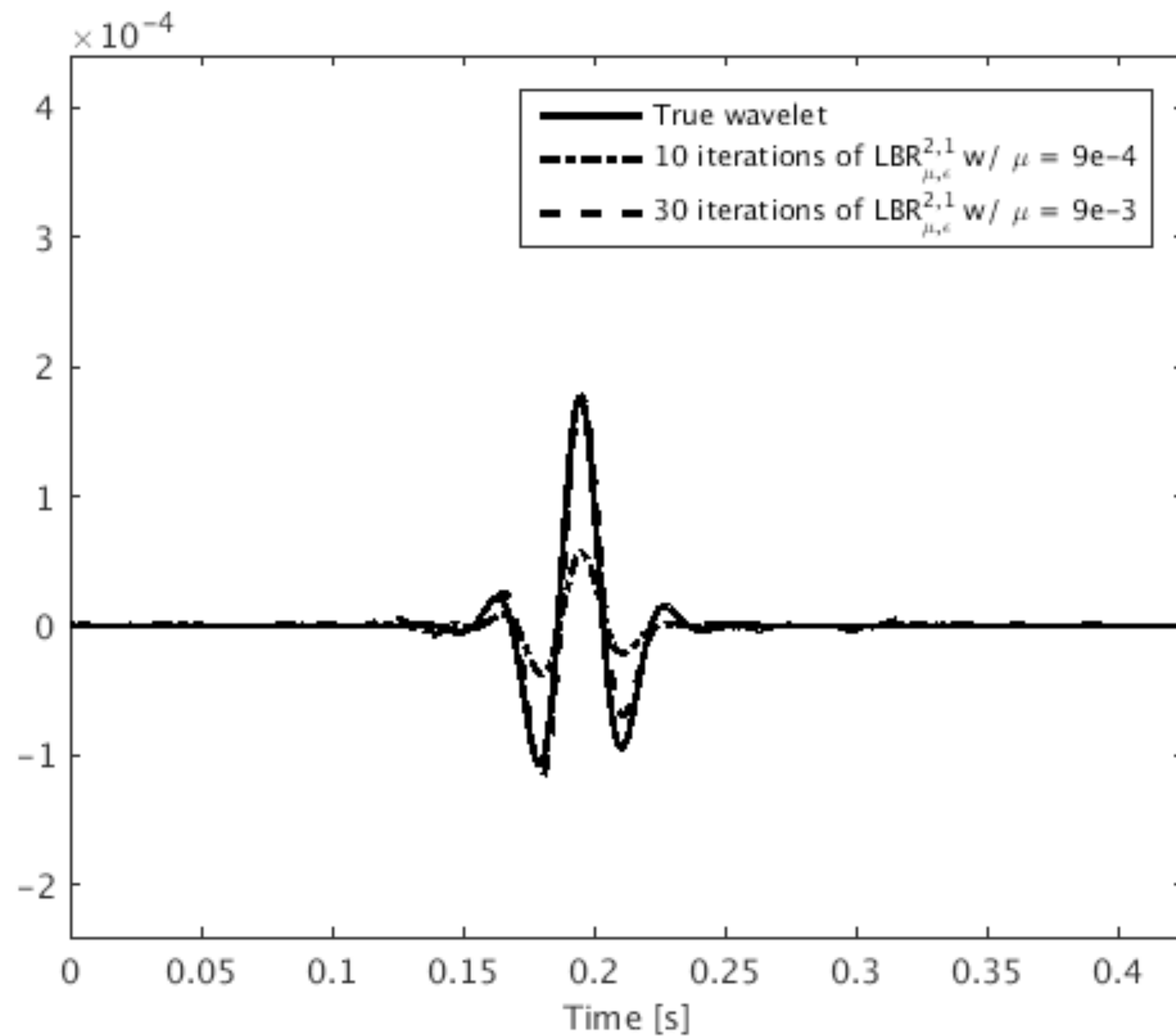
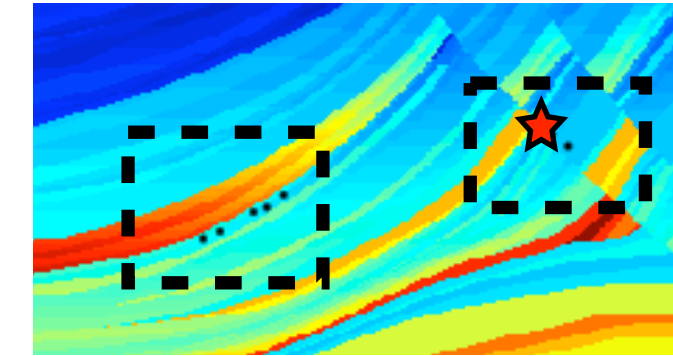
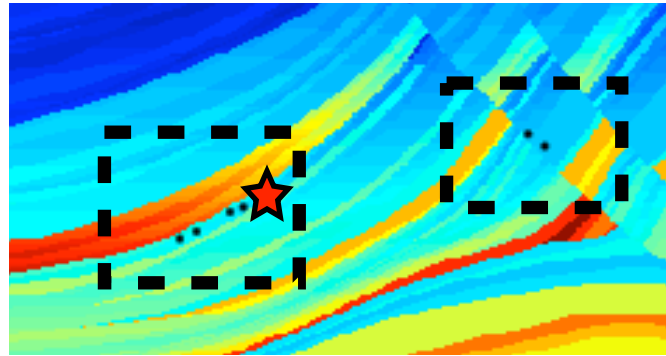




# Wavelet comparison

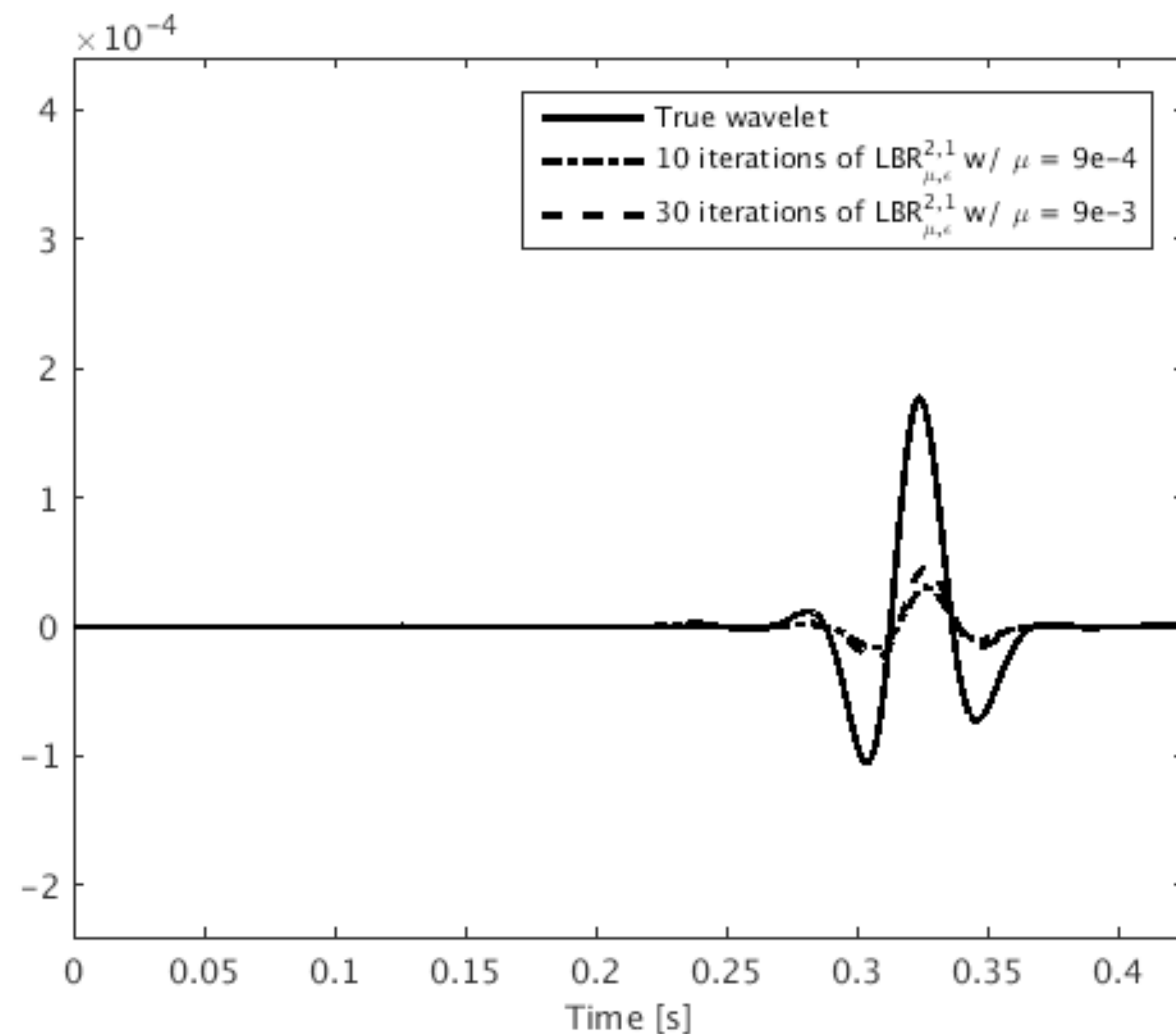
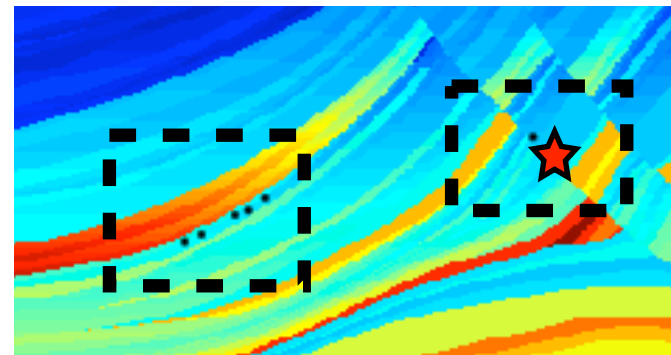


# Wavelet comparison





# Wavelet comparison



In chapter 5

- Debiasing step to correct amplitude and
- Detection of microseismic sources from noisy data

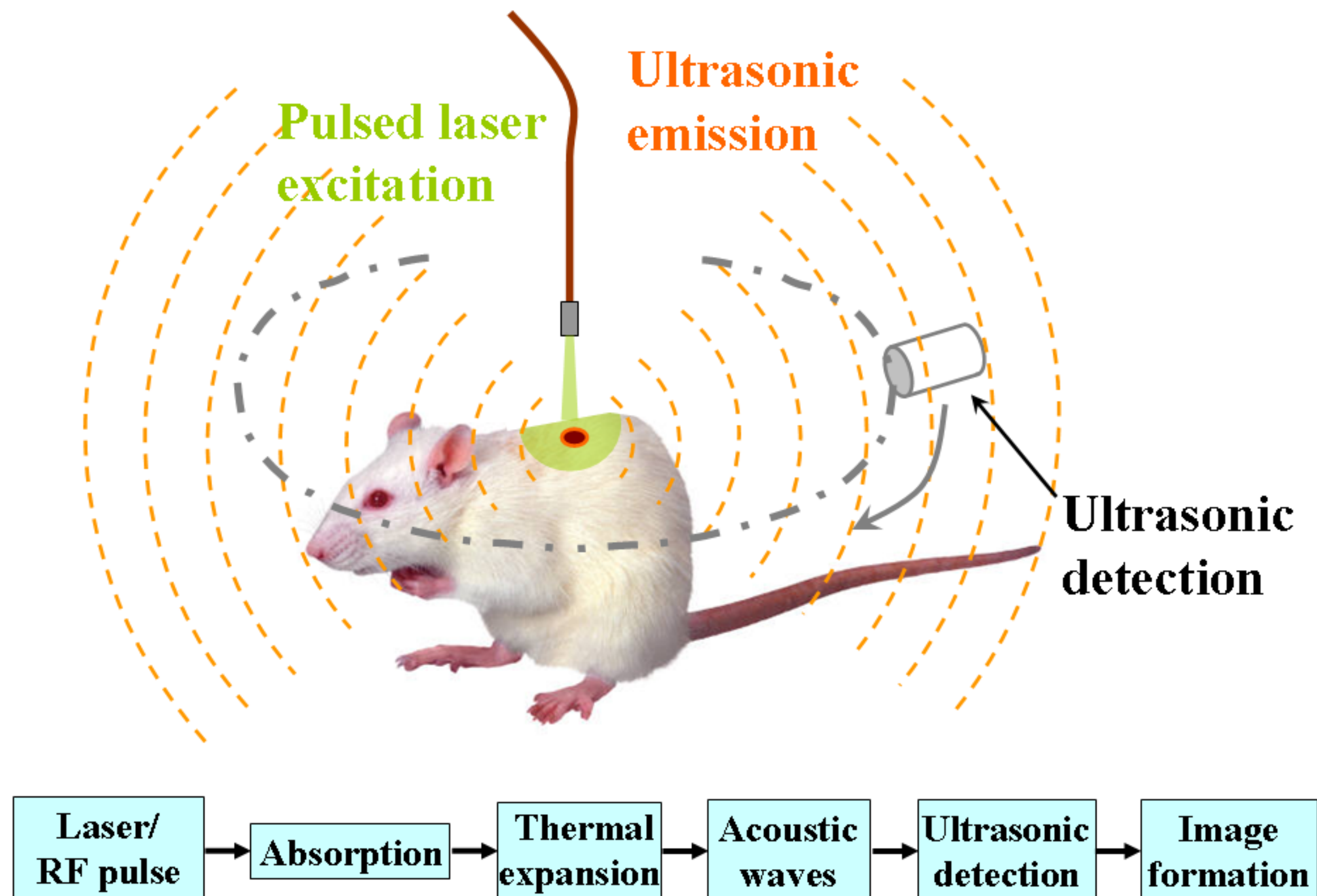
## Key Contributions: Chapter 6

### Sparsity-promoting photo acoustic imaging

- ▶ Simultaneous imaging of absorption map and source estimation
- ▶ With reduced number of transducers and with smooth velocity model



# Photoacoustic Imaging



## Objectives

- ▶ detection of photoabsorbers
- ▶ estimation of associated source-time function

## Challenges

- ▶ Time-reversal methods do not estimate source-time function
- ▶ Require dense transducer coverage

## Solving w/ Linearized Bregman

$$\begin{aligned} & \underset{\mathbf{Q} \in \mathcal{T}_\tau}{\text{minimize}} \quad \|\mathbf{Q}\|_{2,1} + \frac{1}{2\mu} \|\mathbf{Q}\|_F^2 \\ & \text{subject to} \quad \|\mathcal{F}[\mathbf{m}](\mathbf{Q}) - \mathbf{d}\|_2 \leq \epsilon \end{aligned}$$

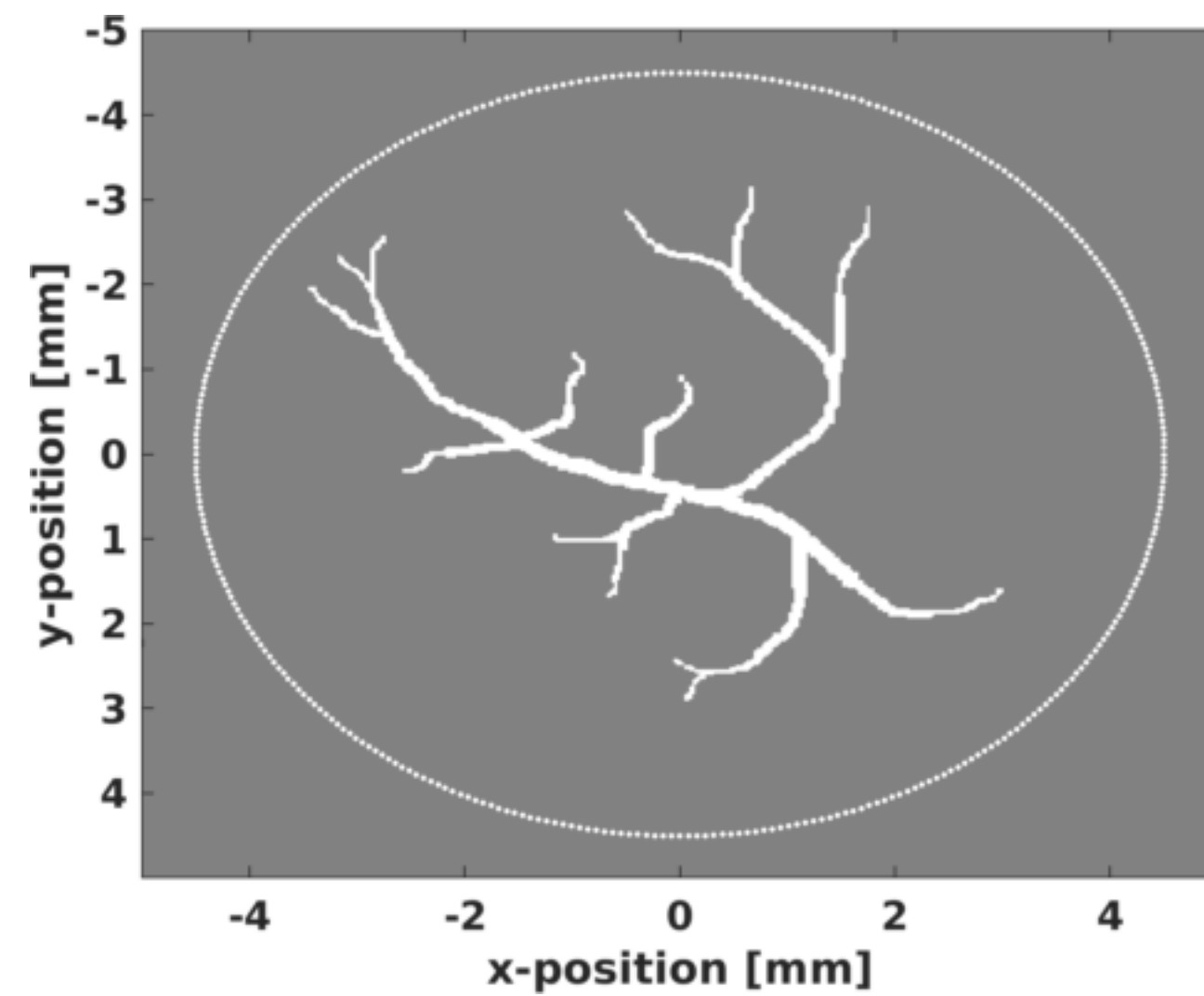
\*where  $\mathcal{T}_\tau = \{\mathbf{Q} | \mathbf{Q}(\cdot, t) = 0, t > \tau\}$

\*where  $\tau$  is the user defined duration

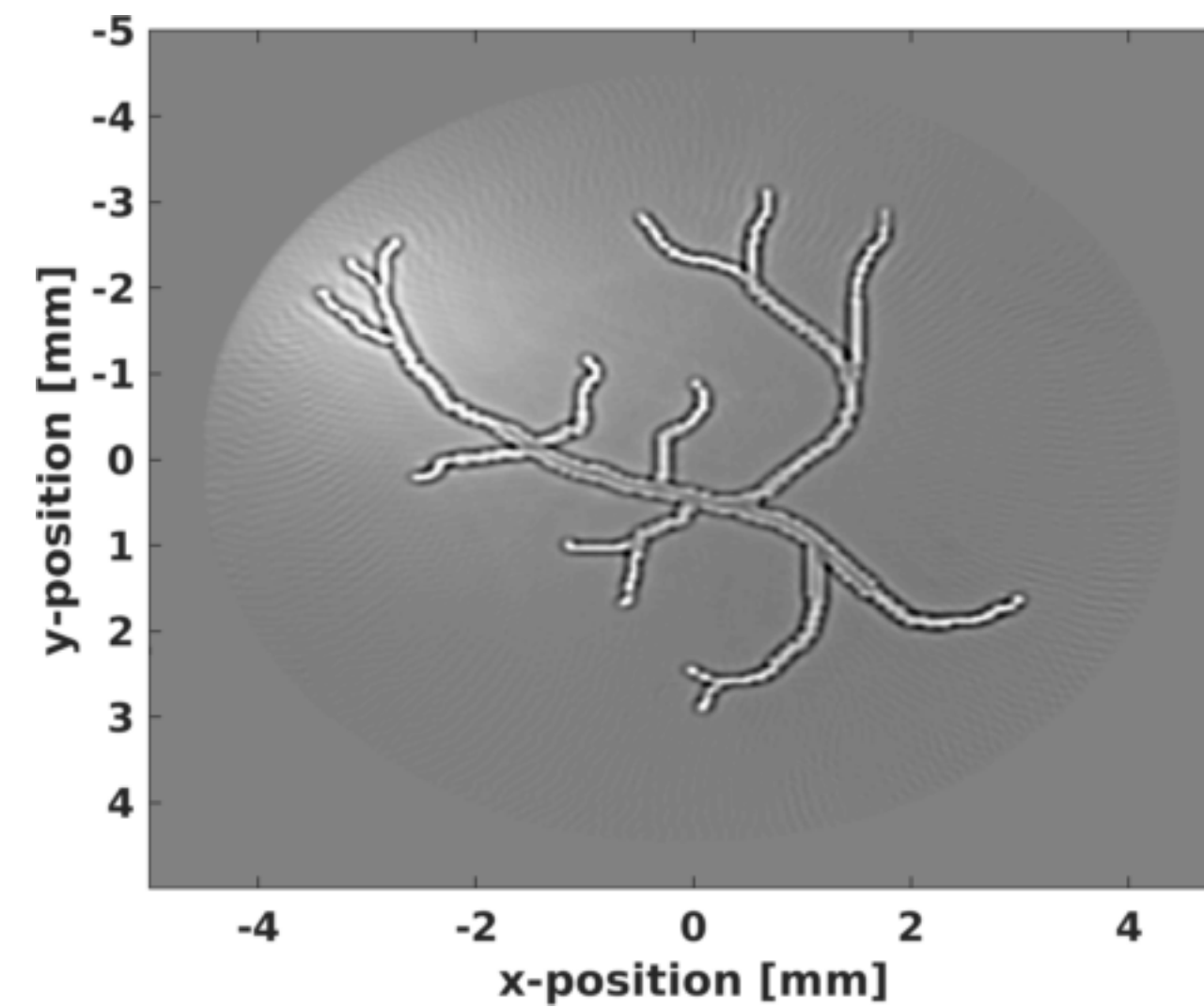


# Case Study: Blood vessel phantom

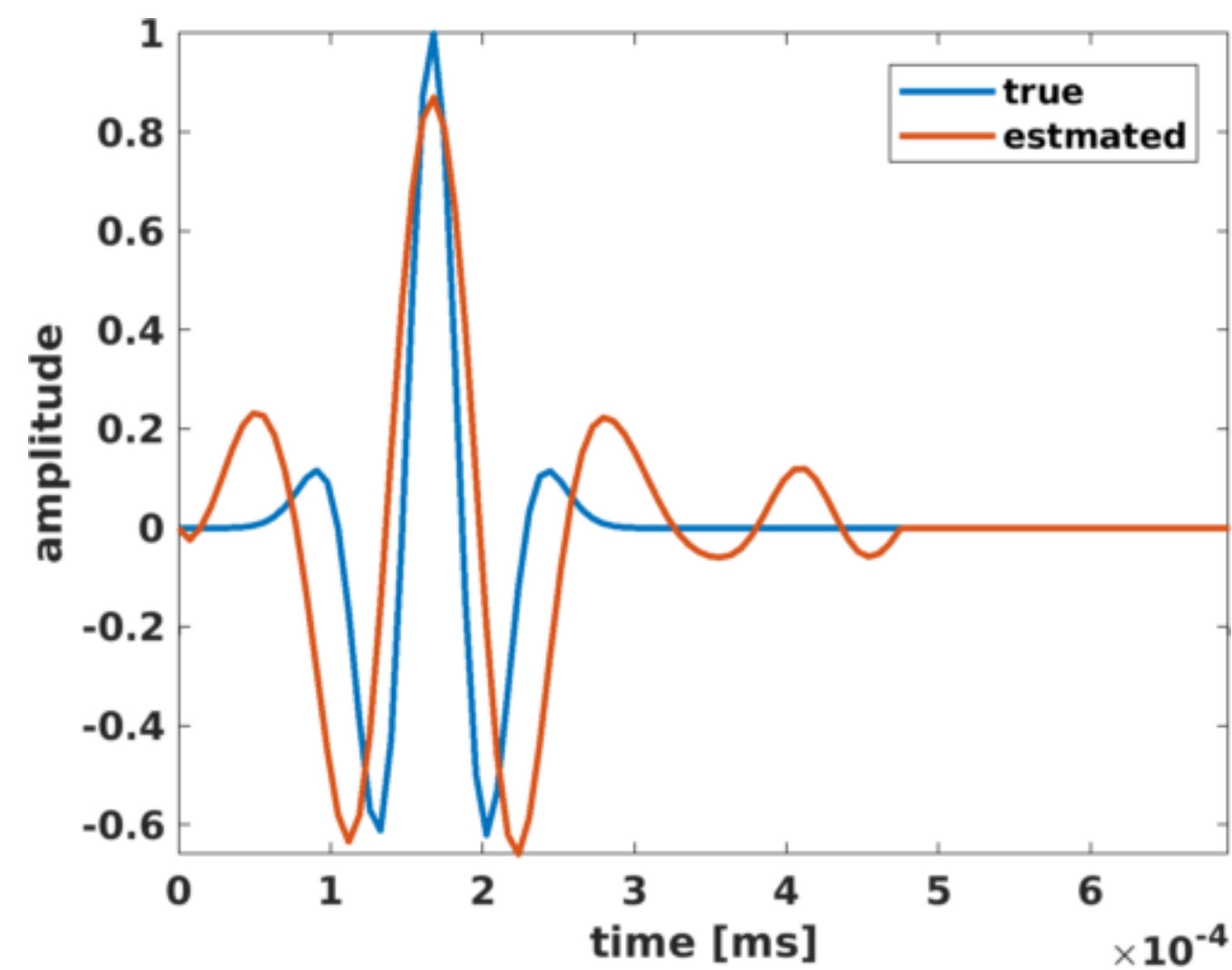
**True Image**



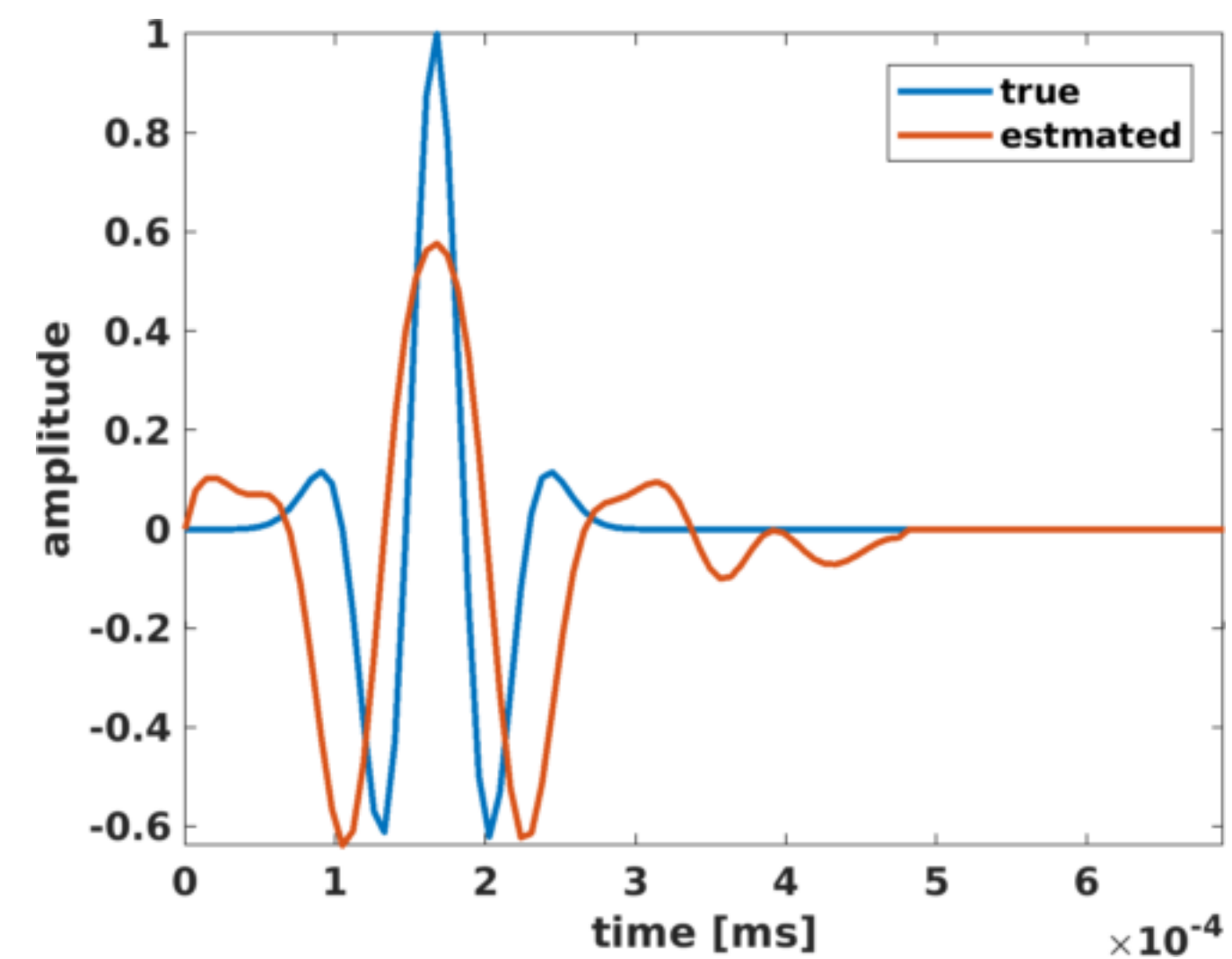
**Estimated Image**



**Wavelet Comparison**



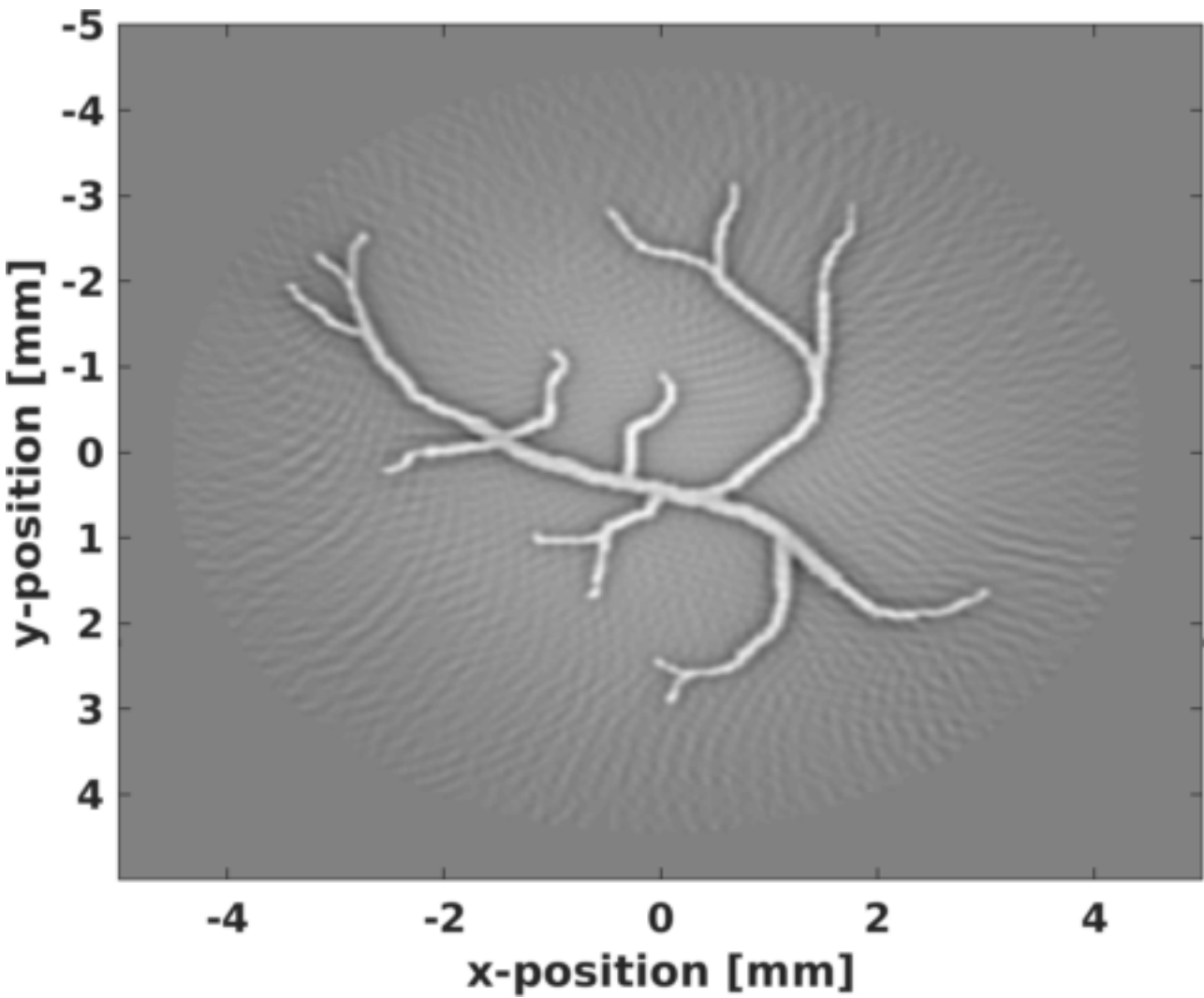
**Wavelet Comparison**



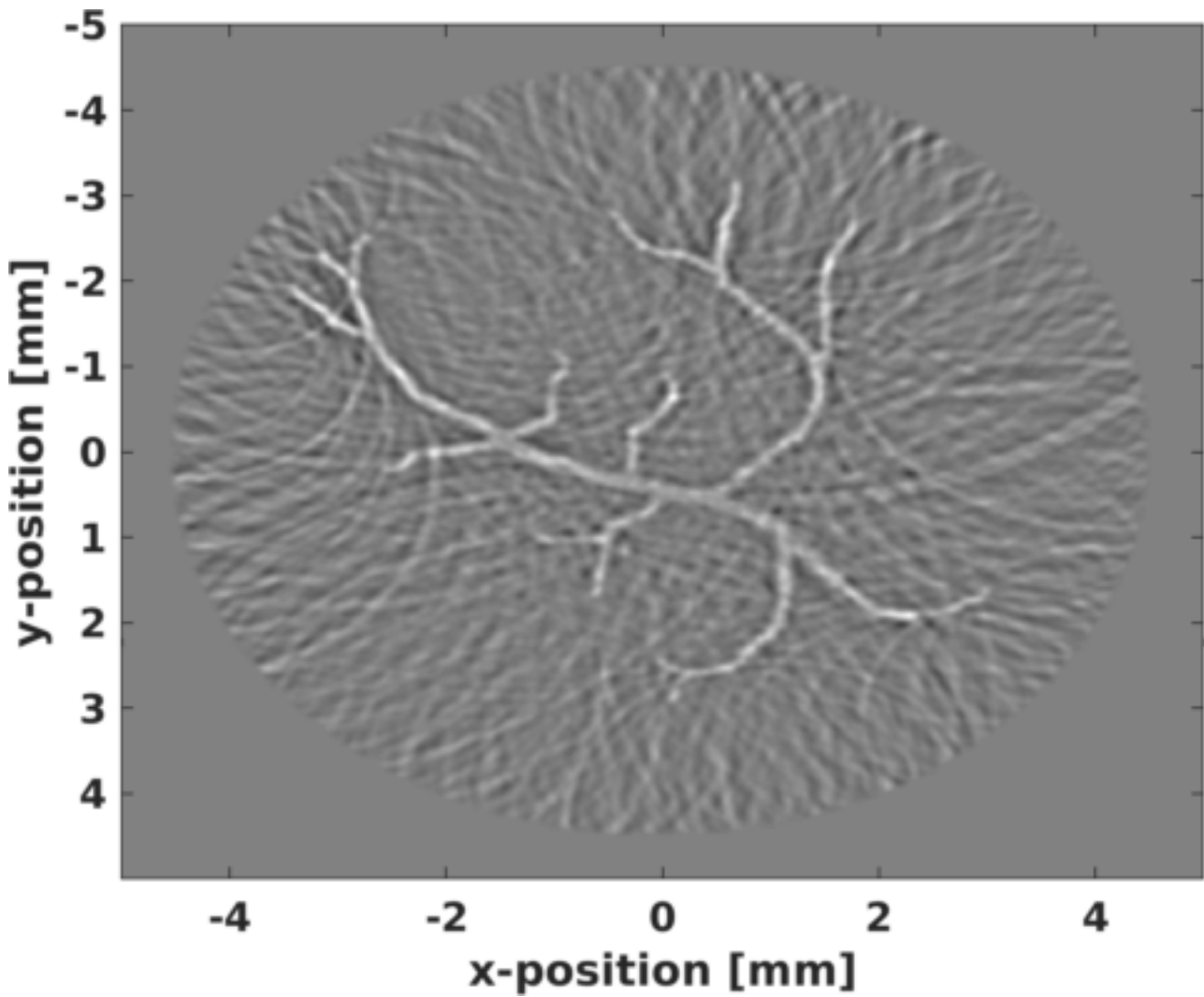
# Effect of transducer sampling

**Sparsity-Promoting**

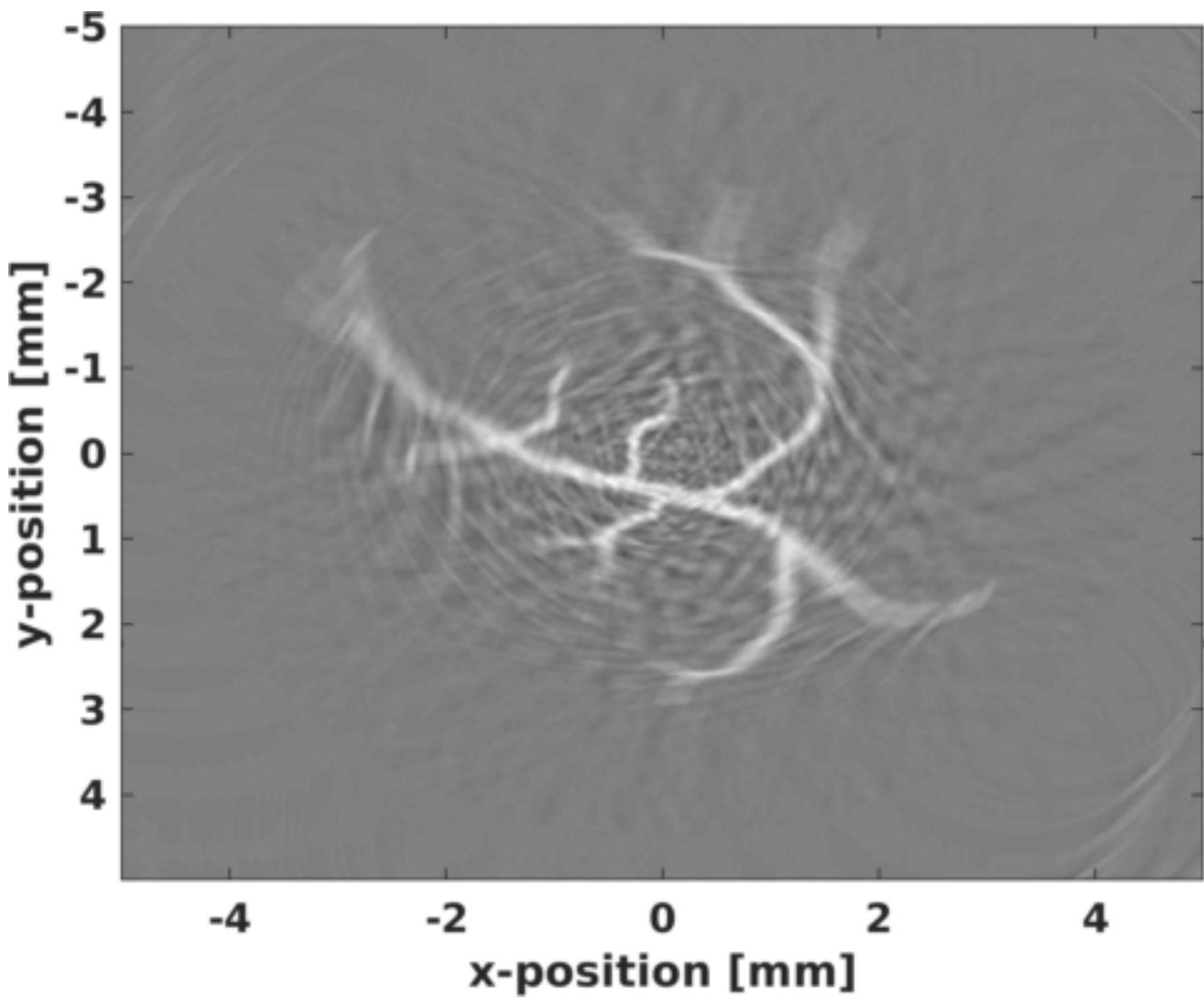
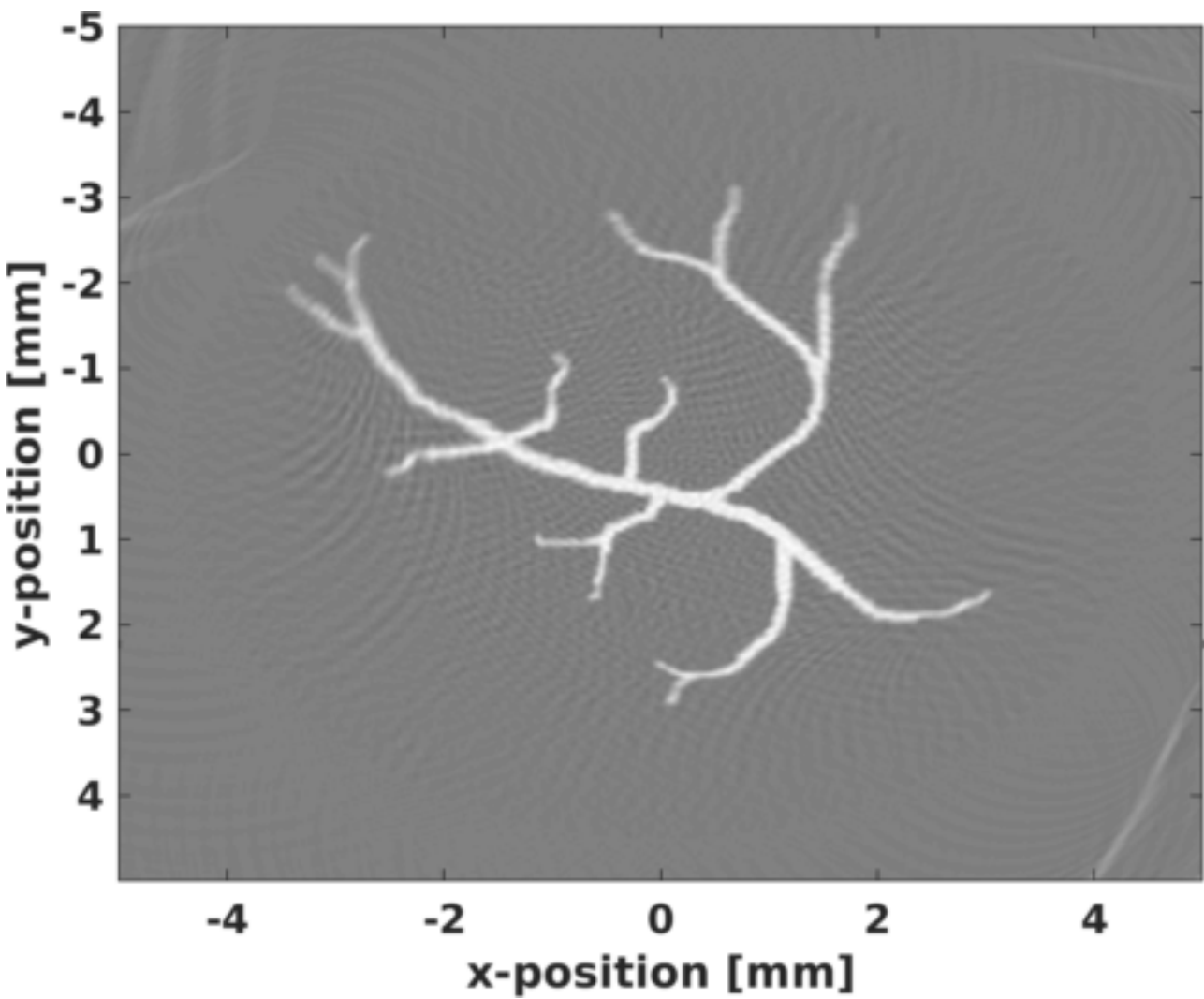
**Transducers every 2 degrees**



**Transducers every 6 degrees**



**Time reversal w/ K-wave**





## Conclusions

Sparsity promotion based method:

- ▶ can simultaneously estimate multiple source locations & source-time functions
- ▶ can provide locations of fractures by resolving microseismic sources within half a wavelength
- ▶ works w/ sources of different frequencies & origin times

Dual formulation provides a computationally efficient scheme.

Wavelet scaling can be corrected using debiasing method

## Future work

Checkpointing strategy to avoid storage of complete source-wavefield

Inclusion of TV-norm instead of  $l_1$  norm in space

- ▶ for sources along a plane
- ▶ with sharp boundaries



1. S. Sharan, Y. Zhang, O. Lopez and F.J. Herrmann, 2020, *Large scale high-frequency wavefield reconstruction with recursively weighted matrix factorizations*, Submitted to Geophysics
2. Y. Zang, S. Sharan, O. Lopez and F.J. Herrmann, 2020, *Wavefield recovery with limited-subspace weighted matrix factorizations*, SEG Technical Program Expanded Abstracts
3. S. Sharan, R. Wang and F.J. Herrmann, 2019, *Fast sparsity-promoting microseismic source estimation*, Geophysical Journal International, vol. 216, pp. 164-181
4. Y. Zhang, S. Sharan and F.J. Herrmann, 2019, *High-frequency wavefield recovery with weighted matrix factorizations*, SEG Technical Program Expanded Abstracts
5. R. Kumar, S. Sharan, N. Moldoveanu and F.J. Herrmann, 2018, *Compressed sensing based land simultaneous acquisition using encoded sweeps*, EAGE Annual Conference Proceedings
6. S. Sharan, R. Kumar, R. Wang and F.J. Herrmann, 2018, *A debiasing approach to microseismic*, SEG Technical Program Expanded Abstracts
7. S. Sharan, R. Kumar, D.S. Dumani, M. Louboutin, R. Wang, S. Emelianov and F.J. Herrmann, 2018, *Sparsity-promoting photoacoustic imaging with source estimation*, IEEE International Ultrasonics Symposium
8. S. Sharan, R. Wang and F.J. Herrmann, 2017, *High resolution fast microseismic source collocation and source time function estimation*, SEG Technical Program Expanded Abstracts
9. R. Kumar, H. Wason, S. Sharan and F.J. Herrmann, 2017, *Highly repeatable 3D compressive full-azimuth towed-streamer time-lapse acquisition — a numerical feasibility study at scale*, The Leading Edge, vol. 36, pp. 677-687
10. R. Kumar, S. Sharan, H. Wason and F.J. Herrmann, 2016, *Efficient large-scale 5D seismic data acquisition and processing using rank-minimization*, SEG Technical Program Expanded Abstracts

# Acknowledgement

Many thanks to

- ▶ my advisor Prof Felix J. Herrmann
- ▶ PhD advisory committee at Georgia Tech and UBC
- ▶ PhD examination committee
- ▶ My colleagues at SLIM Lab
- ▶ Georgia Research Alliance, NSERC, SINBAD consortium
- ▶ Nick Moldoveanu from Schlumberger
- ▶ Developers of open source software packages (Devito, JUDI)